Wisp1 is associated with hepatitis B related human hepatocellular carcinoma and promotes proliferation or migration of HCC derived cell lines.

Dissertation
submitted to the
Combined Faculties for the Natural Sciences and for Mathematics
of the Ruperto-Carola University of Heidelberg, Germany
for the degree of
Doctor of Natural Sciences

presented by
Diplom-Chemist Sonja Lukowski
born in Kiel, Germany

Referees:
Prof. Dr. R. Zawatzky, University of Heidelberg, Germany
Prof. Dr. S. Dooley, University of Heidelberg, Germany

Dissertation

submitted to the

Combined Faculties for the Natural Sciences and for Mathematics

of the Ruperto-Carola University of Heidelberg, Germany

for the degree of

Doctor of Natural Sciences

presented by

Diplom-Chemist Sonja Lukowski

born in Kiel, Germany

Oral-examination**:** 16. October 2012

Wisp1 is associated with hepatitis B related human hepatocellular carcinoma and promotes proliferation or migration of HCC derived cell lines.

"Non esiste vento favorevole per il marinaio che non sa dove andare."

Lucio Anneo Seneca

Zusammenfassung

Das hepatozelluläre Karzinom (HCC) ist weltweit die fünfthäufigste Tumorerkrankung und die dritthäufigste durch Krebs hervorgerufene Todesursache. Mit einer jährlich steigenden Inzidenz und schlechter Prognose, stellt HCC ein großes Gesundheitsproblem dar. Diagnostische Marker zur Früherkennung des hepatozellulären Karzinoms werden benötigt, fehlen aber aufgrund der Komplexität und Heterogenität der Erkrankung.

Das Ziel dieser Arbeit war es, die Wisp1 Expression in unterschiedlichen Tumorstadien zu untersuchen und die Funktionen von Wisp1 in epithelialen- und fibroblastischen HCC abstammenden Zelllinien zu untersuchen. Immunhistochemische Färbungen von HCC Patientenproben wiesen eine erhöhte Wisp1 Expression in ganz frühem und frühem HCC auf, wobei inflammatorische und steatotische Bereiche der Leber ebenfalls positiv für Wisp1 waren. In fortgeschrittenen HCC Stadien wurde hingegen kein Wisp1 detektiert. Diese Befunde wurden durch *in vitro* Untersuchungen ergänzt, die zeigten, dass Wisp1 von HCC Zelllinien (FLC4, HLF) exprimiert und sekretiert wird. Eine Stimulation der epithelialen HCC Zelllinie (FLC4) mit humanem Wisp1 (hWisp1) führte zu einem Anstieg der Proliferation, während hWisp1 einen stimulierenden Effekt auf das Migrationsverhalten der fibroblastischen HCC Zelllinie (HLF) hatte. Interessanterweise wiesen beide Zelllinien eine Aktivierung von Signalwegen über die Phosphorylierung von Fak, Src, Akt und Erk1/2 auf. Alles, in der Entwicklung von HCC, wichtigen Phospokinasen.

In der vorliegenden Arbeit wurde Wisp1 als möglicherweise geeigneter immunhistochemischer Marker für die Früherkennung des HCC identifiziert. Darüber hinaus könnte Wisp1 auch kausal mit der Erkrankung assoziiert sein, da es die Proliferation und Migration von HCC Zellinien reguliert.

Chapter

Chapter

Index

1 Introduction

1.1 Hepatocellular carcinoma (HCC)

Worldwide, hepatocellular carcinoma (HCC) is the fifth most commonly diagnosed solid cancer and the third most common cause of cancer related death with a 5-year survival rate of only 3–5% upon diagnosis [1]. Because of its constantly increasing incidence and its very poor prognosis, HCC represents a major health problem [2]. So far, the underlying mechanism of HCC is poorly understood and available factors, which could be used as early diagnostic markers supporting therapy, are limited. Commonly used biomarkers are, for instance, α–fetoprotein, alkaline phosphatase, gamma-glutamyl transpeptidase (GGT), ferritin and hepatoma-specific gamma-glutamyl transferase isoenzymes [3, 4]. However, none of these factors are specific for HCC, which is a highly complex disease and, due to its heterogeneity, its pathogenesis is understudied when compared to other frequent cancer diseases like breast or lung cancer. Different risk factors, such as hepatitis B and C infection, prolonged exposure to toxins, like Aflatoxin B1 intoxication, and chronic abuse of alcohol may account for the high variability of HCC. Hepatitis B infection and Aflatoxin B1 intoxication are the main risks for HCC in Africa and Asia, whereas hepatitis C infection and alcohol abuse account for HCC in developed countries [5]. Other risk factors have been proposed to play a role in HCC with a lower frequency, including diabetes, non-alcoholic fatty liver diseases (NAFLD) or certain metabolic disorders [6]. HCC can result from chronic liver inflammation on the basis of one of these aforementioned risk factors. Another important factor is gender, since females show a 3 fold lower incidence of HCC than males [7]. HCC affects all parts of the world with some geographical variations; the highest incidence rates can be found in developed countries. Likewise, the geographic distribution of risk factors varies.

1.1.1   Mechanisms of hepatocellular carcinoma

The development of HCC must be understood as a multistep process with an accumulation of genetic and epigenetic alterations in regulatory genes which eventually lead to uncontrolled activation of oncogenes and inactivation, or even loss, of tumor suppressor genes [8]. The molecular contribution of these multiple factors

and their interactions in the development of HCC remain elusive [9]. Finally, these multiple steps trigger the malignant transformation of normal hepatocytes (HCs) into cancer cells [9] (Fig.1-1). One of the first steps toward HCC is the development of hyperplastic nodules; thereby hepatocellular carcinoma is grouped into tumors which are poorly, moderately or well differentiated. Poorly differentiated tumors are the most malignant type of HCC. At advanced-stages of disease, tumor cells may metastasize into other organs such as the lung [10].
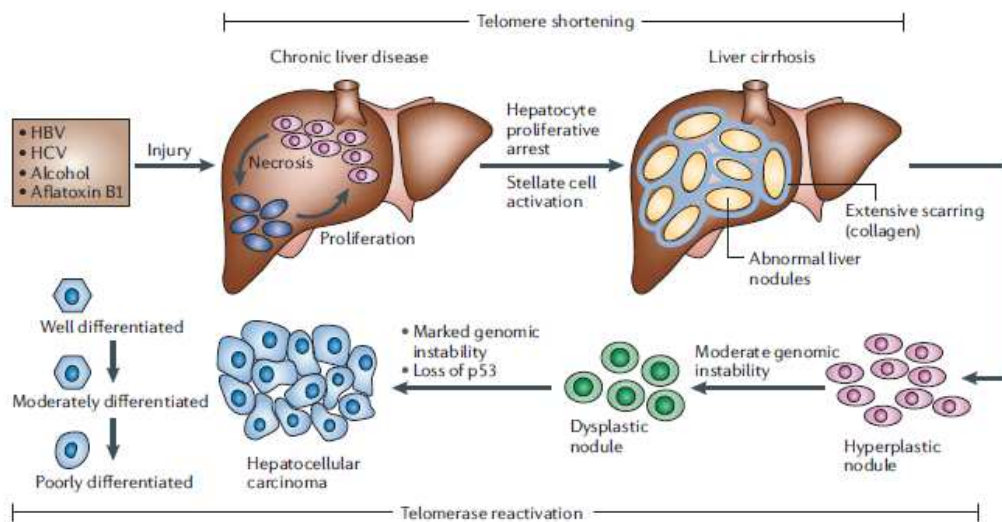
Fig.1-1 Progression of hepatocellular carcinoma. Liver damage due to different risk factors such as hepatitis B or C infection, cirrhosis or chronic alcohol abuse leads to hepatic necrosis followed by hepatocyte proliferation. Continuous regeneration in chronic liver disease is characterized by the formation of hyperplastic nodules which develop into dysplastic nodules and finally into hepatocellular carcinoma (HCC) which can be grouped into well, moderately or poorly differentiated tumors. [From Farazi, P.A. and R.A. DePinho, Hepatocellular carcinoma pathogenesis: from genes to environment. Nat Rev Cancer, 2006. **6**(9): p. 674-87]

Various genetic alterations of different pathways are involved in the progression of hepatocellular carcinoma. For example, molecular analysis of human HCC has shown inactivation of the tumor suppressor gene p53 and E-Cadherin, and deregulation of transforming growth factor beta (TGF-β) and vascular endothelial growth factor (VEGF) dependent signaling [6]. In addition, aberrant DNA methylation patterns have been reported in human HCC and telomere shortening has been described as a key feature of chronic hyperproliferative liver disease [6]. Several genomic alterations can also lead to defects in chromosome segregation, a common cytogenetic feature of cancer cells including HCC [6]. Alterations of the Wnt pathway and its components, e.g., β-catenin and glycogen synthase kinase (GSK-3β), have been proven to be crucial in hepatocarcinogenesis [6].

A common hallmark of all cancers is abnormal growth control. Since multiple signaling pathways and genetic alterations can result in uncontrolled growth or migration, it is very important to understand the complexity of HCC. More information on prognostic factors and molecular biomarkers associated with liver tumorigenesis should bring forward therapeutic approaches.

1.1.2 Therapeutic perspectives for hepatocellular carcinoma and staging systems of the disease

At the present time, limited therapeutic options exist and these options are applicable for just a select number of HCC patients [11]. Standard curative methods are surgical resection or liver transplantation, percutaneous or transanterial interventions, radiation therapy and chemotherapy [9]. However, these curative treatments are applicable for only 30–40 % of HCC patients [12, 13].

The stage of HCC at diagnosis limits treatment options and prognosis. Very early-stage HCC has been defined as the disease in patients with well-preserved liver function; these patients show the best survival rate upon partial hepatectomy. Early-stage HCC has been defined as a tumor between 3 and 5 cm; liver transplantation gives the best possible outcome. This situation is complicated since diagnostic markers for early-stages of HCC, which potentially would allow for effective treatment, are lacking, thus diagnosis is made at an intermediate or advanced-stage of the disease where no radical treatments are applicable. For intermediate or advanced-stage HCC, local ablative therapy is most commonly used. These patients have a survival time of 6 months to 2 years [14]. Promising survival benefit is shown with the treatment of patients with advanced HCC with the multikinase inhibitor sorafenib [14]. Patients with end-stage HCC do not benefit from any known treatment since most die of liver failure and not from tumor progression.

In this context, different HCC staging and grading systems are available and provide a detailed characterization of HCC to find the suitable treatment for each subgroup of patients [13]. Traditionally, the Tumor-Node-Metastasis (TNM) classification system or the Okuda classification is used. Both systems have their limitations, as TNM staging does not include liver function and the Okuda system cannot distinguish

between early and advanced HCC stages. The Barcelona Clinic Liver cancer classification (BCLC) system, first presented in 1999, combines tumor status with liver function and general health status [15]. It has been proposed as the standard means to assess for prognosis of patients with hepatocellular carcinoma.

1.1.3   Epithelial-mesenchymal transition (EMT) during HCC progression

The process of epithelial cells converting into mesenchymal cells is named epithelial-mesenchymal transition (EMT). EMT is a complex process by which differentiated epithelial cells lose their epithelial cell phenotype and obtain features of mesenchymal cells [16]. Epithelial cells express E-Cadherin, whereas mesenchymal cells do not [17]. Epithelial cells show a polygonal-shaped morphology. They form cell layers closely connected by adherent, gap and tight junction proteins. Under normal conditions, they do not leave their epithelial cell layer. Furthermore, epithelial cells show an apical to basolateral polarization, with the apical surface usually facing the lumen of a body cavity and the basolateral membrane in contact with other cells or ECM components. In contrast, mesenchymal cells show a spindle-shaped, fibroblast-like morphology. They are highly mobile, migrating as chains or single cells, lacking the apical to basolateral polarization of epithelial cells [16]. EMT is initiated by a diverse set of extracellular signals, for instance, through extracellular matrix components or growth factors, which further stimulate intracellular factors like members of the GTPase family and Src tyrosine-kinase family members. These signaling pathways eventually lead to the modulation of transcription, and thus, changes in EMT specific gene-expression. EMT plays a central role during cancer progression since cancer cells undergo partial or complete EMT [16]. With this transition, cancer cells acquire a high motility and migrative capacity, which gives them the possibility to break through the basement membrane, invade blood vessels and reach distant organs where they build up cancerous colonies (Fig.1-2).
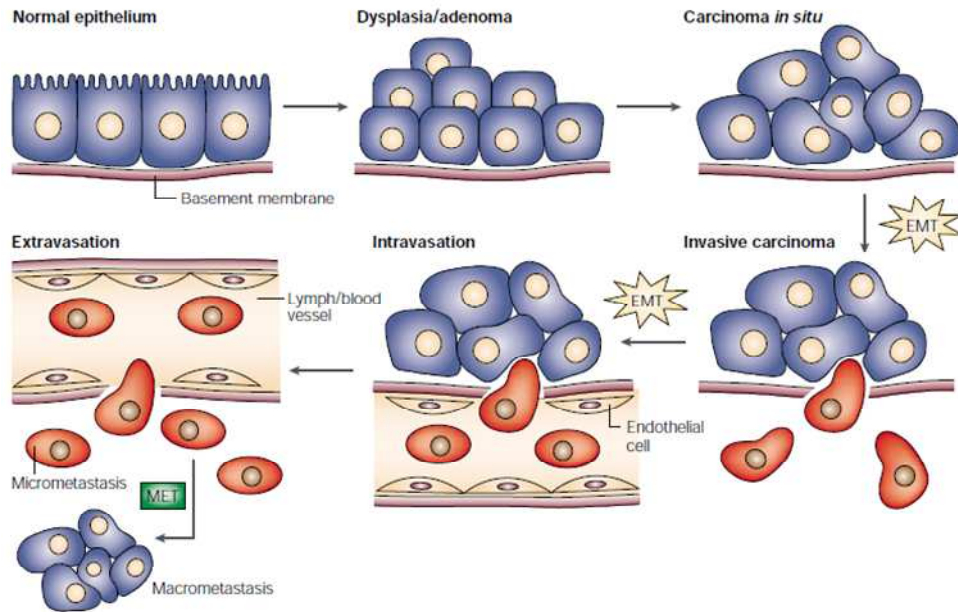
Fig. 1-2 Sites of EMT in the emergence and progression of carcinoma. After tumor initiation, normal epithelium develops into an adenoma. Tumor promotion, including genetic and epigenetic changes, can further lead to the EMT process which is necessary for breaking through the basal membrane and subsequent intravasation and systemic spread. At secondary sites, solitary carcinoma cells can extravasate and either remain solitary (micrometastasis) or form a new carcinoma through a mesenchymal–epithelial transition (MET) [From Thiery, J.P., Epithelial-mesenchymal transitions in tumour progression. Nat Rev Cancer, 2002. 2(6): p. 442-54.]

A key event during EMT is the loss of E-Cadherin, which is a main component of the epithelial cell phenotype, hence having direct consequences for cell shape. E-Cadherins are transmembrane proteins which belong to the superfamily of calcium dependent adhesion glycoproteins. The N-terminal domain plays a fundamental role in the formation of epithelial tissues. The cytoplasmic domain interacts with β-catenin and the actin network, causing assembly and disassembly of actin cytoskeleton, thereby modulating the tension and strength of adhesion within a cell layer. Reduced expression of E-Cadherin is correlated with the disruption of cell-cell contacts and deregulation of adhesion further influencing proliferation and mobility [18]. Knock-out experiments revealed functions of this gene in migration and tumor progression, as well as invasion and metastasis [19].

HCC metastasis is most frequently detected in the lung, followed by regional lymph nodes, kidneys, bone marrow and adrenal glands. Metastasis is a process that depends on many factors including chemokine gradients, detachment of cell-cell contact between neighboring cells and changes in cell-matrix contacts. Thus, cell adhesion, migration and proteolysis of extracellular matrix proteins are important features in the process of metastasis [20, 21]. This is especially of importance in the

liver, where hepatocytes grow in trabecular structures surrounded by a high number of ECM proteins like collagen, lamin and fibronectin. Interactions between HCC cells and ECM proteins are suggested to be essential for tumor metastasis. Interactions between the HCC cells and the ECM components are mediated through integrins, a class of transmembrane receptors [22].

1.1.4 The role of integrin molecules as signal transducing adhesion factors in hepatocellular carcinoma cells

Intergrins are heteromeric transmemebrane receptors. They regulate cell functions in each kind of cell. At least 14 distinct alpha chains and 9 beta subunits are known that can pair up to form more than 20 different receptors [22]. Each subunit has an extracellular and a cytoplasmic domain. While the extracellular domain binds to extracellular-matrix (ECM) proteins, the intracellular domain interacts with signaling molecules and actin binding proteins linking integrins to the components of the cytoskeleton. Integrins have been shown to be important signal transducers; they modulate cell-cell contacts and they participate in cell migration, growth and inflammation. During carcinogenesis, integrins were described to influence tumor growth, differentiation, survival and apoptosis during the metastasis of cancer cells [23, 24]. Integrins mediate signals from the surroundings to the inside ("outside-in") of the cell. On the other hand, "inside-out" signaling pathways involving factors that bind directly to the cytoplasmic tails and phosphorylation events can also modulate integrin function [25]. Many cancer cells interact with cell and matrix components through integrins [22]. Integrin function can be altered by ligands present in, and produced by, HCC [26]. Furthermore, integrin signaling was linked to both cancer suppression and progression [27].

1.2 The CCN family of proteins

The CCN family of proteins was originally discovered in the 1990s. However, they remained mostly understudied in the field of cell and cancer biology until only

recently. It has become clear that the CCN proteins are multifunctional factors which are involved in many important processes including differentiation, tumorigenesis, wound healing, cell proliferation, migration, adhesion and survival [28].

The abbreviation CCN stands for **C**yr61 (cysteine-rich 61), **C**TGF (connective tissue growth factor*)* and **N**ov (nephroblastoma overexpressed), which are the first three discovered and best investigated proteins of this family. Currently, the family comprises six family members including Wisp1, Wisp2 and Wisp3 (WNT1-inducible-signaling pathway proteins). As they were discovered simultaneously by different laboratories, individual proteins often carry different names in literature [29]. To avoid confusion resulting from this nomenclature, they were recently named after the founding proteins (CCN) and numbered 1-6 (Tab.1-1).

Tab. 1-1 Conventional and alternative nomenclature of the CCN protein family.

CCN nomenclatur	Alternative nomenclature
CCN1	**Cyr61**, CEF10, IGFBP-rP4m, βIG-M1, CTGF-2, IGFBP10
CCN2	**CTGF**, βIG-M2, FISp12, IGFBP-rp2, IGFBP8, HCs24, HBGF-0.8
CCN3	**Nov**, IGFBP-rP3, IGFBP9
CCN4	**Wisp1, Elm1**
CCN5	**Wisp2**, CTGF-L, CTGF-3, HICP, rCOP-1
CCN6	**Wisp3**

Importantly, CCN proteins are so called "matricellular proteins", which do not directly play a structural role in the matrix, but serve to modulate cell matrix interactions and cell function [30]. The functions of this group of proteins are achieved by binding to matrix proteins, cell surface receptors or other molecules, such as cytokines or proteases which interact with the cell surface [30]. In general, one of the key features of matricellular proteins, and of CCN proteins in particular, is their enormous range of functions resulting from a multi-modular structure [31]. The typical CCN protein is composed of four potentially functional modules [32]: The N-terminal signal sequence for secretion is followed by four modules including an IGFBP domain, a von Willebrand factor type C (VWC) oligomerization domain, a thrombospondin type 1 repeat (TSP-1) and a carboxyl terminal end (CT) (Fig.1-3). The second remarkable feature of the CCN family is their high cysteine content (about 10% by mass). Despite

the fact that they share a high similarity in structural components, closely related CCN proteins may show both, similar or even opposite effects on, e.g., cell proliferation, migration or survival. Furthermore, it is important to note that the function of CCNs is also dependent on the cellular context and the patho/physiological condition [33].
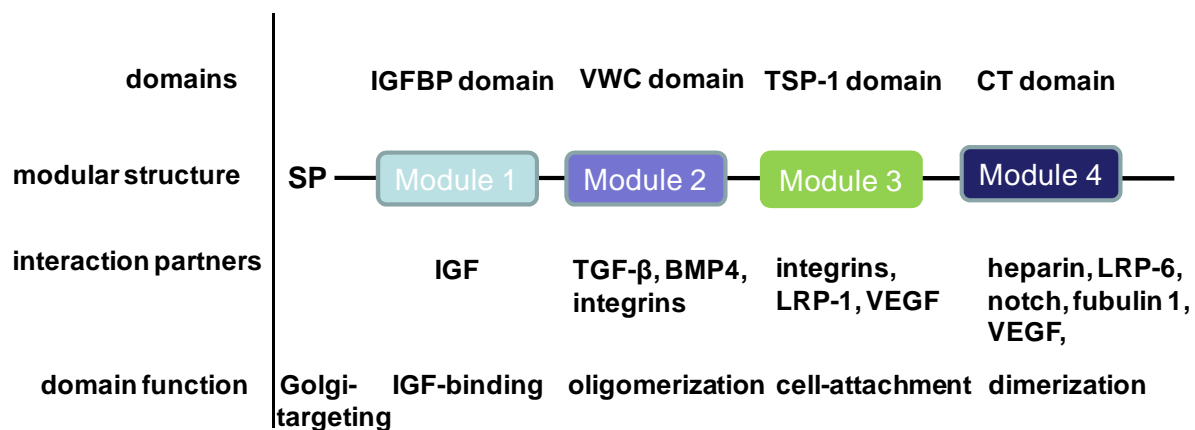
Fig.1-3 Representative structure of CCN proteins. VWC: von Willebrand factor type C, TSP-1: thrombospondin type 1 repeat, CT: carboxyl terminal end, SP: signal peptide, BMP: bone morphogenetic protein, LRP: low density lipoprotein receptor-related protein, VEGF: vascular endothelial cell growth factor, HSPG: heparan sulfate proteoglycans.

The multi-modular structure is the basis for a diverse set of putative CCN interactions and results in multiple CCN functions. Each module has its own biological role and can either act independently or in a cooperative manner with the other modules present in the same CCN protein. Of high interest is that CCN proteins are present in the extracellular milieu as they are secreted proteins. Using specialized transport vesicles, they are transferred to the membrane of the cell surface where they are released. On the other hand, CCN proteins can be internalize in an endocytotic way [34]. Modulation of the IGFBP domain for instance directly affects cell cycle progression or cell death [35]. The most common functions of the von Willebrand factor type C is the regulation of bone morphogenic proteins (BMPs) and transforming growth factor beta (TGF-β), thereby affecting cell adhesion or tissue remodeling [36]. The TSP-1 domain has a huge number of interaction partners such as collagen [37], fibronectin [38], and VEGF [39], affecting cell adhesion or modulating angiogenesis. Additionally, the TSP-1 domain binds to integrins [40] and this integrin binding has been thought to be important for CCN functions [41]. Furthermore, the CT domain of CCN proteins for instance regulates cell

differentiation through Notch1 [42] or binds to heparan sulfate proteoglycans (HSPGs) [43, 44] which are considered to act as a co-receptor for integrins. This complex forms the putative receptor for CCN proteins and mediates some of their functions. Upon binding of CCN ligands and activation of cell surface receptors, integrin–HSPG complexes induce further downstream events in the cytoplasm including activation of different kinases (e.g., MAP-kinases) and gene transcription [33, 41, 42, 44-47] (Fig.1-4).
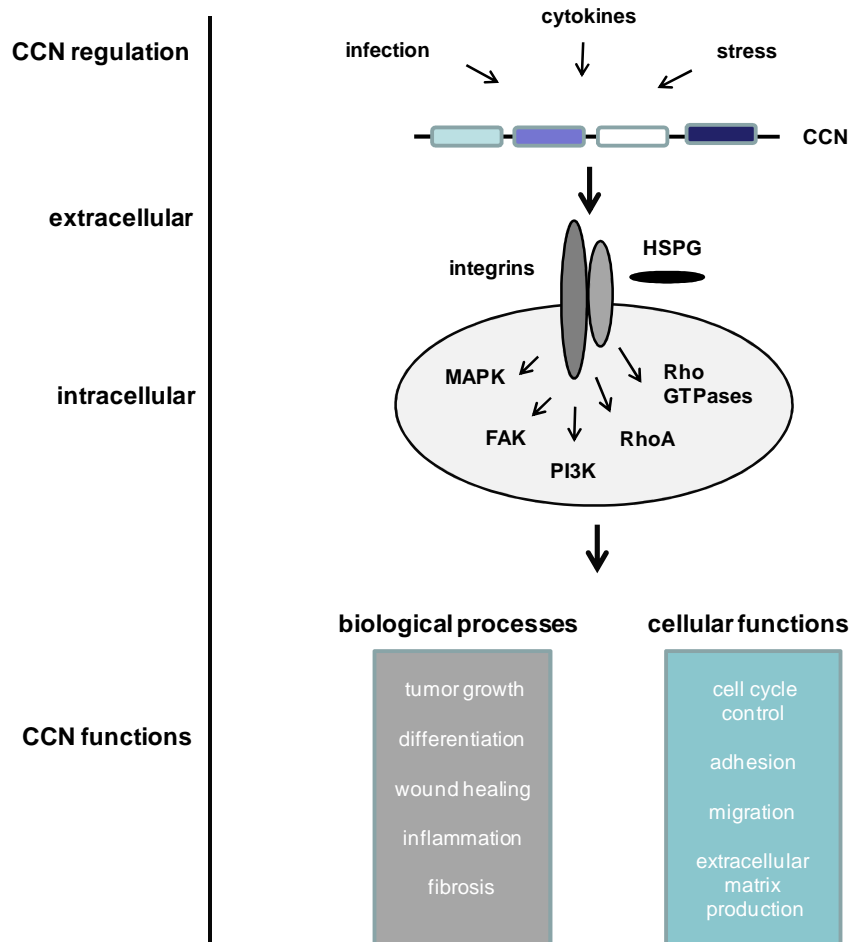
Fig. 1-4 Scheme of CCN protein regulation and function. HSPG: heparan sulfate proteoglycans, MAPK: mitogen-activated protein kinase, FAK: focal adhesion kinase; PI3K: phosphatidylinositol 3-kinase.

Thereby, one of the first functions awarded to CCN members was the deregulation of cell proliferation. Due to their multifunctional properties and expression in different types of cells and tissues, CCN proteins might be important molecules for the prognosis and diagnosis of HCC and may represent promising targets for therapy [29, 41, 48].

1.3 The Wnt-inducible signaling protein 1 (Wisp1/CCN4)

Wnt-inducible signaling protein 1 (Wisp1/CCN4) is a secreted, matricellular, cysteine-rich protein of the CCN family of proteins. It was first described in low metastas type melanoma in the mouse and called Elm1 (expressed in low-metastatic type 1 cells) [49]. Human Wisp1 was later discovered as a Wnt-induced downstream target in the mammary epithelial cell line C57MG [50]. Wisp1 is poorly investigated; very few studies exist which report the analysis of Wisp1 expression and function [51, 52] and those that do exist report on several organs, such as the heart, kidney, breast and lung [53-55]. In general, Wisp1 was found to be expressed during organ development, in diseases linked to fibrotic changes of tissues or organs and in cancer. Wisp1 expression was mainly linked to cell differentiation, proliferation, adhesion, migration and extracellular matrix production. However, the molecular mechanism of Wisp1 function is unclear. Until now, most reports describe PI3K/Akt dependent signaling as an intracellular effector of Wisp1 [53, 54], partially explaining the effect of Wisp1 on cell proliferation and survival. A signaling pathway whereby Wisp1 affects cancer development and metastasis formation has not been reported thus far. In contrast to other members of the CCN family, binding of Wisp1 to integrins has not been shown, however, binding to the soluble and matrix-associated dermatan sulfate proteoglycans, decorin and biglycan, has been described recently [56].

Since Wisp1 was first described as a downstream target of the Wnt signaling pathway [57], an important pathway frequently altered in human hepatocellular carcinoma [58], it is of particular interest to study its expression and function in normal, injured and diseased liver. Subsequently, Wisp1 is suggested to interact with cell-surface receptors, such as integrins [44] , Notch [50] and connexins [59, 60], comprising signaling pathways that play an important role in normal and injured liver [61, 62]. Wisp1 was described as a suppressor of metastasis [49]. Recently, Wisp1 has been found to be overexpressed in cholangiocarcinoma [63]. Using immunohistochemistry, expression of Wisp1 was not detected in normal liver but was detected in about 50% of cholangiocarcinoma tissues. In addition, Wisp1 expression was reported to be significantly associated with lymphatic and perineural invasion of tumor cells [63], an oncosuppressor gene in colorectal cancer [64] and overexpressed in scirrhous gastric carcinoma [59]. Thus, Wisp1 is described to have

either pro- or anti-cancerogenic effects. Recently, Wisp1 was observed to mediate cell signaling not only in an autocrine loop (overexpression resulted in morpholocial alterations of normal fibroblasts) [58], but also in a paracrine loop supporting tumorigenesis [58, 64]. Moreover, expression of Wisp1 and its alternative splice variants was described in different HCC cell lines [60] and in vivo in HCC [61]. A comprehensive approach toward the expression and function of Wisp1 in HCC is missing until now, but could provide helpful insights into one of the most malignant tumor types worldwide.

1.4 Aims of this study

Hepatocellular carcinoma is a malignant liver tumor with the ability to rapidly progress. Since therapeutic regimes for its treatment are limited, diagnosis and intervention at an early-stage is mandatory to improve prognosis.

The aim of the present study was to investigate whether the expression of Wisp1 is associated with different stages of HCC. To elucidate the underlying mechanisms, Wisp1 signaling was studied in human epithelial- and fibroblastoid-type HCC-derived cell lines. *In vivo*, I sought to determine characteristic features of Wisp1 expression during HCC progression which might help to identify early morphological and phenotype specific alterations of hepatocytes at early stages of HCC. *In vitro*, I investigated Wisp1 expression and secretion in HCC derived cell lines of different phenotypes to elucidate further the Wisp1 mechanism of signal transduction and its impact on proliferation and migration.

This study therefore aims to analyze Wisp1 to identify a new marker for early stages of HCC, allowing interventions at an early time point, and should provide evidence that Wisp1 drives cancer specific proliferation and migration.

2 Materials and methods

2.1 Equipment

Agarose chamber	PeqLab, Germany
Analytical balance BL310	Sartorius, Germany
Autoclave	NTAS, Germany
Blotting chamber	PeqLab, Germany
Electrophoresis chamber	Bio-Rad, USA
Cell Incubator, Hera cell	Kendro Laboratory Products, Germany
Centrifuge, Biofuge primo R	Heraeus, Germany
Confocal microscope	Leica, Germany
DMIRE2 confocal microscope	Leica, Germany
DC500 phase contrast/	
ELISA, Infinite Reader M200	Tecan, Germany
Flow cytometer, FACSCalibur	PeqLab, Germany
Fluorescent microscope	Leica, Germany
Hemocytometer	Hecht, Germany
Leica RM 2165 microtome	Leica, Germany
Laminar flow HA2472GS	Heraeus, Germany
Luminescent image analyser	PeqLab, Germany
Magnetic stirrer MR 3001K	Heraeus, Germany
Microwave	Sharp, Germany
MOS52 microscope	Leica, Germany
PCR-thermocycler	Bio-Rad, USA
Spectrometer, Gene Quant Pro	Amersham Bioscience, USA
Thermomixer compact	Eppendorf, Germany
UV transilluminator	NTAS, Germany
Vortexter Heidolph REAX top	Buddeberg, Germany
Water bath	VWR, Germany

2.2 Patients and tissue samples

HCC tissues and corresponding non-cancerous hepatic tissues were obtained with consent from 54 patients who had undergone curative hepatectomy for primary HCC in the Eastern Hepatobiliary Hospital of Second Military Medical University, Shanghai, China. All patients are exclusively Han Chinese. The study protocol was approved by the Ethical Committee of Eastern Hepatobiliary Hospital of Second Military Medical University and conducted in accordance with the official recommendations of the Chinese Community Guidelines. Complete clinical data were available in all cases. The diagnosis was determined according to the UICC TNM classification of primary liver cancer, 6th edition [65]. Immediately after hepatectomy, fresh tumors and non-cancerous hepatic tissues were partly snap-frozen in liquid nitrogen and stored at –80°C. They were partly embedded in freshly molten paraffin in an embedding box and poured paraffin blocks were stored at RT until further histological analysis (see 2.3/2.4).

2.3 Paraffin sectioning of human HCC tissue samples

Tissue of the paraffin blocks (see 2.2) was cut into serial sections of 4 μm thickness. Cuts were transferred to a water bath filled with 37°C dH$_2$O and fixed on poly-L-lysine coated slides. Slides were incubated for 1h at 60°C in an upright position to dry sections and ensure fixation. For further histological applications slides were stored at 4°C (see 2.4).

2.4 Immunohistochemistry

Buffers

Tab. 2-1 Composition of 1x PBS buffer.

	1 l
instamed PBS ddH$_2$O, add to 1 l	9.55 g

Tab. 2-2 Composition of Tris(hydroxymethyl)aminomethane (Tris), pH 7.6.

	MW [g/mol]	1 l	[c]
Tris ddH$_2$O, add to 1l, adjust pH with 1M HCl	121.14	6.057 g	50mM

Tab. 2-3 Antigen-retrieval solution, Ethylenediaminetetraacetic acid (EDTA), pH 8.4.

	MW [g/mol]	1 l	[c]
EDTA ddH$_2$0, add to 1l, adjust pH with 1M HCl	372.2	0.3722 g	1 mM

Tab. 2-4 Composition of 3,3'-diaminobenzidine tatrahydrochloride (DAB) stock solution.

	15 ml	[c]
DAB Tris(hydroxymethyl)aminomethane pH 7.6, add to 15ml	10 mg	0.07%

Tab. 2-5 Composition of DAB staining solution.

	stock	15 ml	[c]
DAB	0.07%	15 ml	0.07%
H$_2$O$_2$	30%	12 µl	0.024%

Reagents

Dual Enzyme Block	Dako, Germany
Xylene	Merck, Germany
Ethanol	Merck, Germany
Hematoxylin solution	Merck, Germany
Malinol	Waldeck GmbH, Germany
PBS	Biochrom, Germany
DAB	Sigma-Aldrich, Germany
Tris	Sigma-Aldrich, Germany
EDTA	Calbiochem, Germany

Background

Immunohistochemistry (IHC) is a method to localize antigens or proteins in tissue sections. Labelled antibody-antigen complexes are visualized by enzymes, fluorescent dyes or colloidal gold. In this study, IHC was used to understand the distribution and localization of Wisp1 in human hepatocellular carcinoma tissues.

Protocol

During the whole procedure, the human HCC tissue slides (see 2.3) were not allowed to dry at any time. Tissue slides were first deparaffinized in three washes of xylene for 5 min each. Rehydration was carried out with two washes of 100% EtOH for 5 min each, followed by one wash of 98% EtOH for 5 min. Afterwards tissue sections were washed 5 min in ddH$_2$O and in PBS. Antigen retrieval was performed by boiling tissue slides for 4 min in EDTA buffer (1 mM) followed by sub-boiling for 10 min (microwave setting 3). Slides were cooled for 30 min at room temperature (RT) and then incubated with dual Enzyme Block solution for 30 min at RT to minimize unspecific binding of the antibodies. After 30 min the blocking solution was removed and replaced by primary antibody solution (see Tab.8-2). The sections were incubated overnight at 4℃ in the primary antibodie s solution using a humidified box. Following overnight incubation, this step was prolonged for one additional hour at RT. Then, the primary antibody solutions were discarded and replaced by secondary antibody solutions (see 7.3.2) for 35 min at RT. Not or unspecifically bound secondary antibodies were removed by three consecutive washing steps in PBS for 5 min each. To visualize the antigen-antibody complexes, tissue slides were incubated for a maximum of 10 min with DAB staining solution. DAB is a substrate for the peroxidase linked secondary antibody used as a chromogen for the immunoperoxidase based staining. Finally, the reaction was stopped by washing the slides with PBS 2 times. Counterstaining of the nuclei with hematoxylin was done by incubating the DAB stained sections for 10 s in Hematoxylin solution, followed by washing with tap water for 5 min. Tissue sections were dehydrated by two washes of 100% EtOH for 15 s each and then cleared by incubation with three washes in xylene. Malinol, a nonaqueous mountant was used to embed the sections using glass-coverslips. The intensity of positive staining was graded from 0 to 3 (0, negative; 1, weak brown staining; 2, moderate brown staining; 3, very strong brown staining).

2.5 Cell culture

2.5.1   HCC cell line culture

Reagents

Cell culture reagents

DMEM medium   Biozol, Germany

Cell culture additives

Fetal bovine serum   Sigma-Aldrich, Germany

L-Glutamin (L-Glu), 200 mM   Cambrex , Belgium

Penicillin-Streptomycin (P/S), 100x   Cambrex , Belgium

Trypsin   PAA Laboratories, Austria

HBSS   PAA Laboratories, Austria

Tab. 2-6 Composition of DMEM complete medium for HCC cell lines.

DMEM	500 ml
FCS	50 ml
L-Glu	5 ml
P/S	5 ml

Tab. 2-7 Composition of DMEM serum-free medium for HCC cell lines.

DMEM	500 ml
L-Glu	5 ml

Background

Human HCC cell lines, FLC4, HLF, Heb3B and HCC-T have been described previously [66-69]. All HCC cell lines were a kind gift from Michael Kern (Institute of Pathology, Heidelberg, Germany). FLC4 cells were established from the human hepatocellular carcinoma cell line JHH-4. The JHH-4 cells were originally resected from a liver tumor (1988). FLC4 cells represent cells of epithelial- phenotype. FLC4 cells are known to have preserved liver functions, such as albumin synthesis, including hepatic enzyme activity that contributes to drug metabolism. In addition, they are well differentiated cells and express E-Cadherin. HLF cells were established

in vitro from the hepatocellular carcinoma of a 68 year old patient (1975). In contrast to FLC4 cells, HLF represents cells of fibroblastoid-phenotype, they are also poorly differentiated cells which show spindle shaped morphology and do not express albumin or E-Cadherin.

Protocol

HCC cells used in this study were cultured up to passage 10 in DMEM complete medium at 37°C in a humidified incubator (5% CO_2, 95% air). For experiments, cells were serum starved overnight. All stimulations were performed in DMEM serum free medium at a cell density of 60-80%.

2.5.2   Hek293T/17 cell culture

Reagents

Cell culture reagents

DMEM medium   Biozol, Germany

Cell culture additives

Fetal bovine serum   Sigma-Aldrich, Germany

L-Glutamin (L-Glu), 200 mM   Cambrex, Belgium

Penicillin-Streptomycin (P/S), 100x   Cambrex, Belgium

Trypsin   PAA Laboratories, Austria

HBSS   PAA Laboratories, Austria

Tab. 2-8 Composition of DMEM complete medium for Hek293T/17 cells.

DMEM	500 ml
FCS	50 ml
L-Glu	5 ml
P/S	5 ml

Tab. 2-9 Composition of DMEM serum-free medium for Hek293T/17 cells.

DMEM	500 ml
L-Glu	5 ml

Background

Hek293T/17 are a human embryonic kidney cell line with epithelial morphology, which was immortalized using adenoviral DNA. These cells contain the SV-40 large T-antigen for an efficient replication of plasmids useful for many transfection experiments [70].

Protocol

In this work Hek293T/17 were used for lentiviral production. They were cultured in complete DMEM medium and, split two times a week at a ratio of 1:4 using trypsin. Frequent passages kept the Hek293T/17 as individual cells to ensure high transfection efficiencies (see 2.22).

2.5.3   HT1080 cell culture

Reagents

Cell culture reagents

RPMI medium   Biozol, Germany

Cell culture additives

Fetal bovine serum	Sigma-Aldrich, Germany
L-Glutamin (L-Glu), 200 mM	Cambrex, Belgium
Penicillin-Streptomycin (P/S), 100x	Cambrex, Belgium
Trypsin	PAA Laboratories, Austria
HBSS	PAA Laboratories, Austria

Tab. 2-10 Composition of RPMI complete medium for HT1080 cell line.

RPMI	**500 ml**
FCS	**50 ml**
L-Glu	**5 ml**
P/S	**5 ml**

Background

The human fibrosarcoma cell line HT1080 (American Type Culture Collection, Rockville, MD) was established from a 35 year old patient. Cells were used in this study as transducer cells to determine lentiviral titers (see 2.22).

Protocol

HT1080 were cultured in RPMI complete medium. They were split one time per week at a ratio of 1:10 using trypsin. Lentiviral transfection was carried out in complete RPMI medium (see 2.22).

2.6 Protein isolation of cultured cells

Buffers

Tab. 2-11 Composition of 1x Ripa Protein Lysate buffer, stock solution.

	MW [g/mol]	300 ml	[c]
Tris	121.14	1.815 g	50 mM
NaCl	58.44	4.383 g	250 mM
Nonident P40	100%	6 ml	2%
EDTA	372.2	0.279 g	2.5 ml
sodium dodecyl sulfate (SDS)	288.38	0.3 g	0.1%
DOC(Deoxycholic acid Na-salt)	392.57	1.6 g	0.5%
ddH$_2$O, add to 300 ml, adjust pH 7.2 with 1 M HCl			

Tab. 2-12 Composition of 1x Ripa Protein Lysate buffer, pre-working solution

1x Ripa Protein Lysate buffer	50 ml
Complete protease inhibitor cocktail tablets	1 x

Reagents

HBSS   PAA, Germany

Complete protease inhibitor cocktail tablets   Roche, Germany

Phosphatase inhibitor cocktail 2   Sigma Aldrich, Germany

Protocol

Medium of cultured cells was aspirated and cells were washed twice with HBSS. Cells were lysed with ice-cold Ripa buffer (Tab.2-12) supplemented with phosphatase inhibitor cocktail 2 (1:100). For 6 well plates, 120 µl Ripa was used and, for 12 well plates 60 µl of Ripa buffer. Cells were further shaken for 20 min on ice. The cell lysate was disrupted by force using a cell scratcher. Cell lysates were collected in 1.5 ml tubes and centrifuged for 20 min at 13.000 rpm. The supernatant was collected and protein concentration was determined (see 2.7)

2.7 Protein quantification

Kits

Biorad protein assay kit (500-0113, 500-0114, 500-0115)   Biorad, Germany

D_c Assay reagent A, alkaline copper tartrate

D_c Assay reagent B, folin reagent

D_c Assay reagent S, surfactant solution for colorimetric assays

Reagents

Bovine serum albumin (BSA) standard solutions (in PBS): 1 µg/ml, 2 µg/ml, 4 µg/ml, 6 µg/ml, 8 µg/ml, 10 µg/ml

Background

Protein quantification according to the Lowry method is a colorimetric assay to determine the total amount of protein in a solution. The Lowry assay is based on reduced copper ions in alkaline solution, which reduce the folin-ciocalteau-reagent by the oxidation of peptide bonds. The reduced folin reagent can be measured by spectrophotometry.

In this study, a modified Lowry assay was used to determine the amount of isolated proteins from HCC cell lines (see 2.5.1) for subsequent Western blot analysis (see 2.8).

Protocol

2 µl of protein lysate, BSA standards and blank value ddH$_2$O were mixed with 20 µl of Assay reagent A and S (10:1) and immediately incubated with 200 µl of Assay reagent B. Reaction mixtures turned slightly blue within 15 min incubation at RT. Absorbance was measured at a wavelength of 690 nm. Total protein concentration was calculated by a BSA standard curve (BSA concentration against absorbance values).

2.8 Western blot analysis

Buffers

Tab. 2-13 Composition of 1M Tris-HCl, pH 8.8/ 6.8.

	MW [g/mol]	1 l	[c]
Tris ddH$_2$O, adjust to 1 l, adjust pH with 1 M HCl	121.14	121.14 g	1 M

Tab. 2-14 Composition of 10% Sodium dodecyl sulfate solution.

Sodium dodecyl sulfate ddH$_2$O, adjust to 100 ml	10 g

Tab. 2-15 Composition of separating gels for Western blot.

	10%	12%
Acrylamide/bisacrylamide solution 5:1	2.5 ml	1.8 ml
1 M Tris-HCl, pH 8.8	1.6 ml	1.4 ml
ddH$_2$O	2.2 ml	2.3 ml
10% sodium dodecyl sulfate solution (SDS)	66.7 µl	56 µl
N,N,N',N'-tetramethylethylenediamine (TEMED)	3.2 µl	2.8 µl
10x ammonium persulfate (APS)	32.5 µl	28 µl

Tab. 2-16. Composition of stacking gel for Western blot.

	4%
Acrylamide/bisacrylamide solution 5:1	0.3 ml
1 M Tris-HCl, pH 6.8	0.5 ml
ddH$_2$O	1.1 ml
10% sodium dodecyl sulfate solution (SDS)	19.1 µl
N,N,N',N'-tetramethylethylenediamine (TEMED)	1.9 µl
10% ammonium persulfate (APS)	9.4 µl

Tab. 2-17 Composition of 10x Lämmli electrophoresis buffer.

	MW [g/mol]	**1 l**	**[c]**
Tris	121.14	30,34 g	250 mM
Glycine	75.07	144 g	1,92 M
10% sodium dodecyl sulfate solution (SDS)		100 ml	1%
ddH$_2$O, add to 1 l			

Tab. 2-18 Composition of Transfer buffer.

	MW [g/mol]	**1 l**	**[c]**
Methanol	100%	200 ml	20%
Nupage® Transfer Buffer	20x	50 ml	1x
ddH$_2$O, add to 1 l			

Tab. 2-19. Composition of 10x TBS.

	MW [g/mol]	**1 l**	**[c]**
Tris	121.14	12.1 g	100 mM
NaCl	58.44	87,66 g	1.5 M
ddH$_2$O, add to 1 l, adjust pH 7.8 with 1 M HCl			

Tab. 2-20 Composition of 1x TBST (0.1% Tween).

10x TBS	100 ml
Tween®20	10 ml
ddH$_2$O, add to 1 l	

Tab. 2-21 Composition of 0.1 M Tris, pH 8.5.

	MW [g/mol]	1 l	[c]
Tris	121.14	12.1 g	100 mM
ddH$_2$O, add to 1 l, adjust pH with 1 M HCl			

Tab. 2-22 Composition of 1x TBST blocking solution (5% milk powder).

1x TBST	50 ml
Milk powder	2.5 g

Tab. 2-23 Composition of ECL Western blotting detection reagent A.

0.1 M Tris, pH 8.5	5 ml
Hydrogen peroxide solution, 30%	3 µl

Tab. 2-24 Composition of ECL Western blotting detection reagent B.

0.1M Tris, pH 8.5	5 ml
p-Coumaric acid	22 µl
Luminol (3 -aminophtolhydrazide)	50 µl

Reagents

Molecular weight standard:

Prestained Protein Ladder	Fermentas, Germany
Loading Buffer	Invitrogen, Germany
p-Coumaric acid	Sigma-Aldrich, Germany
Luminol (3-aminophtolhydrazide)	Sigma-Aldrich, Germany
Hydrogen peroxide	Sigma-Aldrich, Germany
Nitrocellulose membrane	Whatman, Germany
Ponceau S solution	Sigma-Aldrich, Germany
Nupage®Transfer Buffer	Invitrogen, Germany

Filter paper   Whatman, Germany

Background

Western blot analysis is a method to detect specific proteins in a complex protein mixture. The proteins are separated dependent on their size by gel electrophoresis and then transferred to a nitrocellulose membrane where they can be visualized by specific antibody-antigen reactions.

In this study, Western blot was performed to detect Wisp1 expression, secretion and putative components involved in its cellular signaling pathways (see 3.3/3.5/3.6).

Protocol

A protein amount of 20-35 µg was diluted in 4 x Loading Buffer (LB) to a final concentration of 1 x LB in 50 mM DTT. Samples were adjusted with ddH_2O to a final volume of 40 µl. Samples were vortexted for a few seconds and incubated for 10 min at 99℃. Next, the samples are spun down by centrifugation at 10.000 rpm for 5 min. The protein samples were loaded together with 2 µl Prestained Protein Ladder into the gel pockets of a self-poured SDS gel. Proteins were separated by electrophoresis at 60 V for 5 h using 1x Lämmli as running buffer. Then, the proteins were transferred from the gel to a nitrocellulose membrane in ice cold Transfer Buffer. Therefore, wet transfer chambers were filled with wet filter paper, sponges, gel and the membrane and fixed between the electrodes. From anode to cathode the setup of the blotting sandwich was as follows: 2 sponges, 3 sheets of filter paper, gel, nitrocellulose membrane, 3 sheets of filter paper, and 2 sponges. Importantly, attention was given to air bubbles, which were not allowed to be inside the blotting sandwich. The transfer of the proteins was performed at 40 mA per gel for 16 h. After blotting, unspecific binding of antibody was prevented by blocking the membrane in blocking solution for 3 washes of 10 min each. The membrane was then incubated in primary antibody dilutions (see Tab.8-2) overnight at 4℃ on an overhead shaker. The next day, the membrane was washed 3 times in TBST blocking solution for 10 min each and, then incubated in secondary antibody-HRP dilutions (see Tab.8-3) in TBST for 2 h at RT. The antigen/antibody complex was visualized using enhanced chemiluminescent (ECL) reaction of Luminol and p-coumaric acid, catalysed by peroxide. The antigen chemiluminescence emission of light was scanned on a CCD camera.

2.9 Assessment of Wisp1 concentration by calibration

To determine the concentration of Wisp1 necessary to treat HCC cells in cell culture, we needed to identify the level of Wisp1 which is expressed in these HCC cell lines (see 2.5.1) naturally during the time of culture. These cell lines were cultured for a day (when low Wisp1 expression was detected) up to 3 days (when both cell lines, FLC4 and HLF, express higher levels of Wisp1). Cell lysates were harvested (see. 2.6) and the concentration of Wisp1 was estimated using an exact amount of recombinant Wisp1 protein as calibrator. In detail, HCC cell lines were seeded in 6 well plates (350.000 cells/well) and harvested at day 1, 2 and 3. 1/20 of total harvested protein lysate and calibrator (25 and 100 ng/ml recombinant Wisp1 protein) were resolved with SDS PAGE and immunobloted. Immunoblots were quantified with the AIDA Image Analyzer 2.11 software and related to total number of seeded cells. We estimated that FLC4 cells expressed at day 3 85.4 ng of Wisp1 and HLF cells expressed 73.2 ng. Therefore, for this study, a concentration of 100 ng/ml Wisp1 was chosen to treat respective amount of cells at day 1 to simulate natural concentration of Wisp1 which might be found in HCC.

2.10 Quantitative recovery of proteins from diluted solutions using acetone

Reagents

Acetone   Merck, Germany

Protocol

Protein precipitation is a technique to concentrate proteins from a diluted protein mixture or solutions.

In this study, precipitations were performed to detect secreted Wisp1 in conditioned media of HCC cells (see 3.3).

HCC cell lines were grown in 6-well plates in 2 ml of serum free medium. After 1, 2 and 3 days conditioned medium was harvested and mixed with ice cold acetone (1:4). Precipitation was performed overnight at -20℃. Precipitate was spun down for

20 min at 13.000 rpm (Technical Resource, Pierce Biotechnology, Acetone Precipitation of Proteins). The precipitated pellet was dried at RT for 4 h and further resolved on SDS PAGE, transferred to a nitrocellulose membrane and immunoblotted for detection of Wisp1 as described (see 2.8).

2.11 mRNA Isolation, RNA electrophoresis and reverse transcription

Kit

RNeasy QuantiTect Reverse Transcription kit   Qiagen,Germany
(Cat.No. 205314)

Tab. 2-25 RNeasy QuantiTect Reverse Transcription kit.

	stock	20 µl
Reverse transcriptase	10	1 µl
Primer Mix	10	1 µl
RT buffer	5x	4 µl
gDNA wipeout buffer 7x	10 mM	2 µl
RNA		1 µg
ddH$_2$O		add to 20 µl

Buffers

Tab. 2-26 Composition of DEPC water.

	stock	1 l	[c]
DEPC ddH$_2$O, add to 1 l, incubate 12 h at 37℃, autoclave	100%	1 ml	1%

Tab. 2-27 Composition of 20x MOPS running buffer.

	MW [g/mol]	**1 l**	**[c]**
Sodium acetate (NAOAc)	82.03	8.20g	0.1 M
EDTA	372.2	7.45g	20 mM
MOPS	209.26	83.72 g	0.4 M
DEPC water, add to 1 l, incubate 12 h at 37℃, autoclave			

Tab. 2-28 Composition of RNA Loading buffer.

	stock	**12 ml**	**[c]**
MOPS	20x	8.20g	1x
Formamide	100%	6 ml	50%
Formaldehyde	209.26	2.14 ml	2.2 mM
Ficol solution	100%	1,2 ml	10%
Bromphenol blue	669.96 g/mol	1.2 mg	0.15 mM
DEPC water, add to 12 ml			

Reagents

EtOH	Merck, Germany
β-mercapthoethanol	AppliChem, Germany
Agarose	Serva, Germany
Formaldehyde	Merck, Germany
Ethidium bromide solution (10 mg/ml)	AppliChem, Germany
DNA Ladder (100 bp, 1kb)	AppliChem, Germany

Background

RNA isolation is a technique to purify RNA from biological samples. The quantity and integrity of the purified RNA can be determined by gel electrophoresis. For the

reverse transcription of single-stranded mRNA into complimentary DNA (cDNA) the enzyme reverse transcriptase from Qiagen was used.

In this work, total RNA was extracted from cells using the RNeasy kit according to the manufacture's instructions.

Protocol

RNA was isolated from cells grown in 6-well plates. Lysates were obtained by adding 300 µl RLT buffer containing β-mercapthoethanol (100:1). Homogenization was carried with a syringe and needle followed by the addition of 70% ethanol (300 µl) to generate appropriate binding conditions of RNA to the RNeasy spin column membrane. The homogenates were added onto RNA binding spin columns containing silica membranes that selectively bind RNA. After 1 wash using RW1 buffer and centrifugation at 10.000 rpm for 15 s and 2 washes using RPE buffer and centrifugation for 15 s at 10.000 rpm, the isolated RNA was eluted in 35 µl DEPC water. RNA concentration was photometric determined by measuring the RNA solution at 260 nm in a quartz cuvette using a spectrometer before the integrity was analyzed by electrophoresis. Agarose (1.5%) was dissolved in 25 ml ddH$_2$O, boiled in a microwave and placed on a magnetic stirrer. 5 ml of 10x MOPS buffer and 4 ml formaldehyde was added. Ethidium bromide (EtBr) was dissolved in the mixture to a final concentration of 500 ng/ml to visualize the RNA. The gel mixture was poured into a gel chamber and cooled until the mass solidified. 200 ng of isolated RNA was mixed with 15 µl Loading buffer, heated for 10 min at 68 ℃ and separated on the gel for 1 h at 60 V to prove quantity. RNA samples were visualized on a UV transilluminator. cDNA was generated from 1 µg total RNA for further semiquantitative PCR analysis. The reverse transcription reaction was performed upon DNA wipeout using dDNA buffer. DNA-free RNA was then heated for 2 min at 42℃ before primers, buffer and reverse transcripta se (see Tab.2-5) were added. cDNA synthesis was performed for 1h at 42℃. The re action was stopped by inactivation of the reverse transcriptase at 94℃ f or 5 min. For PCR analysis samples were diluted in ddH$_2$O (1:4) (see 2.12).

2.12 Polymerase chain reaction

Kit

FastStart Taq DNA Polymerase Kit Qiagen, Germany

Tab. 2-29 Standard PCR reaction mixture.

	stock	10 µl
Primer forward	10 pM	0.25 µl
Primer reverse	10 pM	0.25 µl
PCR buffer	10x	1 µl
dNTPs	10 mM	0.2 µl
Taq DNA polymerase	5 U/µl	0.05 µl
ddH$_2$O		7.5 µl
cDNA		100 ng/ml

Background

The Polymerase chain reaction (PCR) is a method to amplify copies of a specific DNA sequence. A PCR mixture contains the DNA template for amplification, primers which bind specifically to sequences present in the DNA fragment, deoxynucleoside triphosphates (dNTPs) as basis for new DNA strands, DNA polymerase for amplification and a buffer solution to guarantee an environment suitable for DNA amplification. PCR is a thermal cycling process which starts with the denaturation of the DNA causing double-stranded DNA to separate into two single-stranded DNA chains. During the annealing time the primers bind specifically to the DNA. During the elongation step the DNA polymerase catalyses the synthesis of new DNA strands by adding dNTPs complementary to the template DNA. Standard conditions for amplification were varied depending on the size of the amplified DNA fragment.

Protocol

cDNA was mixed with PCR buffer, dNTPs, Taq DNA polymerase and ddH$_2$O according to Tab. 2-29 in a 200 µl PCR reaction tube. PCR reaction was carried out in a PCR thermocycler (Tab. 2-30).

Tab. 2-30 Standard program for DNA amplification.

Initial denaturation	2 min, 95℃
Denaturation	30 sec, 95℃
Annealing	30 sec, 95℃
Elongation	1 min , 72℃
Final Elongation	4 min, 72℃

x35 (Denaturation, Annealing, Elongation)

2.13 Agarose gel electrophoresis

Buffers

Tab. 2-31 Composition of 10x TBE gel buffer, pH 8.0.

	MW [g/mol]	1 l	[c]
Tris	121.14	108 g	0.9 M
Na$_2$EDTA	372.2	7.45 g	20 mM
Boric acid	61.38	55 g	0.9 M
ddH$_2$O, add to 1l, adjust pH with 1 M HCl			

Tab. 2-32 Composition of 10x Agarose loading buffer.

	MW [g/mol]	stock	30 ml	[c]
Glycerol		85%	20 ml	35%
Bromphenol blue	691.94		0.05 g	2.5 mM

Reagents

Agarose   Serva, Germany

Ethidium bromide solution

(10 mg/ml)   AppliChem, Germany

DNA Ladder (100 bp, 1kb)   AppliChem, Germany

Background

Agarose gel electrophoresis is a method to separate and visualize DNA of different size by applying an electric field. Nucleic acid molecules are separated by size since the negatively charged DNA migrates through an agarose matrix towards the positive electrode. The DNA within the agarose is visualized using Ethidium bromide (EtBr).

EtBr is fluorescent dye that intercalates into DNA and the resulting complex is detectable using ultraviolet light.

In this study, agarose gel electrophoresis was used to detect and quantify the expression of RT-PCR products (see 3.3/ 3.4 /3.7) of Wisp1, different cell cycle markers and migration factors.

Protocol

PCR samples were diluted in loading buffer, mixed, spun down for a few seconds and loaded together with DNA ladder on agarose gels (1-2%). Agarose was dissolved in 1x TBE gel buffer, mixed and boiled in a microwave. Ethidium bromide was added to a final concentration of 500 ng/ml, the gel solution was poured into gel chambers and cooled until it formed a gel. Gel electrophoresis was performed in 1x TBE running buffer at 90 V for 30 to 50 min to detect DNA fragments. PCR samples were visualized on a UV transilluminator.

2.14 Phase contrast and fluorescence microscopy

Phase contrast and conventional epi-fluorescence images were obtained with a Leica IPB microscope equipped with a Leica DC500 camera. For conventional epi-fluorescent images, excitation was performed with an EQB 100 isolated fluorescent lamp. Image acquisition was done with Leica IM50 software.

2.15 Immunofluorescence of FLC4 cells and laser-scanning confocal microscopy

Buffers

Tab. 2-33 Composition of 1xPBS buffer.

	1 l
instamed PBS	9.55 g
ddH$_2$O, add to 1l	

Tab. 2-34 Composition of Permeabilization solution.

	50 ml	**[c]**
Triton-X-100	0.15 ml	0.3%
BSA	0.5 g	1%
1x PBS, add to 50 ml		

Tab. 2-35 Composition of Blocking solution.

	50 ml	**[c]**
BSA	0.5 g	1%
1x PBS, add to 50ml		

Tab. 2-36 Composition of Antibody dilution solution.

	50 ml	**[c]**
BSA	0.05 g	0.1%
1xPBS, add to 50ml		

Reagents

Histofix (4% PFA)	Roth, Germany
Draq5®	Alexis Biochemicals, Germany
DakoCytomation®	
Fluorescent Mounting Medium	Dako Cytomation, Germany

Background

Immunofluorescent staining is a technique to visualize the distribution of target molecules, i.e., proteins (antigens) within a cell by specific fluorescent dyes coupled to the specific antibodies that allow formation of antigen-antibody complexes. Immunofluorescent staining can further be analysed, e.g., with laser-scanning confocal microscopy (LSM), which is an imaging technique that enables the detection of fluorescent dyes in thin optical slices.

In this study immunofluorescent stainings and confocal microscopy techniques were performed to investigate expression and localization of E-Cadherin in HCC cell lines.

Protocol

HCC cells were seeded into 24 well plates (75.000 cells/ well) on glass cover slipes, serum starved overnight and followed by respective treatment. To prepare the FLC4 cells for staining, they were washed two times with PBS and fixed for 10 min at RT with 400 µl Histofix solution, followed by permeabilization using 200 µl of Triton-X solution for 5 min at RT. After two additional washing steps with PBS, unspecific binding of the antibodies was blocked by treating the cells with BSA blocking solution for 1 h at RT. After discarding the blocking buffer, primary antibody solutions (see Tab.8-2) were applied overnight at 4℃. A second washing step was performed the next day by using the BSA blocking solution for an additional 20 min, followed by an incubation of the cells with secondary antibody solutions (see Tab.8-3) for 3 h at RT. Finally, the nuclei were stained with Draq5® for 30 min. Cells were mounted on glass slides using DakoCytomation® Fluorescent Mounting Medium and stored at 4℃. Confocal images were obtained by a laser spectral confocal microscope with an oil objective. The argon laser emitted at 488 nm, the krypton laser emitted at 568 nm and the helium/neon laser at 633 nm. The obtained images were acquired with a TCS SP2 scanner and the Leica Confocal software (vers.2.5).

2.16 Scratch wound healing assay

Background

The scratch wound healing assay is a method to study cell motility. A scratch, simulating an injury within a confluent seeded cell layer is analyzed on an image-based readout.

In this study, the scratch wound healing assay was used to determine migratory activity of HCC cells upon Wisp1 stimulus.

Protocol

HCC cell lines (see 2.5.1) were seeded in 6 well plates at a density of 85% and allowed to adhere for 5 h. Then, the medium was changed to serum free DMEM overnight. At day 1 (100% confluent) the cell layer was injured with a 200 µl pipette tip. Immediately after injury, one washing step with HBSS was performed before the cells were left either untreated or treated with Wisp1 (100 ng/ml) in 1 ml serum free DMEM. Photographs of the scratch area were taken after 4, 6, 8, 10 and 24 h at the same position of the wound using a Leica DM IRB Inverted Research Microscope. The images were analyzed with Leica QWin Vers.3 software. The area of the scratch of each picture was selected manually an the marked area was further determined using the area calculator to get the size of the scratch at each timepoint.

2.17 HCC in vitro adhesion assay

Background

With the cell adhesion assay cell contacts between cells and the dish were studied in the presence or absence of Wisp1.

Protocol

Adhesion assays were performed by seeding HCC cells into 6 well plates. The test cells were serum starved overnight and then trypsinized for 10 min. The detached cells were collected in serum free DMEM medium and sedimented by centrifugation

for 12 min at 600 x g using a swing out rotor. The supernatant was discarded, whereas the pellet containing the cells was resuspended in 1 ml serum free DMEM medium. Then cells (300.000 cells/ml) were either seeded in FCS containing DMEM medium (see 2.5.1), serum free DMEM medium or serum free DMEM medium containing Wisp1 (100 ng/ml). These cell solutions were plated in duplicates into 6 well plates. Pictures were taken 30, 60, 90, 120, 150, 180, 210 and 240 min after plating on a Leica DM IRB Inverted Research Microscope. The percentage of attached cells was obtained by counting the total number of cells and the number of cells that had already attached.

2.18 Cell proliferation assay

Kits

BrdU incorporation assay (Cat.No.11647229001)   Roche, Germany
BrdU labelling reagent (5-bromo-2'-deoxyuridine in PBS)
FixDenat solution
Anti-BrdU-POD (monoclonal antibody from mouse-mouse hybrid cells, conjugated with peroxidase (POD))
Antibody-dilution solution
Washing buffer (10x PBS)
Substrate solution (TMB, tetramethyl-benzidine)

Reagents

Mitomycin C   AppliChem, Germany

Background

The 5-bromo-2'-deoxy-uridine (BrdU) incorporation assay is a method to quantify DNA synthesis during cell proliferation. BrdU is a tymidine analog, which can be incorporated into the newly synthesized DNA. Following immunodetection via specific antibodies the BrdU labelled cells can be visualized.

In this work, the BrdU incorporation assay was performed to investigate DNA synthesis kinetics of HCC cell lines in response to Wisp1 stimulation.

Protocol

The BrdU assay was performed according to manufacturer's instructions. Cell cycle synchronization was induced by serum deprivation for 24 h before the respective treatment followed. 2 h before the treatment started, control HCC cells were preincubated with mitomycin C (5 µg/ml). Cells then were either treated with serum free medium, FCS containing medium, serum free medium containing Wisp1 (100 ng/ml) or mitomycin C (5 µg/ml). Treatment was carried out for 8 h or 16 h. 2 h after the start of treatment 100 µl BrdU labelling substance was added to the culture medium. For BrdU staining, the medium was aspirated and the cells were fixed; the DNA was denatured in one step by adding 100 µl FixDenat solution for 1 h at RT. Denaturation ensures the accessibility of the incorporated BrdU for further antibody detection. Cells were afterwards incubated with the anti-BrdU-antibody (1:100 in Antibody Dilution Solution) for 2 h at RT. Cells were then washed 3 times with PBS and incubated with 100 µl of the calorimetric substrate for 30 min. The reaction product was quantified by measuring the absorbance at 370 nm with a reference wavelength of 492 nm using a scanning multi-well spectrometer (ELISA reader). The developed blue color of the reaction could be directly correlated to the amount of DNA synthesis. Experiments were done in triplicate. Data are presented as an average with SD.

2.19 Dose response curve and antibiotic selection of HCC populations transfected with Puromycin or Neomycin

Reagents

Tab. 2-37 Puromycin stock solution.

	100 ml	**[c]**
Puromycin	5 g	50 mg/ml
ddH$_2$O, add to 100 ml, sterile		

Tab. 2-38 Neomycin stock solution.

	100 ml	**[c]**
Neomycin	5 g	50 mg/ml
ddH$_2$O, add to 100 ml, sterile		

Background

Antibiotic dose response curves determine cell toxicity when they are exposed to different concentrations of an antibiotic. Here, Puromycin and Neomycin dose response curves were performed to first, determine cell toxicity in HCC cell lines and second, to select for cells which contain the resistance gene.

Protocol

HCC cells (60-80% confluent) were seeded in 24 well plates and on day two exposed to a range of concentrations of the respective antibiotics. Viability of cells was examined every two days and new DMEM medium containing fresh antibiotics was added. Cells were cultured up to 14 days. The lowest concentration of antibiotic that killed 100% of the cells in 14 days from the start of antibiotic selection was further used (see 2.22)

2.20 Bacterial culture

Buffers

Tab. 2-39 Composition of LB (lysogeny broth*)* medium.

	1 l
instamed LB	25 g
ddH$_2$O, add to 1 l, autoclave	

Tab. 2-40 Puromycin stock solution.

	100 ml	**[c]**
Puromycin ddH$_2$O, add to 100 ml, sterile	5 g	50 mg/ml

Tab. 2-41 Ampicillin stock solution.

	100 ml	**[c]**
Ampicillin ddH$_2$O, add to 100 ml, sterile	5 g	50 mg/ml

Reagents

Agar	Life Technologies, Germany
LB	Fisher Scientific, Germany
pLKO.1-puro-CMV-TurboGFP	
TRCN0000033350 and	
TRCN0000033351	Sigma Aldrich, Germany
pLKO.1-puro UbC-TurboGFP	Sigma Aldrich, Germany
pCMV 891	Sigma Aldrich, Germany
pMDG	Sigma Aldrich, Germany
pcDNA3.1+ containing	
full length Wisp1	Kind gift from Dr. M. Young (Department of Health & Human Service, Maryland, USA)
One Shot TOP10 Chemically	
Competent E.coli	Invitrogen, Germany

Background

Competent cell bacteria can take up a plasmid which includes a foreign gene. Further, bacteria containing the plasmid are selected using agar plates containing an antibiotic.

In this study, *E.coli* bacterial culture was used for the transformation of plasmids containing shWisp1 constructs or full-length Wisp1.

Protocol

For agar plates, 7.5 g instamed LB and 6 g agar were dissolved in 300 ml ddH$_2$O. The solution was autoclaved and then cooled down to 40℃ before the antibiotic (Puromycin or Ampicillin) was added (60 µg/ml). The solution was poured into Petri dishes and allowed to cool at RT for 30 min. Agar plates were closed, sealed with parafilm and stored at 4℃.

Bacteria (50 µl) were thawed on ice for 30 min. 2 µl of plasmid was added onto the top of the bacteria and incubated on ice for an additional 30 min. Afterwards, bacteria were briefly heat shocked at 42℃ for 1 min, transferred to ice for an additional 5 min and mixed with 150 µl 37℃ warm LB medium and incubated at 37℃ for 45 min at 300 rpm. The bacteria solution was plated out on an antibiotic (Puromycin or Ampicillin) containing agar plates. The agar plates whereas incubated overnight at 37℃ to allow the bacteria to grow which express the antibiotic resistant gene. The agar plates were stored until further use at 4℃ (see 2.21).

2.21 Plasmid purification

Kit

EndoFree® Plasmid Purification Kit (Cat.No. 12362)   Qiagen, Germany

Buffer P1, alkaline buffer 1

Buffer P2, alkaline buffer 2

Buffer P3, precipitating buffer

Buffer QBT, equilibrating buffer

Buffer QC, washing buffer

Buffer QN, DNA eluting buffer

Buffer ER, DNA eluting buffer

Buffer TE, Tris- EDTA buffer

Endoxin-free water

LyseBlue, indicator

Qiagen syring

Qiagen column

Buffers

Tab. 2-42 Composition of LB (lysogeny broth*)* medium.

	1 l
instamed LB	25 g
ddH$_2$O, add to 1 l, autoclave	

Reagents

Agar   Life Technologies, Germany

LB   Fisher Scientific, Germany

Isopropanol Merck, Germany

Background

Based on the alkaline lysis, plasmid DNA is isolated from bacteria. Bacteria containing the plasmid of interest are lysed by a strong alkaline buffer, followed by binding of the plasmid DNA to an anion-exchange resin under low-salt conditions. RNA, proteins and low molecular weight impurities are removed by a medium-salt wash. The plasmid DNA is eluted in a high-salt buffer, concentrated and desalted by isopropanol precipitation.

In this study plasmid purification was used to extract and purify shWisp1 containing vectors and full-length Wisp1 containing vectors (see 2.22).

Protocol

A single colony was picked from an agar plate (see 2.20), placed in 250 ml LB medium containing the selective antibiotic and incubated overnight at 37℃ with shaking at 300 rpm. The next day, the bacterial cells were harvested by centrifugation at 6.000 x g for 15 min at 4℃. The bacterial pellet was resuspended in 25 ml ice cold Buffer P1 containing LyseBlue reagent, an indicator which provides optimal buffer mixing. For efficient lysis of the bacteria the buffer was pipetted up and down until no clumps were visible. 25 ml of Buffer P2 were added and mixed for 5 min by inverting the mixture at RT until the cell suspension turned blue. 25 ml of chilled P3 Buffer was immediately added to the suspension; fluffy, white material appeared containing genomic DNA, proteins and cell debris. The suspension was filtrated using the syringe. 2.5 ml of ER Buffer were added to the clear suspension,

inverted and incubated for 30 min on ice. The column was equilibrated by adding 20 ml of QBT buffer which emptied from the column by gravity. The filtrated lysate was added onto the column followed by two washes with 30 ml of QC Buffer. The DNA was eluted in 15 ml of QN Buffer and precipitated with 0.7 ml volumes of isopropanol. The solution was centrifuged at 15.000 x g for 30 min at 4°C and the supernatant decanted. The DNA pellet was washed with 5 ml of endotoxin-free 70% ethanol and centrifuged at 15.000 x g for 10 min. The supernatant was decanted and the pellet was air-dried for approximately 1h. The DNA was dissolved in 0.5 ml TE Buffer. The DNA concentration was determined by spectrometry at 260 nm.

.

2.22 Lentivirus production and transfection

Buffers

Tab. 2-43 Composition of Na-butyrate stock solution.

	MW [g/mol]	100 ml	[c]
Na-butyrate HBSS, add to 100 ml	110.09	11 g	1 M

Tab. 2-44 Composition of Poly-D-lysine stock solution.

	10 ml	[c]
Poly-D-lysine HBSS, add to 10 ml	10 g	1 mg/ml

Tab. 2-45 Composition of Hexadimethrine bromide stock solution.

	5 ml	[c]
Hexadimethrine bromide ddH$_2$O, add to 5 ml	4 g	800 µg /ml

Reagents

HBSS	PAA, Germany
Metafectene	Biontex, Germany

Background

Lentiviral-based particles permit efficient infection and integration of a specific shRNA constructs into differentiated and non-dividing cells. A lentivirus can integrate into the host cell genome to allow stable, long-term transgene expression.

In this work, lentiviral based infection of shRNA against Wisp1 was performed to produce transient and stable Wisp1 knockdown cell lines.

Protocol

For each virus four cell culture dishes were coated with poly-D-lysine solution for 5 min at RT and then washed with ddH$_2$O for culture of the lentiviral packaging Hek293T cells. Per dish 5x10^6 cells were seeded in 14 ml DMEM (see 2.5.2). Hek293T cells were transfected with a transfection cocktail containing 4.4 µg lentiviral expression plasmids pLKO.1-puro UbC-TurboGFP and 3.4 µg of packaging plasmid pCMV 891 and 2.2 µg pMDG (see. 2.20) using metafectene transfection reagent and Na-butyrate to produce lentivirus particles. Lentivirus containing medium was concentrated after two days post-transfection using Vivaspin-Tubes according to the manufacturer's instructions. Viral titers were determined by counting GFP-positive transfected cells by flow cytometry (see 2.22). Wisp1 silencing cell lines were created by adding 0.5, 1 and 2.5 MOI of the respective lentiviruses to the HCC cell lines cultured in DMEM medium containing FCS supplied with the transfection reagent hexadimethrine bromide (8 µg/ml) for 16 hours. Medium was replaced every day and fresh medium with Puromycin (2.5 µg/ml) was added until resistant colonies could be identified. Cells were further cultured up to 4 weeks in Puromycin containing medium to ensure 100% of transfection efficiency. Wisp1 knockdown was proved by Western blot (see 2.8).

2.23 Caspase 3 assay

Buffers

Tab. 2-46 Caspase 3 assay stock solutions.

	Stock	100 ml	[c]
HEPES	100 mM	50 ml	50 mM
NaCl	750 mM	13.3 ml	100 mM
CHAPS	1%	0.1 g	0.1%
EDTA	100 mM	0.1 ml	100 µM
DTT	1 M	0.1 ml	1 mM
Glycerol	100%	10 ml	10%
ddH$_2$O, add to 100 ml, adjust pH 7.4 with 1 M HCl			

Tab. 2-47 Cell lysate buffer for Caspase 3 assay.

	M [g/mol]	0.5 l	[c]
HEPES	238.31	11.9 g	100 mM
NaCl	58.44	21.92 g	750 mM
EDTA	372.2	18.61 g	100 mM
DTT	154.25	77.125 g	1 M
ddH$_2$O, add respectively to 1 l			

Tab. 2-48 Assay buffer for Caspase 3 assay.

	Stock	100 ml	[c]
HEPES	100 mM	50 ml	50 mM
NaCl	750 mM	13.3 ml	100 mM
CHAPS	1%	0.1 g	0.1%
EDTA	100 mM	0.1 ml	100 µM
DTT	1 M	0.1 ml	1 mM
ddH$_2$O, add to 100 ml, adjust pH 7.4 with 1 M HCl			

Tab. 2-49 Ac-DeEVD-AFC stock solution, caspase 3 substrate.

	Stock	5 ml	[c]
Ac(N-acetyl)-DEVD (Asp-Glu-Val-Asp)-AFC (7-amino-4-trifluoromethylcoumarin) DMSO, add to 5 ml	729.61	5 mg	1.35 mM

Background

Caspase 3 is an intracellular cysteine protease. It becomes activated during the cascade of events which occur during apoptosis. Thereby, caspase 3 cleaves a set of cellular molecules which contain the amino acid motif Asp-Glu-Val-Asp (DEVD). Thus, cells which are undergoing apoptosis are first lysed and further tested for their protease activity by the addition of a caspase-specific peptide which is conjugated to a fluorescent reporter molecule, e.g., 7-amino-4-trifluoromethyl coumarin (AFC). The cleavage of the peptide by the caspase 3 releases a fluorochrome that emits fluorescence light at 505 nm, when excited by light at 400 nm wavelength. The level of caspase enzymatic activity in the cell lysate is directly proportional to the fluorescence signal detected with a fluorescent microplate reader.

Protocol

HCC cells were seeded in 24 well plates (75.000 cells/well) in triplicate and serum starved overnight. On the next day, proteins were isolated (see. 2.6) in 100 µl Caspase 3 cell lysis buffer, followed by determination of protein concentration (see. 2.7). For the assay, cell lysate, assay buffer and Caspase 3 substrate were pipetted into a flat bottom 96 well plate as follows; blank: 90 µl assay buffer, cell lysate: 70 µl assay buffer plus 20 µl cell lysate. 10 µl of the substrate (1:20 in assay buffer) were added to the blank and cell lysate and the plate was incubated for 6 h at 37℃. ELISA measurement of the fluorescence gave the fluorescence signal of each sample. For calculation of relative caspase 3 activity, the blank value was subtracted from the samples volumes and afterwards normalized to the protein concentration.

2.24 Transient overexpression of Wisp1

Buffers

Tab. 2-50 Neomycin stock solution.

	100 ml	[c]
Neomycin ddH$_2$O, add to 100 ml, sterile	5 g	50 mg/ml

Tab. 2-51 Transfection cocktail for HCC cell line.

	Each reagent in 100 ml Optimem
plasmid	5 µg
Lipofectamin2000	4.8 µl
Mix and incubate at	
RT for 20 min	

Reagents

Lipofectamin 2000   Invitrogen, Germany

Optimem   Invitrogen, Germany

Protocol

HCC cell lines (60-80% confluent) were seeded into a T25 culture flask. At day two they were washed twice with PBS and transfected with 5 µg of plasmid containing the full length Wisp1 gene (see. 2.20) using Lipofectamin2000 transfection reagent according to the manufacturer's instruction. After cells remained with transfection cocktail for 6 h, they were i) for transient transfection, switched to starvation medium for 24 h , followed by protein isolation or ii) for stable transfection, switched to culture in full DMEM medium containing Neomycin (800 µg/ml). Medium was changed every second day. When Neomycin resistant colonies could be identified, Wisp1 overexpression was detected by Western blot. Cells were cultured for further experiments.

2.25 Statistical analysis

Data are reported as the mean ± SE. To determine if there was significant difference within each experiment, we performed Student's *t*-test. We considered different significance at *p < 0.05 and **p <0.02. All statistical procedures were carried out using AIDA Image Analyzer 2.11 software. Experiments were done in duplica or triplica.

3 Results

3.1 Wisp1 expression in human HCC samples

To explore possible roles of the Wisp1 protein in human hepatocellular carcinoma, its expression was analyzed using Western blot and immunohistochemistry. We found that Wisp1 levels were increased, decreased or not changed when comparing normal tissue (N) adjacent to a liver tumor and tumor (T) tissue samples (Fig.3-1).
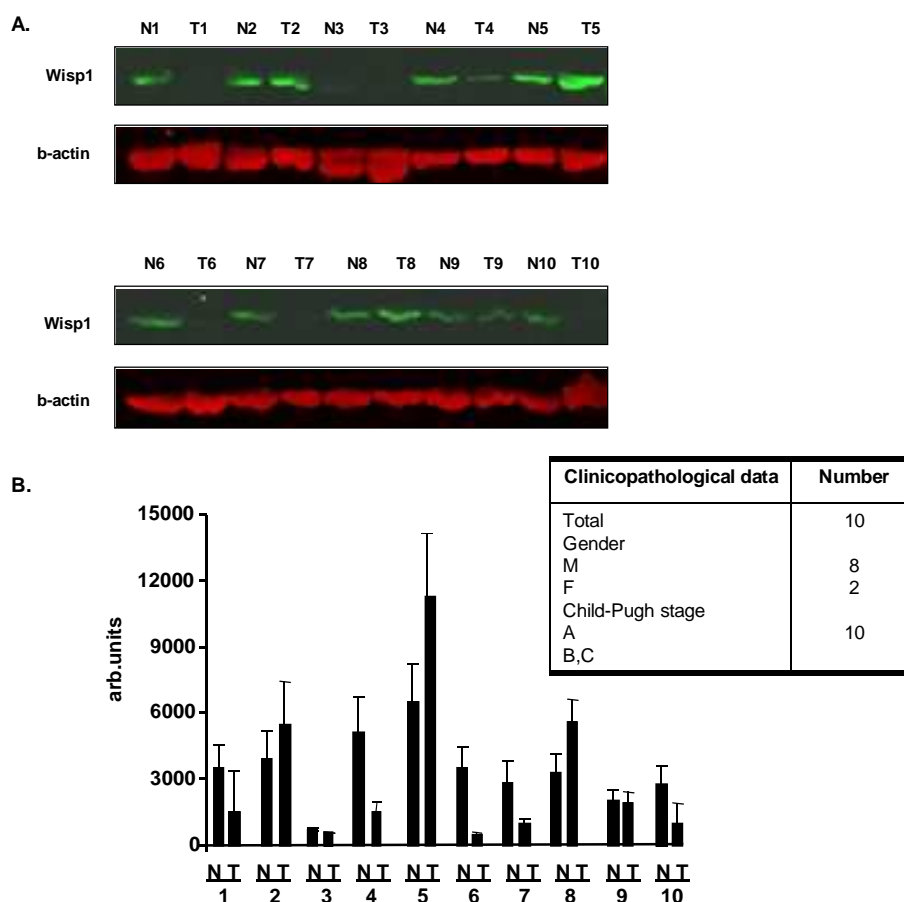
Fig. 3-1 Western blot analysis of Wisp1 in normal (N) liver adjacent to tumor (T) samples. (A) A single band corresponding to the predicted MW of Wisp1 was identified at 48 kDa using an anti-human Wisp1 specific antibody. To demonstrate equal protein loading of the gel, b-actin was detected as a reference in the same samples. (B) Quantification of the immunoblot signal of different intensities was normalized to the reference protein b-actin. Data are presented as the mean. Error bars on data points represent SE of the mean.

In the next step, to explore the tissue expression pattern and localization of Wisp1 in healthy versus hepatocellular carcinoma samples, 48 liver biopsies from HBV-positive HCC patients were analyzed by immunohistochemistry using Wisp1 specific antibodies. Clinicopathological data are summarized in Tab.3-1.

Tab. 3-1 Clinicopathological data of 48 HBV infected patients with liver cancer.

Clinicopathological data	Number
Total	48
Gender	
M	43
F	5
Age	
>50	25
≤50	23
Tumor number	
single	38
multiple	10
Tumor size (cm)	
>5	23
≤5	20
unknown	5
Depth of invasion	
T1,2	20
T3,4	23
unknown	5
Child-pugh class	
A	24
B,C	19
not classified	6
Nodal stage	
N0, 1	48
N2, 3	0
Differentiation grade	
well	6
moderate	22
poor	20

In normal adjacent liver sections, in "healthy" areas fulfilling the main criteria of morphologically non-injuired hepatocytes, Wisp1 was either absent or weak staining was found in the cytoplasm (Fig.3-2A). In normal adjacent liver sections, areas with damaged hepatocytes and multifocal inflammation, represented by an accumulation of lymphocytes, showed a strong positive signal for Wisp1 in hepatocytes in close proximity to the areas of inflammation (Fig.3-2B). Furthermore, hepatic steatosis was present in some patients with HBV-induced liver cancer. In the non-tumorigenic area of these patients, strong Wisp1 expression was found in hepatocytes surrounding fat droplets (Fig.3-2C).

A. Healthy hepatocytes
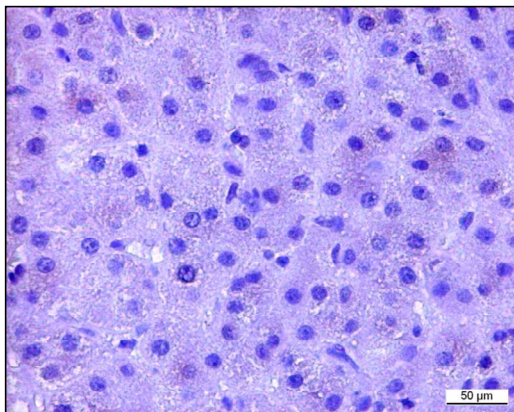
B. Inflamed areas
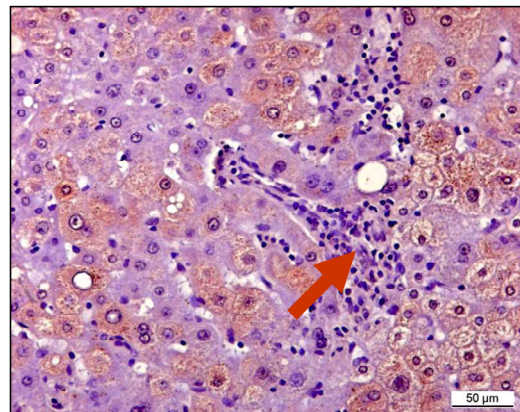
C. Steatotic areas
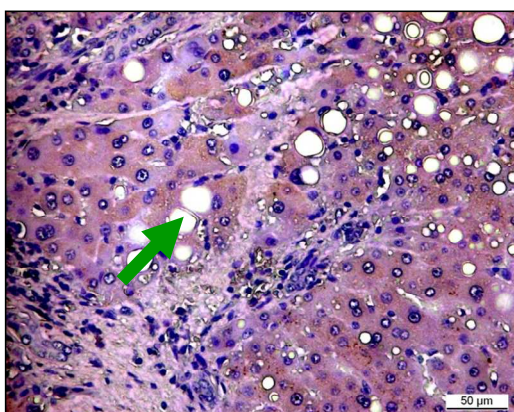
D. Control, 2nd antibody
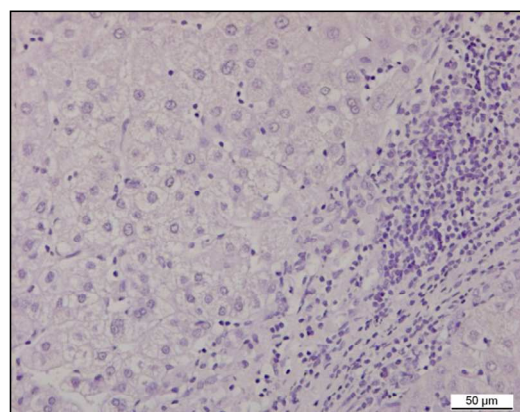
Fig.3-2 Representative pictures of Wisp1 immunohistochemical staining in non-tumorigenic areas of patients with liver cancer (A) No Wisp1 staining in healthy HCs. (B) Strong Wisp1 staining in HCs surrounding the areas of inflammation indicated by the red arrow. (C) Strong Wisp1 signals are present in section with hepatic steatosis in cells surrounding fat droplets indicated by the green arrow. (D) No staining was detectable under control conditions in 4 liver sections when the primary antibody was omitted. The magnifications are indicated by scale bars.

Interestingly, the intensity of Wisp1 signals in liver sections evaluated as tumor regions correlated negatively with the cancer stage of the tumor. In patients with well differentiated hepatocellular carcinoma, strong Wisp1 expression was found in hepatocytes of the tumor. Wisp1 expression was not found in HCs nuclei, endothelial cells of vessels or cholangiocytes of the bile ducts (Fig.3-3A). In patients with moderately differentiated HCC, immunohistochemical staining for Wisp1 showed moderate to low expression of the protein in hepatocytes of the tumor area (Fig.3-3B). In poorly differentiated HCC, Wisp1 expression was not found (Fig.3-3C).

A. Well differentiated
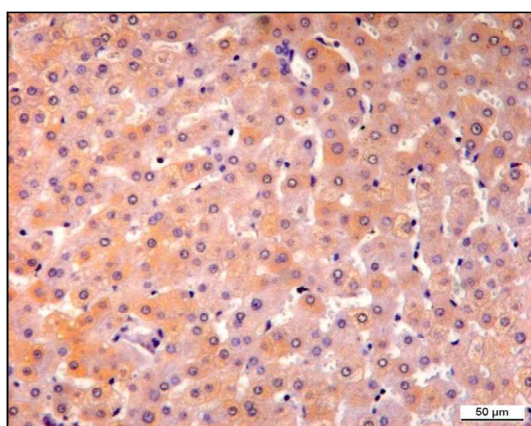
B. Moderately differentiated
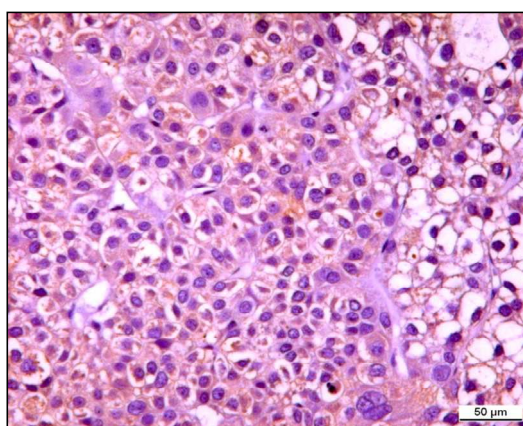
C. Poorly differentiated
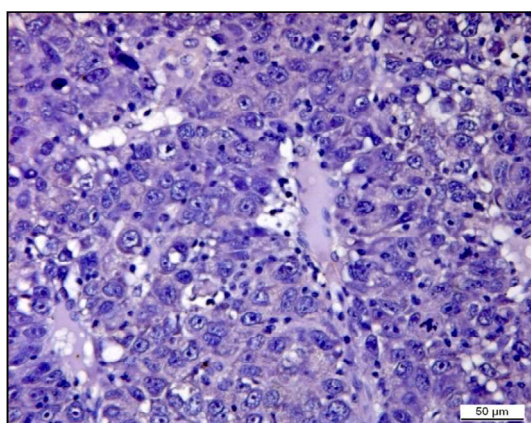
Fig.3-3 Representative pictures of Wisp1 immunohistochemical staining in the tumor area of patients with liver cancer. (A) Strong Wisp1 positive staining (in brown) in HCs of the tumor region of well differentiated HCC. (B) Moderate to low positive staining in HCs of the tumor region of moderately differentiated HCC. (C) Wisp1 was not present in HCs of the tumor region of poorly differentiated HCC. Nuclei are counter-stained in blue by hematoxylin. The magnifications are indicated by scale bars.

However, in patient samples with advanced-stage HCC, Wisp1 staining was detectable in multinicleated hepatocytes (Fig.3-4A) and the tumor stroma (Fig.3-4B).

A. Multinucleated cancer cells
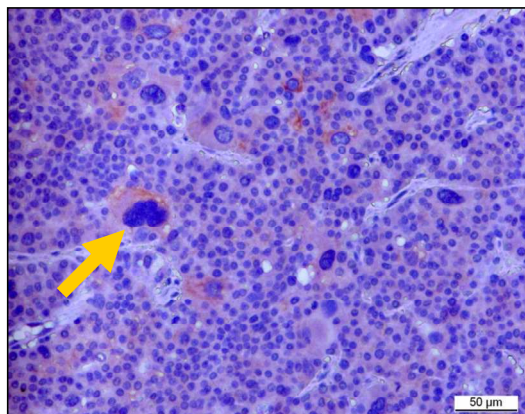
B. Stroma
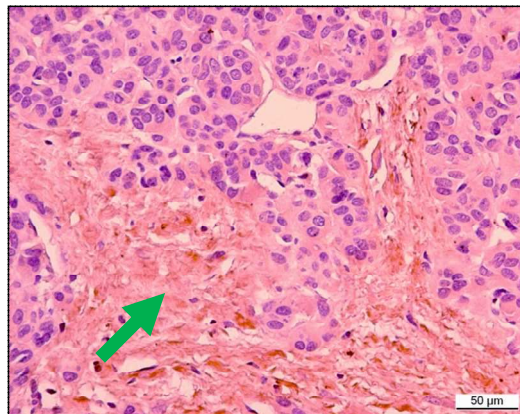
Fig.3-4 Representative picture of Wisp1 immunohistochemical staining from the tumor area of patients of poorly differentiated HCC. Strong positive staining (brown) in multinicleated cancer cells indicated by yellow arrow and (B) in the stroma indicated by green arrow. Nuclei are counter-stained in blue by hematoxylin.The magnification is indicated by scale bars.

Taken together, immunohistochemical staining data (Tab.3-2) revealed that in well differentiated HCC, Wisp1 expression was strong in 83% of patients (5 out of 6 patients). In moderately differentiated HCC, Wisp1 expression was weak to moderate in 82% of patients (18 out of 22 patients). Furthermore, in poorly differentiated HCC, Wisp1 expression was weak in only 30% of patients (6 out of 20 patients).

Tab. 3-2 Wisp1 expression level in tumor region of 48 HBV-positive infected patients with HCC. Wisp1 expression level: 0 no, + weak, ++ moderate, +++ strong.

Differentiation grade	Total no. of samples	0	+	++	+++
well	6			1	5
moderate	22	2	10	8	2
poor	20	12	6	1	1

Table 3-3 gives a detailed overview of Wisp1 expression and its precise localization in liver cancer of 48 patients. Normal liver tissue adjacent to tumors and tumor samples for each patient are shown.

Tab. 3-3 Wisp1 expression in 48 patients with liver cancer.
Wisp1 expression level: 0 no, + weak, ++ moderate, +++ strong

No. of sample	Non-tumor Wisp1 levels	Characteristics of non-tumor areas	Tumor Wisp1 levels	Differentiation grade
1	+++	positive damaged HCs	0	poor
2	+++	positive damaged HCs/ hypertrophic HCs	+	moderate
3	+++	positive damaged HCs, negative multinicleated HCs	+	moderate
4	+++	positive damaged HCs/ multinicleated HCs	+	moderate
5	+++	positive steatotic areas	++	moderate
6	+++	positive multinicleated HCs	++	moderate
7	++	positive damaged HCs	0	moderate
8	++	positive inflamed areas	0	poor
9	++	positive steatotic areas/stroma	0	moderate
10	++	positive stroma	0	poor
11	++	positive damaged HCs	0	poor
12	++	positive steatotic areas	+	poor
13	++	positive steatotic areas	+	moderate
14	++	positive multinicleated HCs	+	moderate
15	+	healthy	0	poor
16	+	positive multinicleated HCs	0	poor
17	+	healthy	0	poor
18	+	healthy	0	poor
19	0	healthy	0	poor
20	0	healthy	0	poor
21	0	healthy	0	poor
22	0	healthy	0	poor
23	0	healthy	0	poor

No. of sample	non-tumor Wisp1 levels	characteristics of non-tumor areas	tumor Wisp1 levels	Differentiation grade
24	+	healthy	+	poor
25	+	healthy	+	moderate
26	+	positive steatotic areas	+	moderate
27	+	positive stroma	+	poor
28	+	positive steatotic areas	+	moderate
29	+	positive multinicleated HCs	+	poor
30	+	healthy	+	moderate
31	++	healthy	++	moderate
32	+++	positive damaged HCs	+++	moderate
33	+++	healthy	+++	well
34	+++	positive damaged HCs	+++	well
35	+++	positive damaged HCs	+++	well
36	0	healthy	+	poor
37	0	healthy	+	poor
38	0	healthy	++	moderate
39	0	healthy	++	moderate
40	0	healthy	++	moderate
41	+	positive stroma	++	well
42	+	positive steatotic areas	++	poor
43	+	positive steatotic areas	++	moderate
44	+	positive HCs/ stroma	++	moderate
45	++	positive multinicleated HCs	+++	moderate
46	++	positive HCs/ steatotic areas	+++	poor
47	++	positive HCs, negative steatotic area	+++	well
48	++	positive HCs/ multinicleated HCs	+++	well

Furthermore, we found specific Wisp1 expression patterns in the peripheral and central part of HCC. Figure 3-5A shows the characteristic histological pattern of the central and peripheral parts of HCC. Marked hepatocellular necrosis is present in the central part. Rich microvessels can be seen in the peripheral part. Figure 3-5B shows the suitable Wisp1 expression pattern in these different regions. Weak (yellow) or no Wisp1 positive staining was detected in the central part. Moderate to strong (brown) Wisp1 positive expression was found in the peripheral part. Wisp1 expression in the periphery of HCC suggests involvement of Wisp1 in tumor growth and migration.

A.   **Central**   **Periphery**

B.
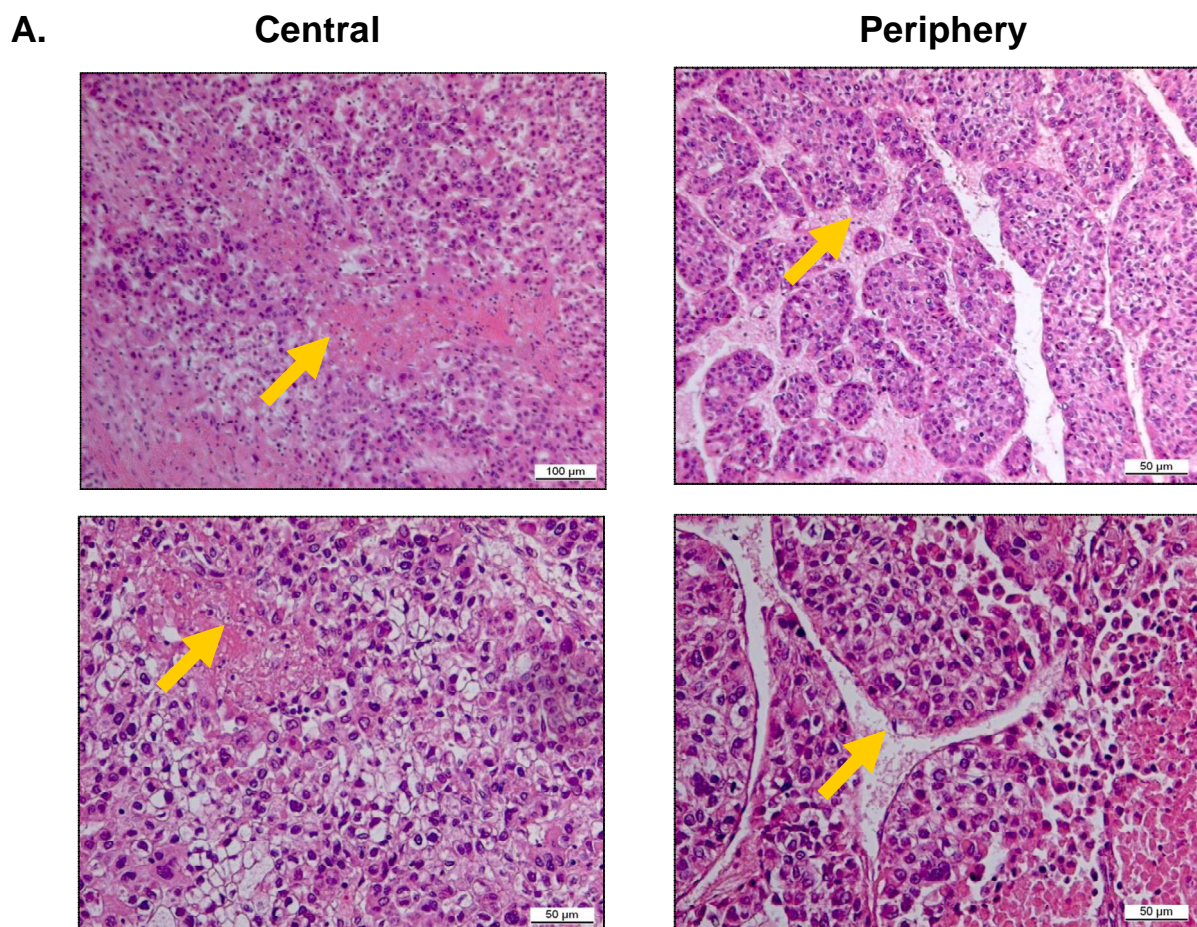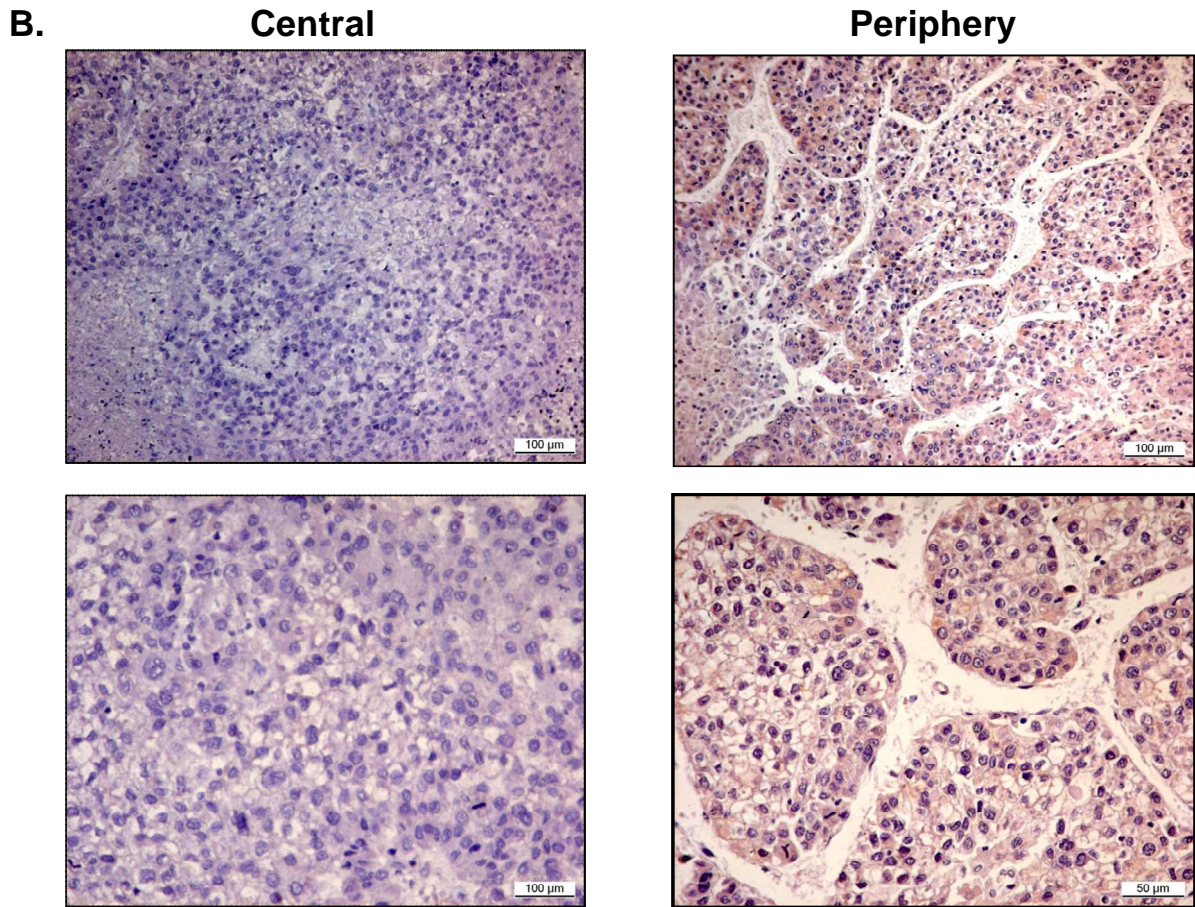
Central   **Periphery**

Fig.3-5 Characteristic histological pattern of the central and peripheral parts of HCC. (A) Hematoxylin staining for nuclei, eosin staining for cytoplasm. Yellow arrows indicate necrotic areas and rich microvessels. (B) Wisp1 weak (yellow) or no staining was detected in the central part. Wisp1 moderate to strong expression (brown) was found in the peripheral part. Nuclei are counter-stained in blue by hematoxylin.

3.2 Positive correlation between Wisp1 and E-Cadherin expression in human HCC samples

Since E-Cadherin plays a key role in the establishment and maintenance of intracellular adhesions and tissue architecture, and as alterations in E-Cadherin expression are associated with dedifferentiation, invasiveness, lymph node and distant metastasis in primary HCC [71, 72], we analyzed human HCC patient samples with immunohistochemistry for E-Cadherin expression and correlated the data to our findings of Wisp1 expression in HCC. With immunohistochemical staining of the various differentiation grades, we found strong membranous expression of endogenous E-Cadherin only in well differentiated HCC (Fig.3-6A). In moderately differentiated HCC, E-Cadherin expression was low, detected by positive brown staining at the membrane and in the cytoplasm of HCs (Fig.3-6B). E-Cadherin expression was not found in poorly differentiated HCC (Fig.3-6C).

A. Well differentiated
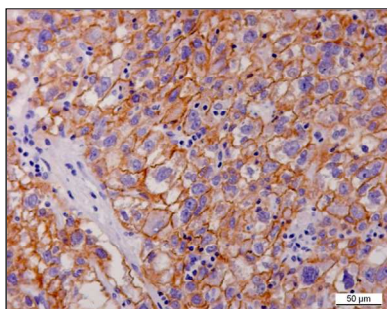
B. Moderately differentiated
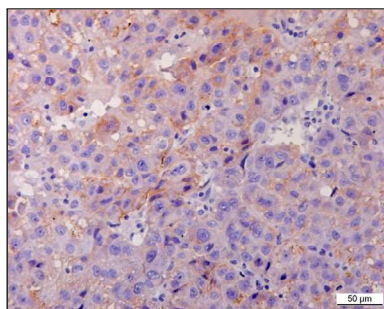
C. Poorly differentiated
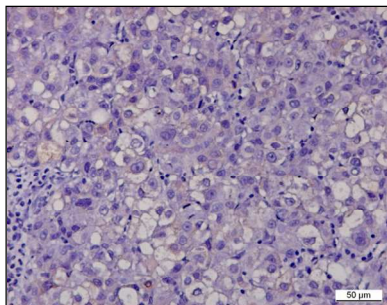
Fig.3-6 Representative pictures of E-Cadherin immunohistochemical staining in the tumor area of patients with liver cancer. (A) Strong E-Cadherin positive staining (in brown) at the cell membrane of cancer cells of well differentiated HCC. (B) Moderate to low positive staining at the cell membrane and cytoplasm of cancer cells of the tumor region of moderately differentiated HCC. (C) E-Cadherin was not present in the tumor region of poorly differentiated HCC. Nuclei are counter-stained in blue by hematoxylin.

Comparison of Wisp1 and E-Cadherin expression intensity in HCC patient samples showed a positive correlation (Fig.3-7). The strong Wisp1 positive cases of early-stage HCC (median 3) also showed strong E-Cadherin staining (median 3). The low Wisp1 positive cases of intermediate-stage HCC (median 1) were accompanied by moderate E-Cadherin staining (median 2). There was no Wisp1 expression in advanced-stage HCC, but low E-Cadherin expression (median 1) was shown.

Differentiation grade	Wisp1 (median)	E-cadherin (median)
well	3	3
moderate	1	2
poor	0	1
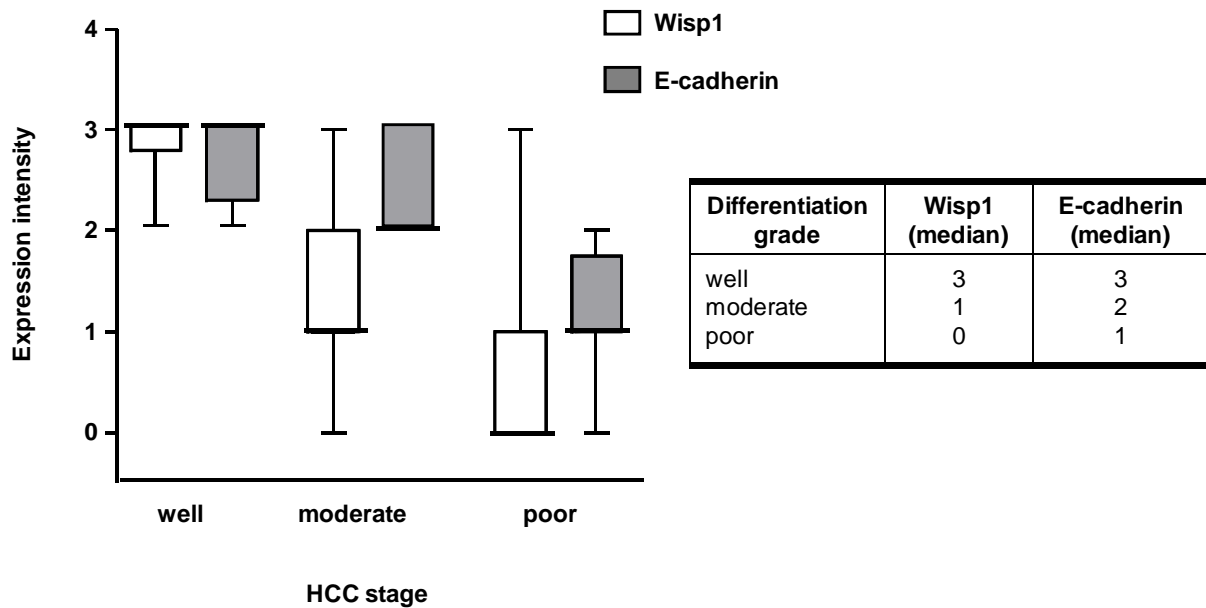
Fig. 3-7 Comparison of Wisp1 and E-Cadherin expression in human HCC patient samples.

Taken together, these findings show that decreased Wisp1 expression correlates positively with decreased E-Cadherin expression. As loss of E-Cadherin expression is a main characteristic of malignant cells, we assume further in our *in vitro* analysis that Wisp1 action depends on E-Cadherin.

3.3 Epithelial and fibroblastoid-type HCC cell lines produce and secrete Wisp1

Since HCC is a very heterogenous disease we anticipated that the tumorigenesis of particular subtypes might depend on Wisp1 induction. To gain insight into the functional significance of Wisp1 up-regulation in early-stage HCC, we studied two different human HCC derived cell lines (Fig.3-8). FLC4 cells are characterized by albumin secretion [67]. In addition, FLC4 cells show a polygonal-shaped morphology, are able to form bile canaliculi and express high levels of E-Cadherin, all together, representing an epithelial phenotype with well-preserved liver function. In contrast, HLF cells show fibroblast-like phenotypes and do not secrete albumin [69]. Both cell lines represent well established in vitro systems for the analysis of human HCC [66].
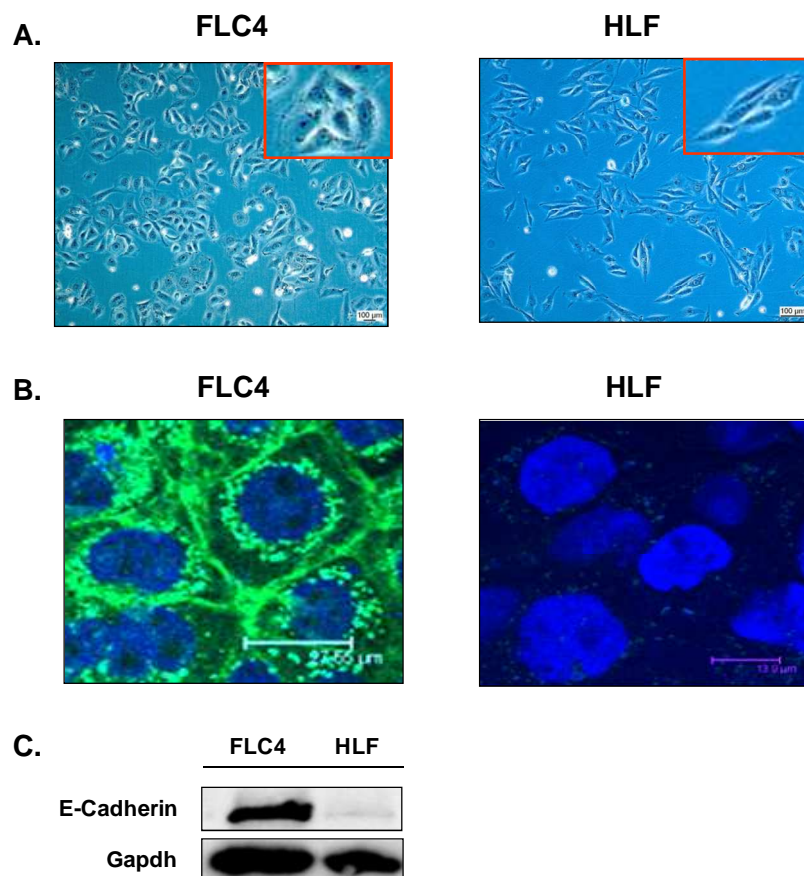
Fig.3-8 Typical features of FLC4 and HLF cell lines. (A) Morphological criteria of epithelial FLC4 and fibroblast-like HLF cells. Representative pictures were taken by light microscopy (objective x10) one day after plating of the respective cells. (B) Immunofluorescence pictures showing E-Cadherin (green) and nuclei (blue) in FLC4 and HLF cells. (C) Immunoblot analysis of E-Cadherin in FLC4 and HLF lysates. Gapdh was used as a loading control.

To determine whether Wisp1 is expressed in HCC cell lines, immunoblots of total protein isolated from FLC4 and HLF cells were performed. Wisp1 was detectable in both cell lines (Fig.3-9A). Since it has been suggested that Wisp1 is a secreted protein [51], the amount of Wisp1 released by FLC4 and HLF cells to the culture medium was determined. Cell-conditioned media was collected at days 1, 2 and 3. Proteins were precipitated with acetone and analyzed by immunoblots using Wisp1 specific antibody. By day 3, the Wisp1 protein was detected in the conditioned medium of both cell lines (Fig.3-9B). It is tempting to speculate that secreted Wisp1 can stimulate cells by autocrine/paracrine signaling. To test this hypothesis, the effects of recombinant human Wisp1 and knockdown was tested *in vitro* on different parameters including cell growth and motility (Fig.3-9C).

A.

	FLC4			HLF		
	1d	2d	3d	1d	2d	3d
Wisp1						
Actin						

B.

	FLC4			HLF		
	1d	2d	3d	1d	2d	3d
Wisp1						

C.

	FLC4					FLC4			
	-	shco	sh0	sh1		-	shco	sh0	sh1
Wisp1					Wisp1				
Tubulin					b-actin				
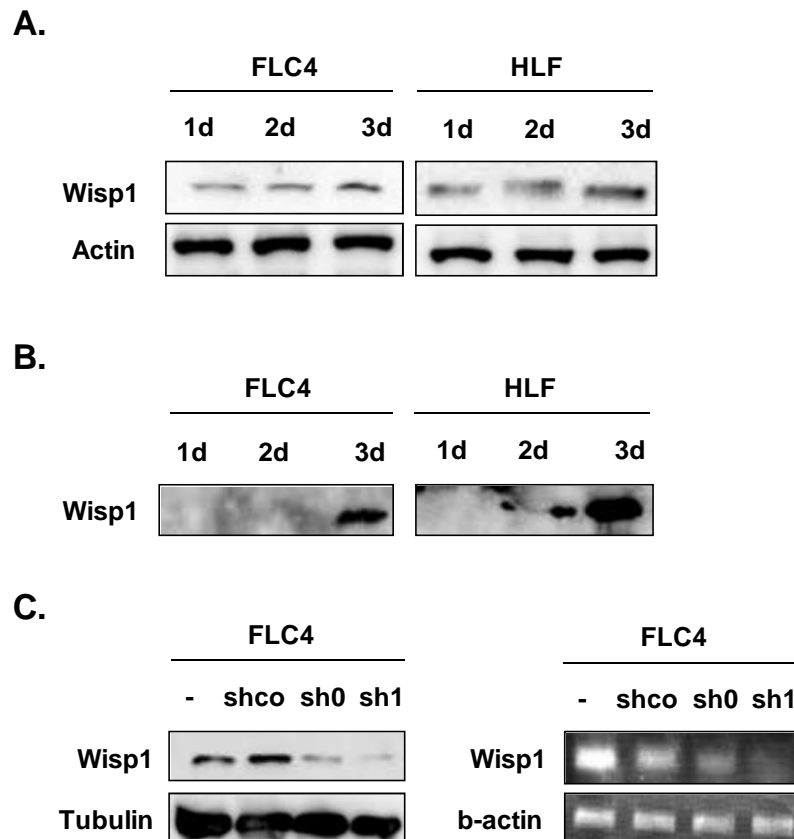
Fig.3-9 HCC cells express and secret Wisp1. (A) FLC4 and HLF cell lines were cultured for 1, 2 and 3 days. 35 ug of total protein lystates were separated on a 12% SDS PAGE gel and then immunoblotted. Wisp1 and actin, as a loading control, were detected by the use of specific antibodies in the same lysates. (B) Secreted proteins were precipitated with acetone from cell conditioned media followed by separation on SDS PAGE and immunoblot (for further details on the precipitation method please consult the materials and methods section). (C) Wisp1 depletion in FLC4 cells. Wisp1 protein and RNA levels were decreased in FLC4 cells using shRNAs targeting Wisp1. Cells were transiently transfected with 1.5 MOI only with shRNA control (shco) or shRNAs for Wisp1 (sh0 and sh1). Endogenous Wisp1 was detected from total protein and RNA lysates.

3.4 Regulation of cell-cycle by Wisp1 in HCC cells

Since it has been shown earlier that the Wisp1 pathway is involved in cell growth, motility, transformation and survival of cells [50, 62, 73, 74], changes in these parameters were investigated in HCC cells upon Wisp1 stimulation or inactivation. Cell growth was arrested by serum deprivation followed by BrdU incorporation and treatment of the cultures with recombinant human Wisp1. To determine whether Wisp1 stimulation affects the growth kinetics of the HCC cell lines, we determined the incorporation at different time points. Wisp1 treatment significantly increased BrdU incorporation of FLC4 cells, whereas the same Wisp1 concentration had no effect on the fibroblast-like HLF cells (Fig.3-10). In the same set of experiments, no changes were detectable between the two cell lines regarding their response to a FCS-dependent stimulation of growth or growth arrest induced by mitomycin C treatment. These results indicate that the general growth properties of FLC4 and HLF cells are comparable, whereas the response to Wisp1 stimulation depends on the specific phenotype of the cell. Furthermore, BrdU incorporation in Wisp1 depleted FLC4 cells was significantly reduced in comparison to control cells transfected with control virus (Fig.3-10C). In comparison to PBS treatment, FCS did not stimulate BrdU incorporation in Wisp1 depleted HCC cells. Wisp1 depleted cells were insensitive to mitomycin C dependent blocking of DNA synthesis, whereas DNA blocking induced by mitomycin C was evident in all experiments analyzing untransfected or control transfected cells. These findings were corroborated by Western blot analysis revealing reduced protein levels of the proliferation marker PCNA upon Wisp1 knockdown (Fig. 3-10D).
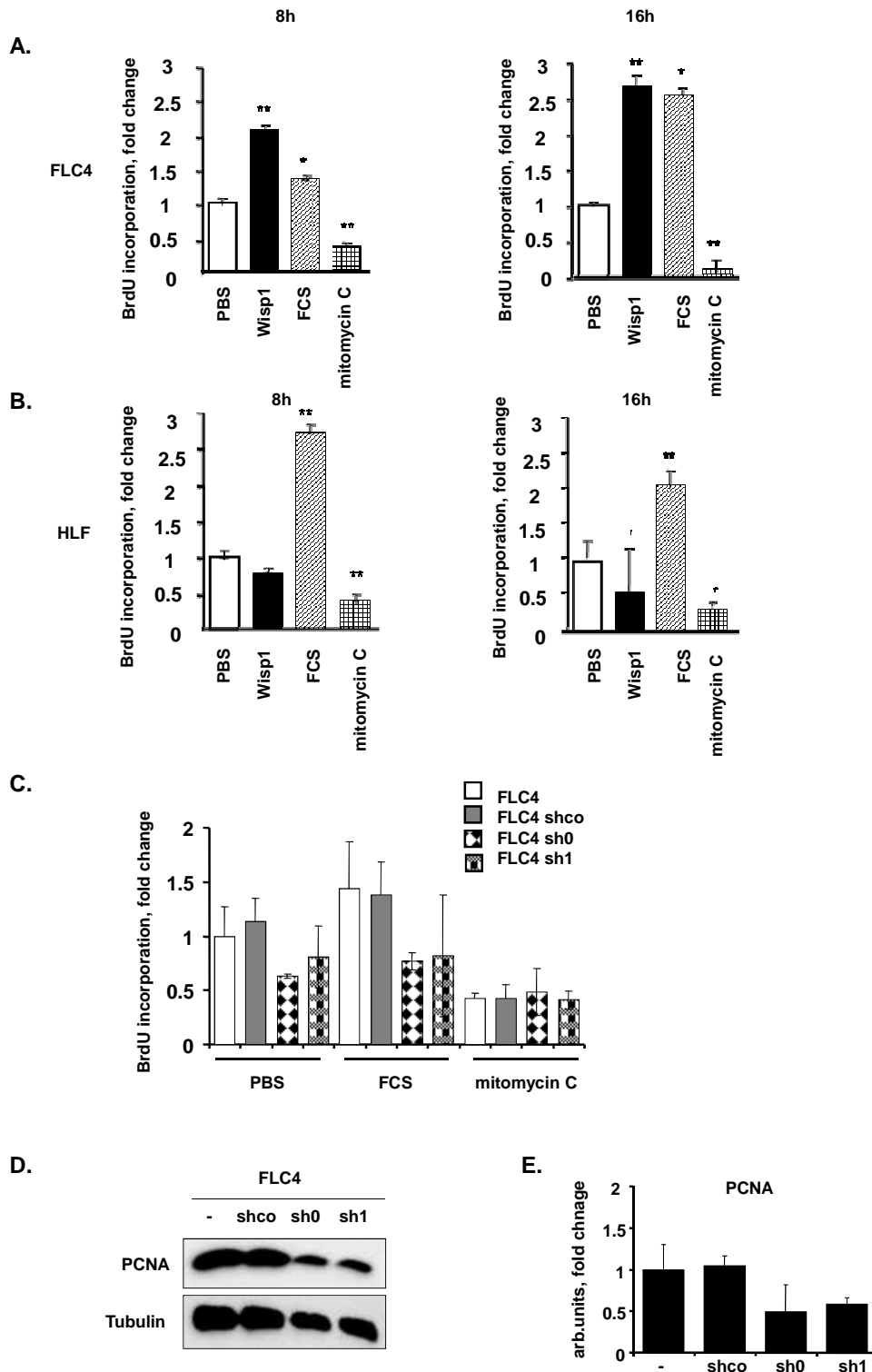
Fig.3-10 Wisp1 affects FLC4 proliferation response and has no effect on HLF cells. (A) FLC4 and (B) HLF cell lines were either treated for 8h or 16h with Wisp1 (100 ng/ml), PBS (vehicle), FCS or mitomycin C (5 µg/ml). Proliferation was analyzed by the BrdU incorporation assay. (C) Wisp1 knockdown attenuates proliferation of FLC4 cells. Again, FLC4 cells transfected with 1.5 MOI control hairpin vector (shco) and shRNA targeting Wisp1 (sh0/sh1) were either treated with PBS (vehicle), FCS (positive control) or mitomycin C (5 µg/ml, negative control). Proliferation was measured by the BrdU incorporation assay. (D) Immunoblot analysis for PCNA. Tubulin was used as a loading control. (E) Quantification of signal intensities representing gene expression was normalized against tubulin. Data are presented as the mean of 2 experiments. Error bars represent SE.

To further support these findings, additional HCC cell lines including epithelial-type Hep3B [75] and fibroblast-type HCC-T cells [76] were stimulated with Wisp1 followed by the BrdU incorporation assay. Wisp1 effects on Hep3B and HCC-T cells were similar to the previous results using FLC4 and HLF cells, and thus dependent on the HCC cell phenotype (Fig.3-11).
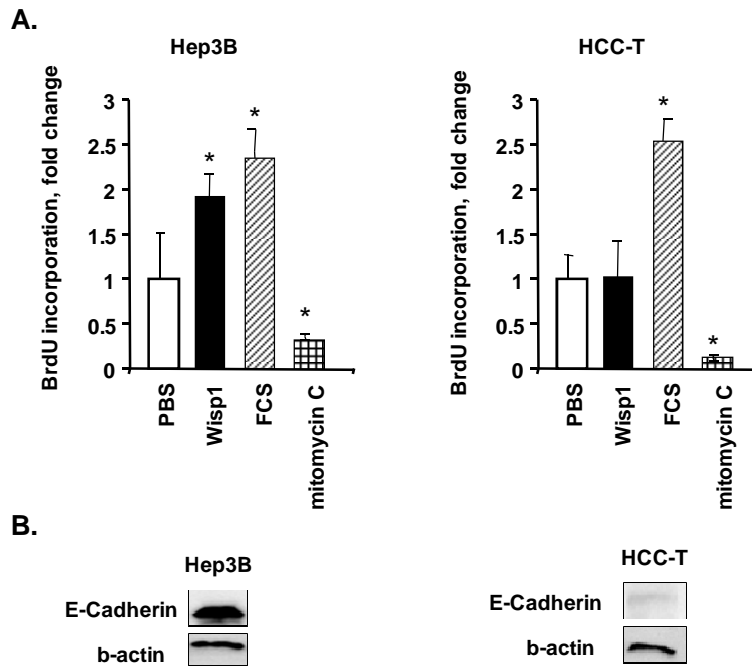
Fig.3-11 Wisp1 increases the proliferation of Hep3B but not of HCC-T cells. (A) HCC cell lines were either treated for 8h and 16h with Wisp1 (100 ng/ml), PBS (vehicle), FCS (positive control) or mitomycin C (5 µg/ml, negative control) and then proliferation was analyzed using a BrdU incorporation assay. (B) Immunoblot analysis of E-Cadherin in Hep3B and HCC-T lysates. B-actin was used as a loading control.

Next, we analyzed the expression of marker genes during cell cycle progression ± Wisp1 treatment (Fig.3-12). HCC cell lines were left either untreated or were stimulated for 24 h with recombinant human Wisp1 (100 ng/ml) and mRNA levels of the different marker genes were assessed using a semi-quantitative RT-PCR method. In line with the BrdU data, Wisp1 did not change the cyclin expression levels in the HLF cell line), but induced the expression of early cyclinD1 more than 1.5 fold and of cyclinE1 more than 2 fold in the FLC4 cell line (Fig.3-12A/B). In addition, we analyzed effects of Wisp1 silencing on expression of cell cycle markers. Wisp1 knockdown in FLC4 cells resulted in an almost complete ablation of the early cyclinD1, whereas cyclinA2 expression levels were significantly reduced by more than 50% as compared to untransfected cells (Fig.3-12C/D).
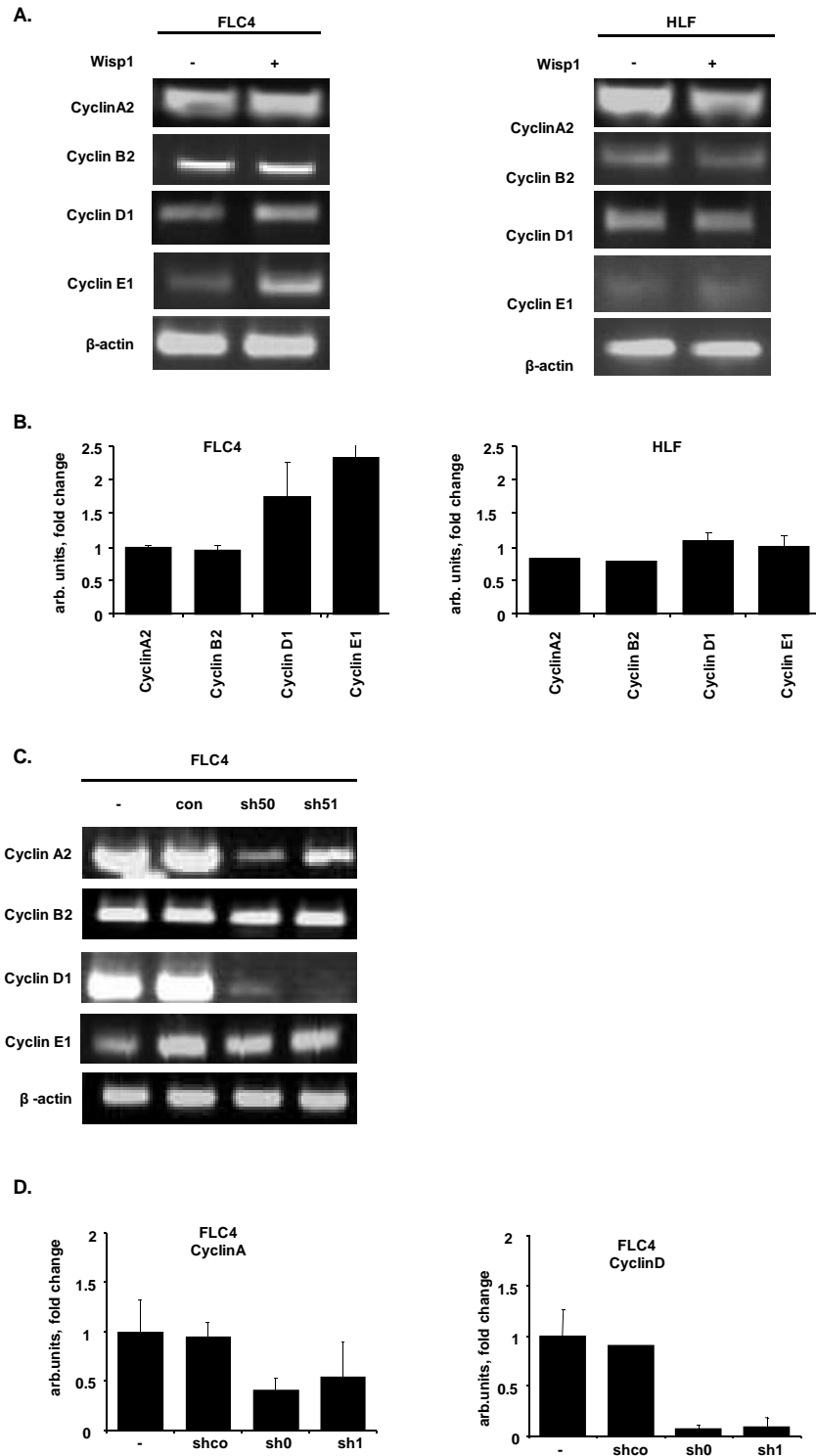
Fig.3-12 Wisp1 effects proliferation of FLC4 but not of HLF cells. (A) Total RNA was extracted from FLC4 and HLF cell lines using the RNeasy kit according to the manufacturer's instructions. Semiquantitative RT-PCR analysis demonstrates the response of cell cycle markers (cyclins) to 24 h Wisp1 stimulation. (B) Cyclin expression was quantified against beta-actin using AIDA Image Analyzer 2.11 software. Data are presented as the mean ± SE. (C) Expression of cell cycle markers in Wisp1 depleted FLC4 cells. A representative semi-quantitative RT-PCR analysis of untransfected (-) control transfected (shco) and Wisp1 knockdown cells (sh0/sh1) is shown. (D) Quantification of signal intensities representing gene expression levels. Cyclin expression was normalized against beta-actin. Data are presented as the mean. Error bars represent SE.

73

To test whether overexpression of Wisp1 would mimic the effects of exogenous Wisp1 treatment, both cell lines were transiently transfected using a mammalian Wisp1 expression vector. In FLC4 cells, but not in HLF cells, Wisp1 overexpression increased DNA synthesis and PCNA protein levels in comparison to control transfections using an empty vector (Fig.3-13). Together, these results suggest that Wisp1 stimulates the proliferation of epithelial FLC4 cells, but does not change the growth properties of the fibroblast-like HCC cell line HLF.

A.
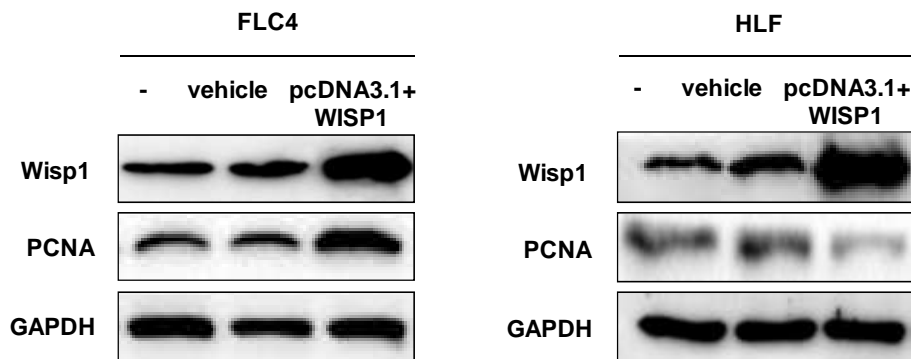
B.
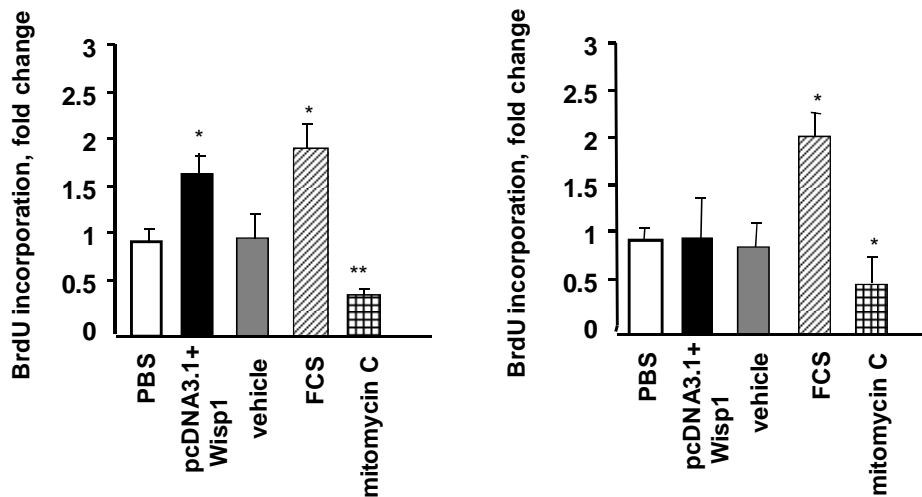
Fig.3-13 Wisp1 overexpression increases proliferation of FLC4 but does not affect the HLF cell line. (A) HCC cell lines were transiently transfected using 1 µg control plasmid DNA or plasmid containing a Wisp1 expression cassette. 30 h after transfection, protein lysates were harvested and analyzed by immunoblot using Wisp1 specific antibodies. The Wisp1 overexpressing cells were further analyzed for changes in PCNA protein levels and (B) the effects on DNA synthesis by BrdU incorporation.

3.5 Mitogenic effects of Wisp1 depend on E-Cadherin

It is well-known that FLC4 cells, in contrast to HLF cells, express high levels of the epithelial-cadherin (E-Cadherin). In addition, it was reported that interactions of CCN members with cadherins modulate signaling pathways [41, 77, 78]. To investigate whether the response of FLC4 cells to Wisp1 depends on E-Cadherin, we examined the effect of Wisp1 on proliferation and cell cycle progression upon E-Cadherin depletion. We found, that the E-Cadherin knockdown largely abolished the Wisp1 mediated proliferative response of FLC4 cells (Fig.3-14B). These results could be reproduced by the use of four different siRNAs specifically targeting different parts of the E-Cadherin mRNA, whereas a scrambled siRNA oligo had no effect (Fig.3-14A). Importantly, the depletion of E-Cadherin did not affect BrdU incorporation to FLC4 cells per se. These data suggest that E-Cadherins are important for Wisp1 dependent effects in epithelial-type HCC cell lines.
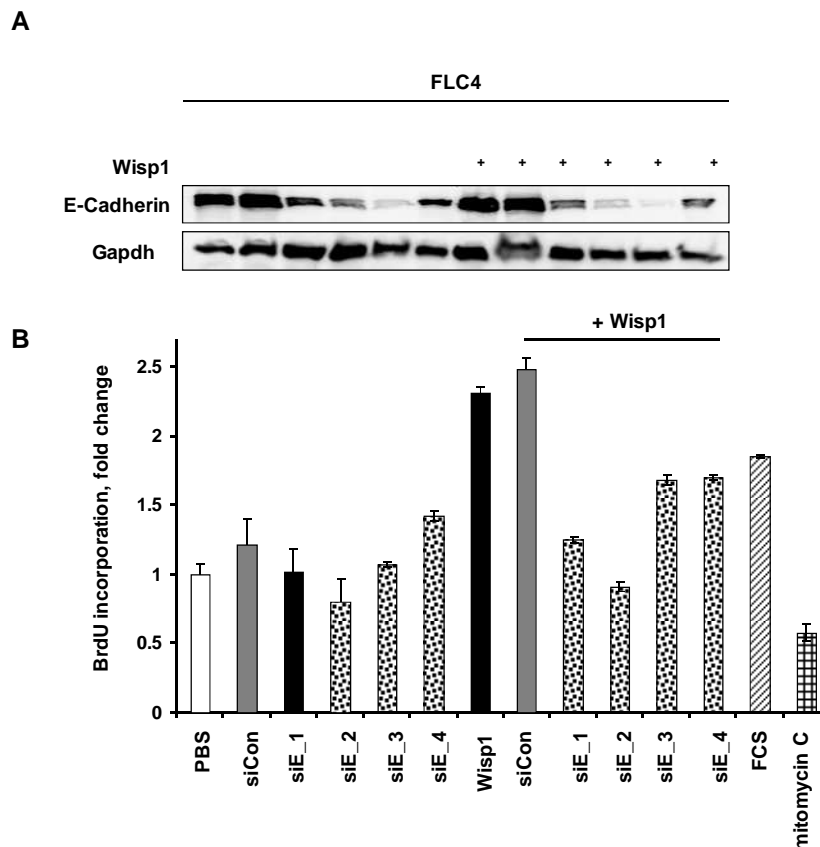
Fig.3-14 Knockdown of E-Cadherin decreases Wisp1-dependent proliferation of FLC4 cells. (A and B). FLC4 cells were transfected with control (siCon) or specific siRNA targeting E-Cadherin mRNA (siE1-siE4). 48 h later, the cells were treated with Wisp1 (100 ng/ml), PBS (vehicle), FCS (positive control) or mitomycin C (negative control) for an additional 16 h and then analyzed for proliferation by the BrdU incorporation assay. Data are normalized against PBS. Data are presented as the mean. Error bars represent SE.

3.6 Wisp1 activates multiple signaling pathways in epithelial and fibroblast-like HCC cell lines

Since binding of CCN proteins via their thrombospondin domain to integrins was reportedly detected [41, 44, 79], we analyzed the activation of kinases which mediate cellular effects downstream of integrins including cell proliferation, migration and survival. Immunoblot with phospho-specific antibodies demonstrated a rapid phosphorylation of Fak (Tyr-397), Src (Tyr-416), Akt (Ser-473) and Erk1/2 (Typ-204) in both HCC cell lines upon Wisp1 treatment (Fig.3-15A). Fak and Src activation were detected only after 15 min of Wisp1 stimulation, while Akt and Erk1/2 phosphorylation were detected after 30 min of stimulation. Immunoblot analysis revealed that the respective total protein kinase levels were not changed by Wisp1. Other kinases, like p38 and cJun, were not activated by Wisp1. These data show that Wisp1 activates Fak, Src, Akt and Erk1/2 in both epithelial- (FLC4) and fibroblast-like (HLF) HCC cell lines. To determine which signaling pathways are affected by Wisp1 silencing in FLC4 cells, we performed immunoblots using phospho-Fak, -Src, -Akt and -Erk1/2 antibodies and antibodies for total protein detection (Fig.3-15C). Wisp1 knockdown in the FLC4 cells caused a decrease in pFak and pErk1/2, whereas Fak and Erk1/2 levels were unaffected. Phospho-Akt protein level was not altered upon Wisp1 knockdown, but pAkt protein level was decreased. Src protein expression was lower than in untransfected cells and, consequently, pSrc level was also decreased.

A.

B.

C.
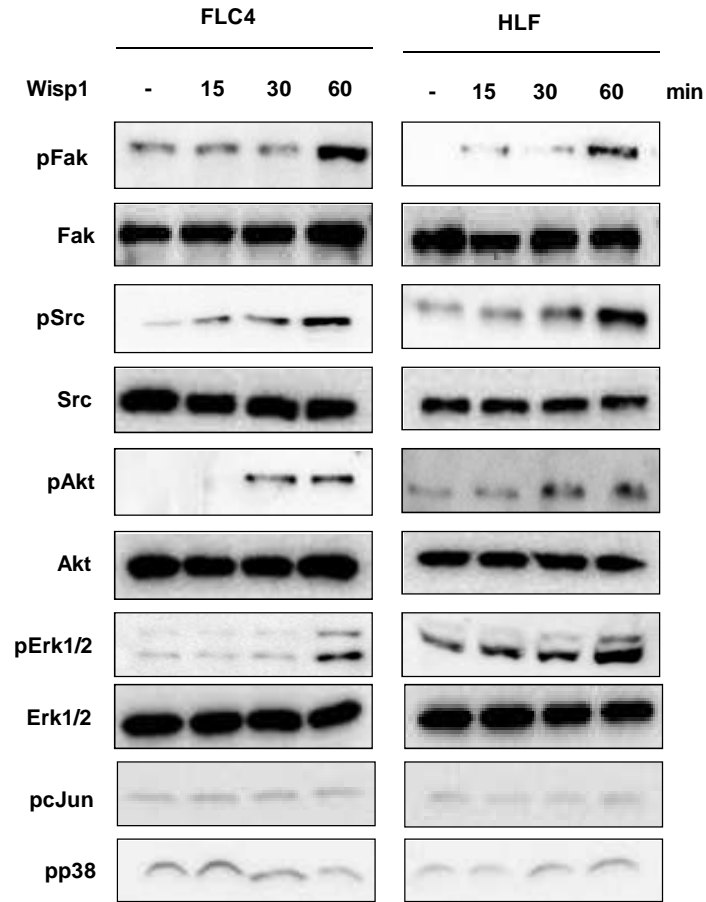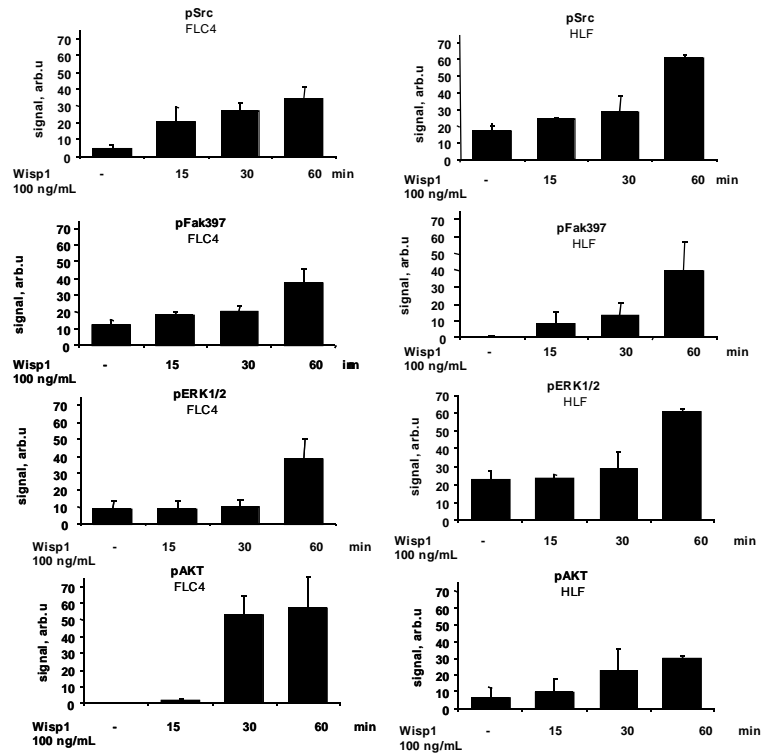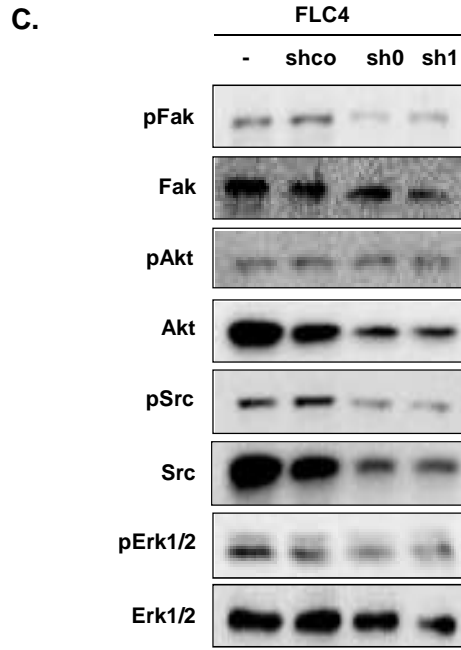
D.
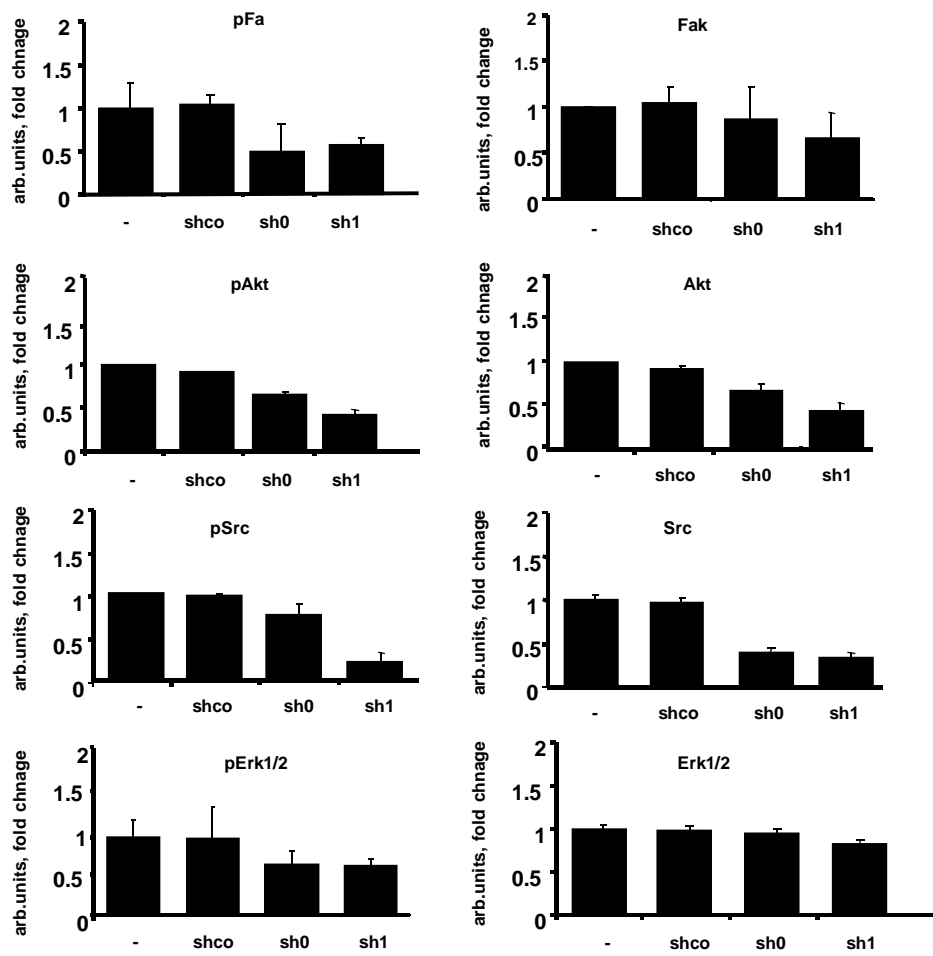
Fig.3-15 Wisp1 induced changes in integrin-dependent signaling pathways. (A) Representative immunoblot analysis of phospho-Fak (Tyr-397), phospho-Src (Tyr-416), phospho-Akt (Ser-473), phospho-Erk1/2 (Tyr-204), phospho-p38 (Thr-180/Tyr-182), phospho-c-Jun (Ser-63) and the respective un-phosphorylated proteins from FLC4 and HLF cell lysates treated ±Wisp1 (100 ng/ml). (B) Quantification of the immunoblot signal intensities was normalized to the reference protein GAPDH. Data are presented as the mean of 2 independent experiments. Error bars on data points represent SE of the mean. (C) Signal transduction in FLC4 Wisp1 knockdown cell lines. Again, FLC4 cells were transfected with 1.5 MOI control hairpin vector (shco) and shRNA targeting Wisp1 (sh0/sh1). Immunoblot analyses of phospho-Fak (Tyr-397), phospho-Src (Tyr-416), phospho-Akt (Ser-473), phospho-Erk1/2 (Tyr-204) and the respective un-phosphorylated proteins.

3.7 Wisp1 increases the migration of fibroblast-like HCC cells

Metastasis formation refers to the spread of cancer in the body involving malignant cells that exhibit increased migration ability. It has been suggested that integrins and Wisp1 [47] can modulate the mobility of cancer cells. As we found, Wisp1 activates multiple kinases (Fig.3-15) in the HLF cell line which do not lead to an increase in proliferation (Fig.3-8), therefore, we compared the migration ability of Wisp1 stimulated and untreated HLF cells by the scratch wound-healing assay. Scratch coverage by HLF cells was increased upon Wisp1 treatment (Fig.3-16A and B). Directed migration depends on the formation of new adhesions, which promote cell attachment. Interestingly, in the presence of Wisp1, the attachment of HLF cells to the cultured dish was faster (Fig.3-16C). Furthermore, it has been reported that CCN members have an effect on multiple MMPs (Metalloproteinases) and their inhibitors TIMPs (Tissue Inhibitors of Metalloproteinases) which play a key role in migration [80-82]. We found that Wisp1 stimulation downregulated TIMP1 expression in the HLF cell line.

Taken together, the migration and adhesion assays demonstrate increased cell motility upon Wisp1 treatment indicating that secretion of Wisp1 by HCC might promote tumor growth and metastasis. In addition, it is possible that solid tumors fine-tune their microenvironment via Wisp1 secretion to differentially regulate growth and/or migration.
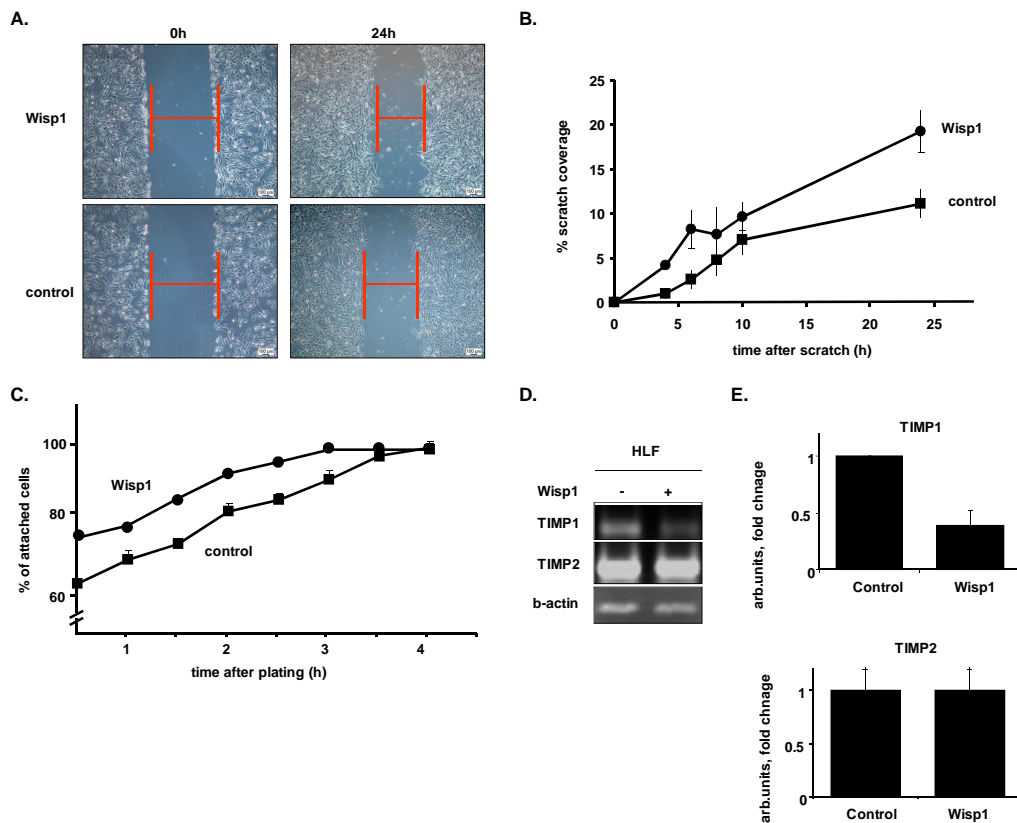
Fig.3-16 Wisp1 increases the migration rate of HLF cells. (A and B) *In vitro* scratch wound healing assay of HLF cells. Panels show representative images (5x objective) of untreated and Wisp1 stimulated cells at day 1 (immediately after injury) for baseline measurements and again at 24 h upon scratching and ±Wisp1 (100 ng/ml) stimulation. (B) Quantitative representation of results in A. Data were calculated on the basis of 3 independent experiments. Data are presented as the mean. Error bars represent SE. (C) Cell attachment of HLF cells in the cell adhesion assay. The data was collected after 30 min to 4 h after plating, n = 3, in triplicates. Data are presented as the mean. Error bars represent SE. (D) Total RNA was extracted from the HLF cell line using the RNeasy kit according to the manufacturer's instructions. The semiquantitative RT-PCR analysis demonstrates the response of TIMP1 and TIMP2 to 24 h of Wisp1 stimulation. (E) TIMP expression was quantified against beta-actin using AIDA Image Analyzer 2.11 software. Data are presented as the mean ± SE.

3.8 Apoptotic cell death is induced by Wisp1 inhibition in HCC cell lines

Inactivation of apoptosis, programmed cell death, is a hallmark of cancer progression [83]. Inactivation of the apoptotic response of cancer cells contributes to their resistance against cancer treatments [83]. Understanding of pro-and anti-apoptotic proteins would help to predict cancer treatment options. Evidence exists that CCN proteins regulate cell survival and show pro- or anti-apoptotic effects [54, 84, 85].

Therefore, apoptosis was studied in Wisp1 control and knockdown HCC cell lines. Caspase 3 activity assays revealed that Wisp1 depletion by shRNAs results in an increase in FLC4 cell apoptosis (Fig.3-17A), whereas Wisp1 treatment of Wisp1 depleted cells reduced Caspase 3 activity. Furthermore, the anti-apoptotic protein BCL-XL is known to regulate cell death by inhibiting caspase activation and, consistently, immunoblot analysis showed a decrease in protein level of the anti-apoptotic marker BCL-XL (Fig.3-17B). Higher MOI of virus infection resulted in complete cell death after 2 weeks in the shWisp1 infected FLC4 cells while control transfected cells survived. Indeed, we suggest that Wisp1 is important for the survival of cancer cells.
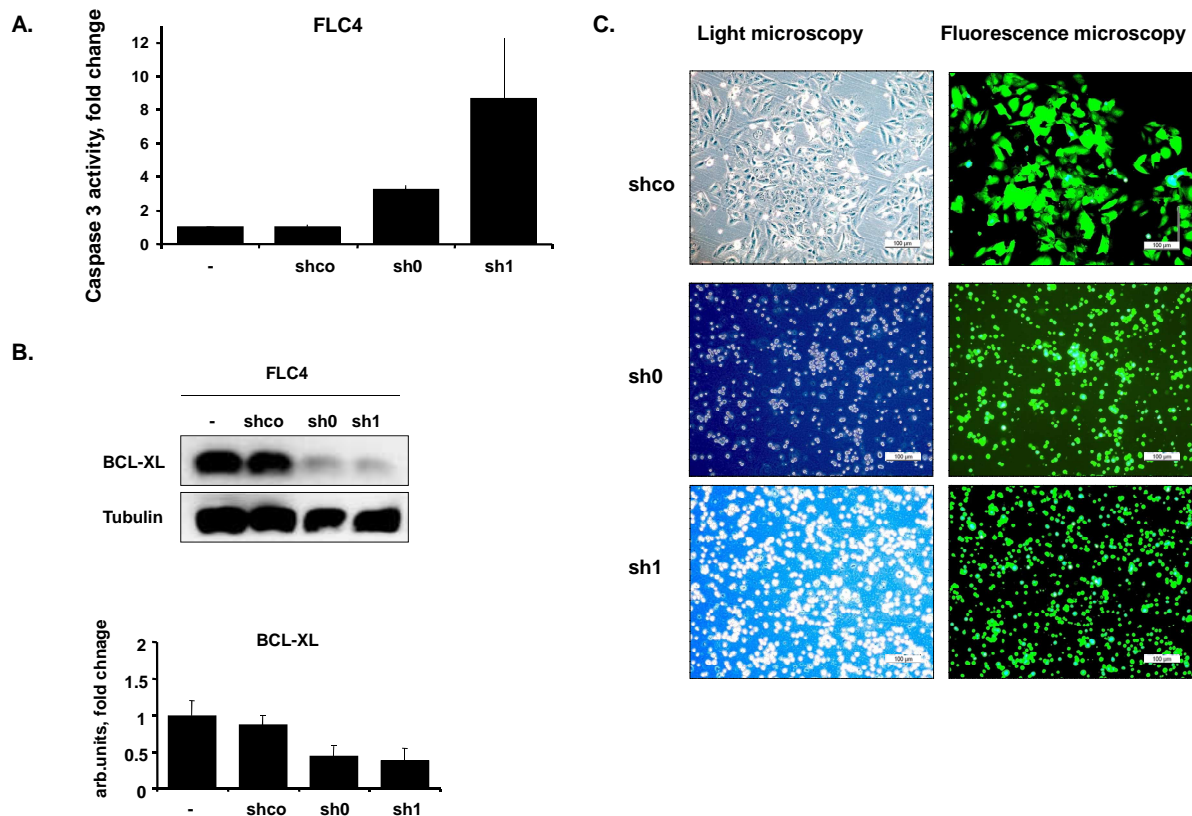
Fig.3-17 Effects of Wisp1 knockdown on FLC4 cell apoptosis. (A). Caspase 3 enzymatic activity assay in untransfected FLC4 cells, with 1.5 MOI control transfected cells (shco) and Wisp1 knockdown cells (sh0/sh1). (B) Immunoblot analysis for BCL-XL and loading control tubulin. Quantification of signal intensity representing gene expression was normalized against tubulin. Data are presented as the mean. Error bars represent SE. (C) Light microscopy and fluorescence microscopy pictures of FLC4 cells which were transiently transfected with 5 MOI shRNA control (shco) or shRNAs to Wisp1 (sh0 and sh1). Cells were cultured up to 2 weeks before they died in culture.

4 Discussion

The aim of the present study was to elucidate whether the matricellular CCN protein Wisp1 is associated with the development of hepatocellular carcinoma in humans and to investigate the mechanisms of Wisp1 function in HCC and HCC-derived cell lines. We provide evidence that Wisp1 is up-regulated in cancer cells found in well differentiated hepatocellular carcinoma. Using different approaches, we also found that the proliferation of epithelial-type cancer cells and the migration of fibroblast-like cancer cells depend on functional Wisp1 indicating that Wips1 is a potential biomarker and involved in tumor progression. These results are of interest since HCC exhibits a poor prognosis due to currently insufficient therapies and new diagnostic markers for the early detection of the disease or novel targets for therapy are highly desired. Unfortunately, early HCC lacks the typical characteristics of advanced HCC including an increase in the common tumor markers α-fetoprotein, (AFP) etc. or histological alterations [76]. Thus, HCC usually is first diagnosed in patient when liver cirrhosis [86, 87] is established and HCC had advanced to treatment resistant stages [73].

Expression and localization of Wisp1 in liver biopsies of patients with hepatocellular carcinoma

Very recently, other groups reported altered levels of Wisp1 expression in different cancer entities [50, 74] and associated them with the malignancy of the disease [50, 62]. To our knowledge, the present study is the first attempt towards a comprehensive analysis of the CCN protein Wisp1 in HCC. It was hypothesized that Wisp1 could be used as an immunohistochemical marker for HCC staging. To investigate the expression pattern and localization of Wisp1 in hepatocellular carcinoma we stained 48 HCC patient samples together with normal adjacent liver tissue from the same individuals (Tab.3-1). First, the immunohistochemical study shows that Wisp1 is very specific for hepatocytes. Second, our results indicate for the first time that uninjured hepatocytes were negative for Wisp1 or showed only a low Wisp1 signal (Fig.3-2). In contrast, increased Wisp1 expression was observed in

damaged hepatocytes surrounding focal areas of inflammation and in hepatocytes with multi nuclei, as well as in cancerogenous hepatocytes of patients with well to moderately differentiated HCC (Fig.3-3/3-4). In contrast, poorly differentiated HCC Wisp1 expression was not found. Hence, when damaged hepatocytes are transformed they express higher levels of Wisp1, whereas Wisp1 expression is lost again in advanced stages of the tumor. These findings, in particular in regard to the overexpression of Wisp1 during inflammation of well differentiated cancer, suggests that Wisp1 expression may be valuable as a useful bio-marker for the early diagnosis of HCC, as well differentiated histology is exclusively seen at early stages and is rare in advanced HCC. These data also suggest a dual role of Wisp1 in HCC, depending on the differentiation stage. Published data already indicate a close association of b-catenin mutations and Wnt signaling with a low tumor stage [88]. Our findings also indicate that Wisp1 is located in the tumor stroma (Fig.3-4) suggesting that binding of Wisp1 to collagen is via its TSP-1 and other CCN domains [89, 90]. Binding of CCN proteins to ECM components such as fibronectin or collagen has been reported [91-93] and mutated TSP domains in CCN have been linked to different types of tumors [33, 94]. In addition, diffuse fatty changes of well differentiated tumor cells are often investigated in HCC. Interestingly, steatotic regions of fatty livers were also positive for Wisp1 (Fig.3-2). Wisp1 was recently shown to be associated with marked attenuation of lung fibrosis, including decreased collagen deposition, suggesting that functional Wisp1 antagonists are of therapeutic value for fibrotic lung diseases [74]. In neoplastic diseases, Wisp1 expression levels were associated with lymphatic and perineural invasion of tumor cells, as well as a poor clinical prognosis in cholangiocarcinoma [59]. In breast cancer, Wisp1 expression was correlated with tumor size, staging, lymph node status and invasion and metastasis [95]. Furthermore, Wisp1 has been shown to be involved in epithelial cell hyperplasia in breast cancer cell lines such as MCF-7, ZR-75, T47D and SKBR2 [58]. In lung cancer, Wisp1 expression was positively correlated to tumor histology, patient age and with lung cancer metastasis [96]. In esophageal cancer, Wisp1 positive cases were closely associated with tumor size and type, lymph node metastasis and poor prognosis [97]. In this line, we find Wisp1 up-regulation by immunohistochemistry in hepatocytes that show a pre-cancerogenous cell morphology. As HCC is a very heterogeneous disease [98], it is very unlikely that one individual marker can be correlated with all features of HCC onset and progression. However, we could detect

the specific Wisp1 expression patterns in all HBV infected HCC patient samples. Presently, available markers for routine immunohistochemistry of HCC show different sensitivity towards the tumor stage and only very few of them are actually specific for HCC [99-102]. Together with AFP and GP-3 (member of the heparan sulfate proteoglycan family), Wisp1 might improve early detection of HCC in HBV patients.

To test whether the up-regulation of Wisp1 in well differentiated HCC was of any functional significance we investigated different HCC cell lines since CCN protein functions have been shown to depend on the cell-type.

HCC cell line proliferation or migration mediated by Wisp1

Recent evidence indicates that Wisp1 can cause proliferation and migration of cancer *cells* and is involved in survival pathways [63, 103-105]. Importantly, Wisp1 is not limited to cancer cells since it has been found in different cell types including epithelial cells as well mesenchymal cells of different organs and tumors [51]. Thus, it remains unclear whether Wisp1 exerts its effects in the tumor cell itself or via the cellular microenvironment of the tumor.

At the onset of our study, we were aware that hepatocellular carcinoma is highly heterogenous and ranges from well differentiated tumors to poorly differentiated neoplasms [9, 16]. Thus, we chose for *in vitro* studies two heterogenic HCC cell lines selected by the epithelial cadherin, E-Cadherin, which regulates cell-cell adhesions, mobility and proliferation of epithelial cells. The human hepatocellular carcinoma cell line FLC4 is well-differentiated, shows an epithelial phenotype and expresses E-Cadherin (Fig.3-8). In contrast to the FLC4 cell line, the HCC cell line HLF is poorly differentiated, shows fibroblastoid phenotype and does not express E-Cadherin (Fig.3-5). We found that Wisp1 is expressed in both cell types (Fig.3-9). Expression of Wisp1 and its alternative splice variants were described in different HCC cell lines [60] and *in vivo* in HCC [61]. We also showed Wisp1 secretion from HCC cell lines in serum-free conditioned medium (Fig.3-9), suggesting Wisp1 as a serum marker for HCC and HCC specific serum markers are of great need [106, 107]. Recently, it was shown that Wisp1 overexpression resulted in morphological alterations of normal fibroblasts [57] and supports tumorigenesis [50, 57]. We further assumed a function of Wisp1 in HCC progression. Deregulation in cell proliferation and uncontrolled

growth have essential roles in carcinogenesis and are responsible for the cancer phenotype. The present study implies that Wisp1 exposure to the epithelial-cell type, either exogenous stimulation or overexpression, promotes DNA synthesis, while gene silencing of Wisp1 attenuates DNA synthesis in the FLC4 cell line (Fig.3-10 and Fig.3-12). In addition, we demonstrated that PCNA protein expression, accompanied by cyclinD1 and cyclinE1 RNA expression, is induced by Wisp1 in FLC4 cells whereas Wisp1 depletion is accompanied by reduced PCNA, cyclinA2 and cyclinD1 levels. No effect was observed in response to Wisp1 stimulation in the fibroblastoid-type HLF cell line. PCNA has been reported to be an indicator for cell proliferation; in HCC patients, high PCNA immunolabeling is associated with poor prognosis [108, 109]. *In vitro* an increased amount of PCNA is expressed in the late G1 and S phases [110, 111]. An increase in cyclins, especially in cyclinD and cyclinE, are common in cancers, including HCC, as cyclins promote cell proliferation [112-114]. Especially the G1-phase cyclins (cyclinD1-3 and cyclinE) are discussed in this manner [115-118], as they trigger the cells from the G1 to the S phase and this process determines the frequency of cell proliferation. In addition, the S-phase cyclinA [118] accompanies the cells through the S-phase [119, 120]. In the current study, we provide evidence that Wisp1 induced DNA synthesis in the epithelial-type HCC cell line is associated with promoting G1/S-phase and S-phase transition. Whereas Wisp1 is also described to be a negative regulator of proliferation, our data are in line with recent reports showing a proliferative effect of Wisp1 on epithelial cells [57, 58].

In this study, we provide further evidence that Wisp1 induced proliferation is cell type dependent. Since E-Cadherin is a marker of epithelial cell origin and an indicator of the epithelial phenotype, it has a pivotal role in epithelial cell behavior during cancer progression and as it is down-regulated in numerous solid cancers, including hepatocellular carcinoma [121], we observed further the proliferative capacity of FLC4 E-Cadherin knockdown cells. We provide evidence that the proliferative capacity of E-Cadherin knockdown cells was not altered in comparison to control transfected cells, but Wisp1 induced proliferation in FLC4 cells was blocked after E-Cadherin knockdown (Fig.3-14). However, E-Cadherin's effect on proliferation is suggested to be complex and the decrease of proliferation in E-Cadherin transfected cancer cells has been described in numerous studies [122, 123], as well as increased cell proliferation [124, 125]. We suggest that the loss of E-Cadherin in FLC4 cells is associated with the loss of the epithelial cell phenotype, so that cells do not

proliferate after Wisp1 stimulation. Indeed the fibroblastoid phenotype HLF cells, which do not express E-Cadherin, do not proliferate after exposure to Wisp1 (Fig.3-10). These findings can be attributed to cross-talk between E-Cadherin and integrins since recent investigations propose integrins as the main cell-surface receptors for CCN proteins [41, 77, 78]. There exists a large body of evidence that adhesion complexes of E-Cadherin and integrins effect carcinoma cell behavior [126] and especially hepatocellular carcinoma cells require integrins and cadherins for a a large number of cellular functions [127-129], thus the effects of Wisp1 in HCC are for certain complex.

Furthermore, the loss of cell adhesions and, consequently, the invasion of surrounding tissue is although a major milestone during cancer development. CCN members are cell adhesive proteins to the ECM, they provide cell adhesion and motility. The fibroblastoid-type HLF cell line is described to strongly adhere, migrate and spread [66, 69]. In this work we were able to demonstrate that Wisp1 stimulation enhances both migration and adhesion in HLF cells (Fig.3-16) via downregulation of TIMP1. The balance between MMPs and their inhibitor TIMPs is associated with tumor cell mobility. According to our data, it has been reported that TIMP1 is an antimigrative factor [130-132] in liver diseases, but there is also evidence that TIMP1 upregulation promotes cell migration [133]. Former studies show the effect of Wisp1 on migration [47, 74] and recent evidence shows increased Wisp mediated migration via MMP2 expression in human chondrosarcoma cells through integrin receptors Fak, Mek, Erk, p65 and NF-κB signaling transduction [134]. Other studies also show that Wisp1 overexpression downregulates motility and invasion of lung cancer cells [47] or transfected Wisp1 K-1735 M-2 melanoma cells show decreased metastatic formation [49].

Taken together, these data are in accordance with previous studies that show that the effects of CCN proteins on cell proliferation or migration are cell type dependent. For instance, in fibroblasts CCN1-3 induce DNA synthesis [78], although only CCN2 (CTGF) is able to induce DNA synthesis in osteoblasts and chondrocytes [103, 104]. CCN3 mediates migration of Ewing's sarcoma cells but blocks their proliferative capacity [135]. While CCN3 and CCN5 decrease vascular smooth muscle cell proliferation and migration, CCN1 and CCN2 act positively on the processes [105, 136].

In the present study, we provide *in vitro* evidence that Wisp1 mediates proliferation of epithelial-type and migration of fibroblastoid-type cells. Whether these effects are in fact cell phenotype limited remains to be investigated deeper. Consistent with these *in vitro* data, revealed by immunohistochemical staining, we found a positive correlation between expression of E-Cadherin and Wisp1 (Fig.3-7). In early stage HCC, cancer cells are still in close connection due to strong cell-cell adhesions mediated by E-Cadherin. These cancer cells proliferate but do not leave their cell network. Due to EMT, these cancer cells lose E-Cadherin and their epithelial phenotype and at advanced stages of HCC start to migrate and to form metastasis. Furthermore, as it has been suggested that the functional properties of Wisp1 is dependent upon its ability to interact with a large number of partners involved in diverse signaling pathways, we further focussed our efforts on different HCC associated signaling targets.

Wisp1 mediated signaling

Detailed molecular pathways which play a pivotal role in the development of liver tumors are until now not fully identified [9, 137]. The mechanism through which Wisp1 mediates its diverse set of cellular and biological functions in isolated cell systems remains to be identified. However, current stories report a specific binding site for CCN proteins in integrin receptors [41, 45, 79, 138, 139]. In addition, activation of MAP kinases in general has been shown to be the main feature of several CCN family members, but their outcome varies, resulting in the same, different or even opposite effect on, for instance, proliferation, migration, adhesion or survival [54, 77, 140]. Thus, we focussed our work on oncogenic kinases which have been shown to be important mediators during HCC progression [116, 141, 142]. Rapid phosphorylation of focal adhesion kinases (Fak) and Src-kinases results in the activation of further downstream targets like P13/Akt or Ras/Raf/Erk, which are all important signal transduction pathways in hepatocellular carcinoma [44, 46, 143, 144]. Clinical studies showed the critical involvement of Akt phosphorylation in the aggressiveness of HCC [145] and activation of Erk has been described to be adhesion-dependent [146, 147]. In this study, we demonstrate that Wisp1 treatment causes activation of Fak, Src, Akt and Erk1/2 via phosphorylation, whereas no

activation of p38 or c-Jnk was observed (Fig.3-15). Activation of these signaling targets was comparable in epithelial- and fibroblastoid-type HCC cell lines. Moreover, silencing of endogenous Wisp1 expression leads not only to alterations in phosphoprotein but also in unphosporylated protein level in the epithelial-type HCC cell line FLC4 (Fig.3-15). These findings are supported by other studies which show the involvement of the Fak signaling pathway in response to Wisp1 in chondrosarcoma cells [134] or which demonstrate Akt activation in response to Wisp1 [54, 74], whereas Wisp1 induced cell motility of the HuCCT1 cholangiocarcinoma cell line and was shown to be mediated through activation of p-p38 [62].Thus, our findings demonstrate first, Wisp1 mediated signaling in HCC cell lines and second, signaling is cell type independent but results in cell type dependent effects. Previous studies show that Wisp1 attenuated p53 mediates apoptosis through activation of Akt [54] and induces expression of BCL-2 and BCL-XL [73]. Since activation of Akt pushes for cells survival and blocks apoptosis by involvement of BCL-XL and activation of the intrinsic caspase mechanism [148, 149], we found consequently that Wisp1 FLC4 knockdown cells show a decrease of anti-apoptotic BCL-XL protein level, an increase in Caspase 3 activity, and increase in Akt level and go into apoptosis and not into proliferation in culture (Fig.3-10 and Fig.3-17). The impact of CCN proteins on apoptosis has mainly been shown for CCN1-3 which activate tumor necrosis factor (TNF) to induce apoptosis [150]. In contrast, Wisp1 inhibits TNF-induced cell death in cardiomyocytes [151]. This study shows that Wisp1 mediated mechanisms of inflammation in HCC cell lines is associated with regulation of apoptotic pathways. As apoptosis is inhibited in cancer cells and this inhibition contributes to cancer progression, many anticancer reagents activate apoptosis of cancer cells [152, 153]. As we have shown that Wisp1 depletion in cancer cells increases apoptosis, it is tempting to conclude that and increase in the level of Wisp1 is a pro-apoptotic protein would be suitable for cancer treatment.

In conclusion, we provide evidence that Wisp1 might serve as a marker for the early detection of HCC since we found its expression is associated with well differentiated HCC and its expression and secretion in phenotype differing HCC derived cell lines. Our studies show in addition that Wisp1 mediated signaling in HCC cell lines is cell type independent and leads to a cell type dependent response (Fig.4-1).

A. Main findings- in vivo

B. Main findings- in vitro
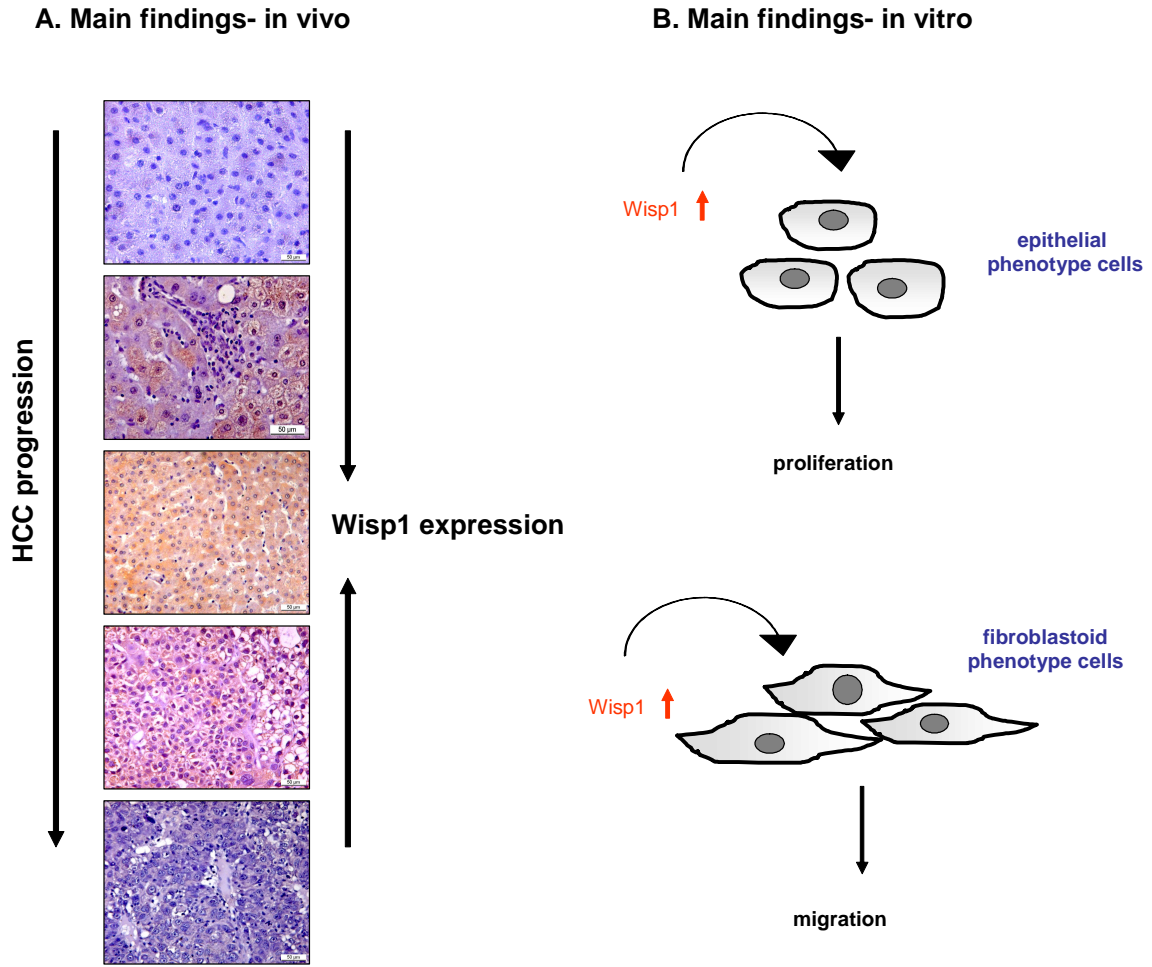
Fig.4-1. Scheme of the main findings of this study. A. *In vivo* and B. *In vitro.*

5 Summary

Worldwide, primary hepatocellular carcinoma is the fifth most commonly diagnosed solid cancer and the third most common cause of cancer related death. Because of its constantly increasing incidence in developed countries and its poor prognosis, HCC represents a major health problem. Diagnostic markers for early-stage HCC are of great need but still lacking due to the high complexity and heterogeneity of HCC. The purpose of this study was to examine Wisp1 expression in different liver tumor stages and its functional role in epithelial- and fibroblastoid-type HCC cell lines. By immunohistochemical staining of HCC patient samples, we demonstrated that Wisp1 expression is enhanced in well- and moderately differentiated HCC and is associated with inflammation and steatosis, but is absent in poorly differentiated HCC. Furthermore, we found that Wisp1 is expressed and secreted in HCC cell lines (FLC4, HLF). Treatment of the epithelial-type HCC cell lines with human recombinant Wisp1 led to an increase in proliferation, while fibroblastoid-type HCC cell lines showed an increase in migration. Interestingly, both types of cell lines displayed the activation of the same phosphokinases upon Wisp1 stimulation. Knockdown of Wisp1 with shRNA in the epithelial-type HCC cell line consequently decreased proliferation and, more importantly, led to apoptosis.

Our study thus identified Wisp1 as a novel immunohistochemical marker for the detection of well differentiated, early-stage HCC as well as a regulator of proliferation in the epithelial-type HCC cell line and a regulator of migration in the fibroblastoid-type HCC cell lines via activation of distinct HCC related phosphokinases. These results pose Wisp1 as a possible diagnostic marker for HCC for which currently only poor therapies are available.

6 List of figures

7 List of tables

8 Appendix

8.1 Abbreviations

AFP	α–fetoprotein
BrdU	5-bromo-2'-deoxy-uridine
Bromo-phenol Blue	3',3",5',5"-tetrabromo-ophenolsulfonphthalein
BSA	bovine serum albumin
CCN	Cystein61/CTGF/Nov
cDNA	copy deoxyribonucleic acid
CHAPS	3-[(3-Cholamidopropyl) dimethylammonio]-1-propanesulfonate
CTGF	connective tissue growth factor
d	days
DAB	3,3´-diaminobenzidine-tetrahydrochloride
dH_2O	distilled water
ddH_2O	double distilled water
DEPC	Diethylpyrocarbonate
DMEM	Dulbecco's modified Eagle's medium
DMSO	dimethyl sulfoxide
DNA	deoxyribonucleic acid
dNTP	deoxynucleotide triphosphate
DOC	Deoxycholic acid Na-salt
DTT	1,4-Dithiothreitol
E.coli	Escherichia coli
EtBr	Ethithium bromide
EtOH	ethanol
ECL	enhanced chemiluminescent
EDTA	ethylenediamine-tetraacetic acid tetrasodium salt
EMT	epithelial-mesenchymal transition
f	forward primer
FCS	fetal calf serum
Fig.	figure
FS	forward scatter

g	grams
GFP	green fluorescent protein
GSK-3β	glycogen synthase kinase beta
kDa	kilo Dalton
h	hour
HBV	hepatitis B virus
HCV	hepatitis C virus
HCC	hepatocellular carcinoma
HC	hepatocytes
HSPG	heparan sulfate proteoglycan
L-Glu	L-glutamine
LSM	laser-scanning confocal microscopy
NOV	nephroblastoma overexpressed
NAFLD	non-alcoholic fatty liver disease
M	moles per liter
MAPK	mitogen-activated protein kinase
mM	millimoles per liter
μM	micromoles per liter
mol	mole
MOPS	3-(N-morpholino)-propanesulfonic acid
MW	molecular weight
mol	mole
NaOH	sodium hydroxide
NaOAc	Sodium acetate
PBS	phosphate buffered saline
PCNA	proliferating cell nuclear antigen
PCR	Polymerase chain reaction
PFA	Paraformaldehyde
POD	peroxidase
P/S	Penicillin-streptomycin
r	reverse primer
RNA	ribonucleic acid
RT	room temperature
SDS	sodium dodecyl sulfate
sec	seconds

shco	short hairpin control
SS	side scatter
shRNA	short hairpinRNA
Tab.	table
TBE	Tris-borate-EDTA buffer
TBS	Tris-buffered saline
TBST	Tris-Tween-buffered
TE	Tris-EDTA buffer
TEMED	N,N,N',N'-Tetramethyl-ethylenediamine
TGF-β	transforming growth factor beta
TMB	tetramethyl-benzidine
Tris	Tris(hydroxymethyl)-aminomethane
U	units
VEGF	vascular endothelial growth factor
Wisp1	Wnt-inducible signaling protein 1

8.2 Primers

Tab. 8-1 Table of primer sequences.

gene	sequence	primer
beta-actin	5'-cacccacactgtgcccatc-3'	beta-actin _f
	5'-ctcctgcttgctgatccac-3'	beta-actin _r
cyclin A2	5'-gcaccccttaaggatcttcc-3'	cyclin A2 _f
	5'-cctctcagcactgacatgga-3'	cyclin A2 _r
cyclin B2	5'-gtatctcaggcagctggagg-3'	cyclin B2 _f
	5'-gaagccaagagcagagcagt-3'	cyclin B2 _r
cyclin D1	5'-catgaactacctggaccgct-3'	cyclin D1 _ f
	5'-tcactctggagaggaagcgt-3'	cyclin D1 _r
cyclin E1	5'-ggtatacttgctgcttcggc-3'	cyclin E1 _f
	5'-tctttggtggagaaggatgg-3'	cyclin E1 _r
Timp1	5'-cctgtgtcccaccccaccca-3'	Timp1_f
	5'-caggcaggcaaggtgacggg-3'	Timp1_r
Timp1	5'-ggcagtgtgtggggtctcgc-3'	Timp2_f
	5'-cggtgccaaggcagggactg-3'	Timp2_r
Wisp1	5'-atgaggtggctcctgcct -3'	Wisp1 _f
	5'-caaaggctctggtgtccaa -3'	Wisp1 _r

8.3 Antibodies

8.3.1 Primary antibodies

Tab. 8-2 Table of primary antibodies.

antibody	origin	application (dilution)	source
Akt	polyclonal rabbit	Western blot (1:1,000)	Cell Signaling (9272)
BCL-XL	polyclonal rabbit	Western blot (1:1,000)	Cell Signaling (2764)
E-Cadherin	polyclonal mouse	Western blot (1:1,000) Immunohistochemistry (1:200) Immunofluorescence (1:100)	BD Bioscience (610181)
Erk1/2	polyclonal mouse	Western blot (1:1,000)	Santa Cruz (sc-135900)
Fak	polyclonal rabbit	Immunofluorescence (1:100)	Santa Cruz (sc-557)
GAPDH	polyclonal rabbit	Western blot (1:1,000)	Santa Cruz (sc-25778)
Wisp1	polyclonal rabbit	Western blot (1:1,000) Immunohistochemistry (1:200)	Abcam (ab10737)
pAkt	polyclonal mouse	Western blot (1:1,000)	Cell Signaling (4051S)
PCNA	polyclonal mouse	Western blot (1:1,000)	Santa Cruz (sc-25280)
pErk1/2	polyclonal rabbit	Western blot (1:1,000)	Santa Cruz (sc-7383)
pFAk397	polyclonal rabbit	Western blot (1:1,000)	Santa Cruz (sc-11765-R)
pSrc	polyclonal rabbit	Western blot (1:1,000)	Cell Signaling (2113-S)
Src	polyclonal rabbit	Western blot (1:1,000)	Cell Signaling (2109)
Tubulin	polyclonal rabbit	Western blot (1:1,000)	Abcam (ab4074-100)

8.3.2 Secondary antibodies

Tab. 8-3 Table of secondary antibodies.

antibody	origin	application (dilution)	source
anti-rabbit-HRP	goat	Western blot (1:5,000)	Santa Cruz (sc-2301)
anti-mouse-HRP	goat	Western blot (1:1,000)	Santa Cruz (sc-2005)
anti-rabbit-immunoglobulins/HRP	swine	Immunohistochemistry (1:200)	Dako (2016-02)
Alexa®488 anti-rabbit	goat	Immunofluorescence (1:300)	Invitrogen (A11029)
Alexa®488 anti-mouse	goat	Immunofluorescence (1:300)	Invitrogen (A11008)

9 References

1. Bruix, J., et al., *Focus on hepatocellular carcinoma.* Cancer Cell, 2004. **5**(3): p. 215-9.
2. El-Serag, H.B. and A.C. Mason, *Rising incidence of hepatocellular carcinoma in the United States.* N Engl J Med, 1999. **340**(10): p. 745-50.
3. Lau, W.Y., *Future perspectives for hepatocellular carcinoma.* HPB (Oxford), 2003. **5**(4): p. 206-13.
4. Pang, R.W., et al., *Biology of hepatocellular carcinoma.* Ann Surg Oncol, 2008. **15**(4): p. 962-71.
5. El-Serag, H.B. and K.L. Rudolph, *Hepatocellular carcinoma: epidemiology and molecular carcinogenesis.* Gastroenterology, 2007. **132**(7): p. 2557-76.
6. Farazi, P.A. and R.A. DePinho, *Hepatocellular carcinoma pathogenesis: from genes to environment.* Nat Rev Cancer, 2006. **6**(9): p. 674-87.
7. Sherman, M., *Hepatocellular carcinoma: epidemiology, risk factors, and screening.* Semin Liver Dis, 2005. **25**(2): p. 143-54.
8. Tischoff, I. and A. Tannapfe, *DNA methylation in hepatocellular carcinoma.* World J Gastroenterol, 2008. **14**(11): p. 1741-8.
9. Blum, H.E. and H.C. Spangenberg, *Hepatocellular carcinoma: an update.* Arch Iran Med, 2007. **10**(3): p. 361-71.
10. Schwartz, M., S. Roayaie, and M. Konstadoulakis, *Strategies for the management of hepatocellular carcinoma.* Nat Clin Pract Oncol, 2007. **4**(7): p. 424-32.
11. Burroughs, A., D. Hochhauser, and T. Meyer, *Systemic treatment and liver transplantation for hepatocellular carcinoma: two ends of the therapeutic spectrum.* Lancet Oncol, 2004. **5**(7): p. 409-18.
12. Llovet, J.M., A. Burroughs, and J. Bruix, *Hepatocellular carcinoma.* Lancet, 2003. **362**(9399): p. 1907-17.
13. Llovet, J.M. and J. Bruix, *Systematic review of randomized trials for unresectable hepatocellular carcinoma: Chemoembolization improves survival.* Hepatology, 2003. **37**(2): p. 429-42.
14. Llovet, J.M., et al., *Sorafenib in advanced hepatocellular carcinoma.* N Engl J Med, 2008. **359**(4): p. 378-90.
15. Llovet, J.M., C. Bru, and J. Bruix, *Prognosis of hepatocellular carcinoma: the BCLC staging classification.* Semin Liver Dis, 1999. **19**(3): p. 329-38.
16. Thiery, J.P., *Epithelial-mesenchymal transitions in tumour progression.* Nat Rev Cancer, 2002. **2**(6): p. 442-54.
17. Peinado, H., F. Portillo, and A. Cano, *Transcriptional regulation of cadherins during development and carcinogenesis.* Int J Dev Biol, 2004. **48**(5-6): p. 365-75.
18. Kemler, R., *From cadherins to catenins: cytoplasmic protein interactions and regulation of cell adhesion.* Trends Genet, 1993. **9**(9): p. 317-21.
19. Larue, L., et al., *E-Cadherin null mutant embryos fail to form a trophectoderm epithelium.* Proc Natl Acad Sci U S A, 1994. **91**(17): p. 8263-7.
20. Murphy, G. and J. Gavrilovic, *Proteolysis and cell migration: creating a path?* Curr Opin Cell Biol, 1999. **11**(5): p. 614-21.
21. Bianchi, F.B., et al., *Basement membrane production by hepatocytes in chronic liver disease.* Hepatology, 1984. **4**(6): p. 1167-72.

22.   Hynes, R.O., *Integrins: a family of cell surface receptors.* Cell, 1987. **48**(4): p. 549-54.

23.   Hemler, M.E., B.A. Mannion, and F. Berditchevski, *Association of TM4SF proteins with integrins: relevance to cancer.* Biochim Biophys Acta, 1996. **1287**(2-3): p. 67-71.

24.   Dedhar, S. and G.E. Hannigan, *Integrin cytoplasmic interactions and bidirectional transmembrane signalling.* Curr Opin Cell Biol, 1996. **8**(5): p. 657-69.

25.   Roskelley, C.D., A. Srebrow, and M.J. Bissell, *A hierarchy of ECM-mediated signalling regulates tissue-specific gene expression.* Curr Opin Cell Biol, 1995. **7**(5): p. 736-47.

26.   Bennett, V. and P.J. Stenbuck, *Identification and partial purification of ankyrin, the high affinity membrane attachment site for human erythrocyte spectrin.* J Biol Chem, 1979. **254**(7): p. 2533-41.

27.   Ruoslahti, E., *Integrin signaling and matrix assembly.* Tumour Biol, 1996. **17**(2): p. 117-24.

28.   Holbourn, K.P., B. Perbal, and K. Ravi Acharya, *Proteins on the catwalk: modelling the structural domains of the CCN family of proteins.* J Cell Commun Signal, 2009. **3**(1): p. 25-41.

29.   Brigstock, D.R., et al., *Proposal for a unified CCN nomenclature.* Mol Pathol, 2003. **56**(2): p. 127-8.

30.   Bornstein, P., *Diversity of function is inherent in matricellular proteins: an appraisal of thrombospondin 1.* J Cell Biol, 1995. **130**(3): p. 503-6.

31.   Hohenester, E. and J. Engel, *Domain structure and organisation in extracellular matrix proteins.* Matrix Biol, 2002. **21**(2): p. 115-28.

32.   Bork, P., *The modular architecture of a new family of growth regulators related to connective tissue growth factor.* FEBS Lett, 1993. **327**(2): p. 125-30.

33.   Perbal, B., *CCN proteins: multifunctional signalling regulators.* Lancet, 2004. **363**(9402): p. 62-4.

34.   Allan, B.B. and W.E. Balch, *Protein sorting by directed maturation of Golgi compartments.* Science, 1999. **285**(5424): p. 63-6.

35.   Jones, J.I. and D.R. Clemmons, *Insulin-like growth factors and their binding proteins: biological actions.* Endocr Rev, 1995. **16**(1): p. 3-34.

36.   Bleau, A.M., N. Planque, and B. Perbal, *CCN proteins and cancer: two to tango.* Front Biosci, 2005. **10**: p. 998-1009.

37.   Takagi, J., et al., *A single chain 19-kDa fragment from bovine thrombospondin binds to type V collagen and heparin.* J Biol Chem, 1993. **268**(21): p. 15544-9.

38.   Sipes, J.M., et al., *Inhibition of fibronectin binding and fibronectin-mediated cell adhesion to collagen by a peptide from the second type I repeat of thrombospondin.* J Cell Biol, 1993. **121**(2): p. 469-77.

39.   Inoki, I., et al., *Connective tissue growth factor binds vascular endothelial growth factor (VEGF) and inhibits VEGF-induced angiogenesis.* FASEB J, 2002. **16**(2): p. 219-21.

40.   Tong, Z.Y. and D.R. Brigstock, *Intrinsic biological activity of the thrombospondin structural homology repeat in connective tissue growth factor.* J Endocrinol, 2006. **188**(3): p. R1-8.

41.   Lau, L.F. and S.C. Lam, *The CCN family of angiogenic regulators: the integrin connection.* Exp Cell Res, 1999. **248**(1): p. 44-57.

42.   Sakamoto, K., et al., *The nephroblastoma overexpressed gene (NOV/ccn3) protein associates with Notch1 extracellular domain and inhibits myoblast*

differentiation via Notch signaling pathway. J Biol Chem, 2002. **277**(33): p. 29399-405.

43. Brigstock, D.R., et al., *Purification and characterization of novel heparin-binding growth factors in uterine secretory fluids. Identification as heparin-regulated Mr 10,000 forms of connective tissue growth factor.* J Biol Chem, 1997. **272**(32): p. 20275-82.

44. Chen, N., C.C. Chen, and L.F. Lau, *Adhesion of human skin fibroblasts to Cyr61 is mediated through integrin alpha 6beta 1 and cell surface heparan sulfate proteoglycans.* J Biol Chem, 2000. **275**(32): p. 24953-61.

45. Gao, R. and D.R. Brigstock, *Connective tissue growth factor (CCN2) induces adhesion of rat activated hepatic stellate cells by binding of its C-terminal domain to integrin alpha(v)beta(3) and heparan sulfate proteoglycan.* J Biol Chem, 2004. **279**(10): p. 8848-55.

46. Chen N, C.N.-N., Lau LF, *The angiogenic factors Cyr61 and CTGF induecs adhesive signalling in primary human skin fibroblasts.* J Biol Chem, 2001. **276**: p. 10443-10452.

47. Soon, L.L., et al., *Overexpression of WISP-1 down-regulated motility and invasion of lung cancer cells through inhibition of Rac activation.* J Biol Chem, 2003. **278**(13): p. 11465-70.

48. Kubota, S., et al., *Report on the fourth international workshop on the CCN family of genes.* J Cell Commun Signal, 2007. **1**(1): p. 59-65.

49. Hashimoto, Y., et al., *Expression of the Elm1 gene, a novel gene of the CCN (connective tissue growth factor, Cyr61/Cef10, and neuroblastoma overexpressed gene) family, suppresses In vivo tumor growth and metastasis of K-1735 murine melanoma cells.* J Exp Med, 1998. **187**(3): p. 289-96.

50. Pennica, D., et al., *WISP genes are members of the connective tissue growth factor family that are up-regulated in wnt-1-transformed cells and aberrantly expressed in human colon tumors.* Proc Natl Acad Sci U S A, 1998. **95**(25): p. 14717-22.

51. Yanagita, T., et al., *Expression and physiological role of CCN4/Wnt-induced secreted protein 1 mRNA splicing variants in chondrocytes.* FEBS J, 2007. **274**(7): p. 1655-65.

52. Hashimoto, G., et al., *Matrix metalloproteinases cleave connective tissue growth factor and reactivate angiogenic activity of vascular endothelial growth factor 165.* J Biol Chem, 2002. **277**(39): p. 36288-95.

53. You, Z., et al., *Wnt signaling promotes oncogenic transformation by inhibiting c-Myc-induced apoptosis.* J Cell Biol, 2002. **157**(3): p. 429-40.

54. Su, F., et al., *WISP-1 attenuates p53-mediated apoptosis in response to DNA damage through activation of the Akt kinase.* Genes Dev, 2002. **16**(1): p. 46-57.

55. Gellhaus, A., et al., *Connexin43 interacts with NOV: a possible mechanism for negative regulation of cell growth in choriocarcinoma cells.* J Biol Chem, 2004. **279**(35): p. 36931-42.

56. Desnoyers, L., D. Arnott, and D. Pennica, *WISP-1 binds to decorin and biglycan.* J Biol Chem, 2001. **276**(50): p. 47599-607.

57. Xu, L., et al., *WISP-1 is a Wnt-1- and beta-catenin-responsive oncogene.* Genes Dev, 2000. **14**(5): p. 585-95.

58. Saxena, N., et al., *Differential expression of WISP-1 and WISP-2 genes in normal and transformed human breast cell lines.* Mol Cell Biochem, 2001. **228**(1-2): p. 99-104.

59. Tanaka, S., et al., *A novel variant of WISP1 lacking a Von Willebrand type C module overexpressed in scirrhous gastric carcinoma.* Oncogene, 2001. **20**(39): p. 5525-32.

60. Cervello, M., et al., *Expression of WISPs and of their novel alternative variants in human hepatocellular carcinoma cells.* Ann N Y Acad Sci, 2004. **1028**: p. 432-9.

61. Calvisi, D.F., et al., *Activation of the canonical Wnt/beta-catenin pathway confers growth advantages in c-Myc/E2F1 transgenic mouse model of liver cancer.* J Hepatol, 2005. **42**(6): p. 842-9.

62. Tanaka, S., et al., *Human WISP1v, a member of the CCN family, is associated with invasive cholangiocarcinoma.* Hepatology, 2003. **37**(5): p. 1122-9.

63. French, D.M., et al., *WISP-1 is an osteoblastic regulator expressed during skeletal development and fracture repair.* Am J Pathol, 2004. **165**(3): p. 855-67.

64. Li, C.L., et al., *A role for CCN3 (NOV) in calcium signalling.* Mol Pathol, 2002. **55**(4): p. 250-61.

65. Wittekind, C., et al., *TNM residual tumor classification revisited.* Cancer, 2002. **94**(9): p. 2511-6.

66. Tsuboi, S., et al., *Persistence of hepatitis C virus RNA in established human hepatocellular carcinoma cell lines.* J Med Virol, 1996. **48**(2): p. 133-40.

67. Aoki, Y., et al., *A human liver cell line exhibits efficient translation of HCV RNAs produced by a recombinant adenovirus expressing T7 RNA polymerase.* Virology, 1998. **250**(1): p. 140-50.

68. Matsuguchi, T., et al., *Production of interleukin 6 from human liver cell lines: production of interleukin 6 is not concurrent with the production of alpha-fetoprotein.* Cancer Res, 1990. **50**(23): p. 7457-9.

69. Chang, R.S., *Continuous subcultivation of epithelial-like cells from normal human tissues.* Proc Soc Exp Biol Med, 1954. **87**(2): p. 440-3.

70. Sena-Esteves, M., et al., *Single-step conversion of cells to retrovirus vector producers with herpes simplex virus-Epstein-Barr virus hybrid amplicons.* J Virol, 1999. **73**(12): p. 10426-39.

71. Takeichi, M., *Cadherin cell adhesion receptors as a morphogenetic regulator.* Science, 1991. **251**(5000): p. 1451-5.

72. Hayashi, Y., et al., *Liver enriched transcription factors and differentiation of hepatocellular carcinoma.* Mol Pathol, 1999. **52**(1): p. 19-24.

73. Venkatesan, B., et al., *WNT1-inducible signaling pathway protein-1 activates diverse cell survival pathways and blocks doxorubicin-induced cardiomyocyte death.* Cell Signal. **22**(5): p. 809-20.

74. Konigshoff, M., et al., *WNT1-inducible signaling protein-1 mediates pulmonary fibrosis in mice and is upregulated in humans with idiopathic pulmonary fibrosis.* J Clin Invest, 2009. **119**(4): p. 772-87.

75. Knowles, B.B., C.C. Howe, and D.P. Aden, *Human hepatocellular carcinoma cell lines secrete the major plasma proteins and hepatitis B surface antigen.* Science, 1980. **209**(4455): p. 497-9.

76. Saito, H., et al., *Establishment of a human cell line (HCC-T) from a patient with hepatoma bearing no evidence of hepatitis B or A virus infection.* Cancer, 1989. **64**(5): p. 1054-60.

77. Jun, J.I. and L.F. Lau, *Taking aim at the extracellular matrix: CCN proteins as emerging therapeutic targets.* Nat Rev Drug Discov. **10**(12): p. 945-63.

78. Chen, C.C. and L.F. Lau, *Functions and mechanisms of action of CCN matricellular proteins.* Int J Biochem Cell Biol, 2009. **41**(4): p. 771-83.

79. Jain, A., et al., *Three SIBLINGs (small integrin-binding ligand, N-linked glycoproteins) enhance factor H's cofactor activity enabling MCP-like cellular evasion of complement-mediated attack.* J Biol Chem, 2002. **277**(16): p. 13700-8.

80. Chen, C.C., N. Chen, and L.F. Lau, *The angiogenic factors Cyr61 and connective tissue growth factor induce adhesive signaling in primary human skin fibroblasts.* J Biol Chem, 2001. **276**(13): p. 10443-52.

81. Chen, C.C., F.E. Mo, and L.F. Lau, *The angiogenic factor Cyr61 activates a genetic program for wound healing in human skin fibroblasts.* J Biol Chem, 2001. **276**(50): p. 47329-37.

82. Fan, W.H. and M.J. Karnovsky, *Increased MMP-2 expression in connective tissue growth factor over-expression vascular smooth muscle cells.* J Biol Chem, 2002. **277**(12): p. 9800-5.

83. Brown, J.M. and L.D. Attardi, *The role of apoptosis in cancer development and treatment response.* Nat Rev Cancer, 2005. **5**(3): p. 231-7.

84. Lin, M.T., et al., *Cyr61 expression confers resistance to apoptosis in breast cancer MCF-7 cells by a mechanism of NF-kappaB-dependent XIAP up-regulation.* J Biol Chem, 2004. **279**(23): p. 24015-23.

85. Xie, D., et al., *Cyr61 is overexpressed in gliomas and involved in integrin-linked kinase-mediated Akt and beta-catenin-TCF/Lef signaling pathways.* Cancer Res, 2004. **64**(6): p. 1987-96.

86. Sun, V.C. and L. Sarna, *Symptom management in hepatocellular carcinoma.* Clin J Oncol Nurs, 2008. **12**(5): p. 759-66.

87. Sakamoto, M., *Early HCC: diagnosis and molecular markers.* J Gastroenterol, 2009. **44 Suppl 19**: p. 108-11.

88. Yuzugullu, H., et al., *Canonical Wnt signaling is antagonized by noncanonical Wnt5a in hepatocellular carcinoma cells.* Mol Cancer, 2009. **8**: p. 90.

89. Subramaniam, M.M., et al., *Expression of CCN3 protein in human Wilms' tumors: immunohistochemical detection of CCN3 variants using domain-specific antibodies.* Virchows Arch, 2008. **452**(1): p. 33-9.

90. Lazar, N., et al., *Domain-specific CCN3 antibodies as unique tools for structural and functional studies.* J Cell Commun Signal, 2007. **1**(2): p. 91-102.

91. Francischetti, I.M., et al., *Cyr61/CCN1 displays high-affinity binding to the somatomedin B(1-44) domain of vitronectin.* PLoS One. **5**(2): p. e9356.

92. Chen, Y., et al., *CCN2 (connective tissue growth factor) promotes fibroblast adhesion to fibronectin.* Mol Biol Cell, 2004. **15**(12): p. 5635-46.

93. Latinkic, B.V., et al., *Xenopus Cyr61 regulates gastrulation movements and modulates Wnt signalling.* Development, 2003. **130**(11): p. 2429-41.

94. Brigstock, D., L. Lau, and B. Perbal, *Report and abstracts of the 3rd International Workshop on the CCN Family of Genes. St Malo, France, 20-23 October 2004.* J Clin Pathol, 2005. **58**(5): p. 463-78.

95. Hu, R., et al., *[The expression and clinical significance of Wnt-1 induced secreted protein-1 in breast carcinoma].* Sichuan Da Xue Xue Bao Yi Xue Ban. **41**(2): p. 231-4.

96. Chen, P.P., et al., *Expression of Cyr61, CTGF, and WISP-1 correlates with clinical features of lung cancer.* PLoS One, 2007. **2**(6): p. e534.

97. Nagai, Y., et al., *Clinical significance of Wnt-induced secreted protein-1 (WISP-1/CCN4) in esophageal squamous cell carcinoma.* Anticancer Res. **31**(3): p. 991-7.

98. Thorgeirsson, S.S. and J.W. Grisham, *Molecular pathogenesis of human hepatocellular carcinoma.* Nat Genet, 2002. **31**(4): p. 339-46.

99. Sanyal, A.J., S.K. Yoon, and R. Lencioni, *The etiology of hepatocellular carcinoma and consequences for treatment.* Oncologist. **15 Suppl 4**: p. 14-22.

100. Bruix, J. and M. Sherman, *Management of hepatocellular carcinoma.* Hepatology, 2005. **42**(5): p. 1208-36.

101. Daniele, B., et al., *Alpha-fetoprotein and ultrasonography screening for hepatocellular carcinoma.* Gastroenterology, 2004. **127**(5 Suppl 1): p. S108-12.

102. Andreana, L., et al., *Surveillance and diagnosis of hepatocellular carcinoma in patients with cirrhosis.* World J Hepatol, 2009. **1**(1): p. 48-61.

103. Nakanishi, T., et al., *Effects of CTGF/Hcs24, a product of a hypertrophic chondrocyte-specific gene, on the proliferation and differentiation of chondrocytes in culture.* Endocrinology, 2000. **141**(1): p. 264-73.

104. Abdel-Wahab, N., et al., *Connective tissue growth factor and regulation of the mesangial cell cycle: role in cellular hypertrophy.* J Am Soc Nephrol, 2002. **13**(10): p. 2437-45.

105. Lake, A.C., et al., *CCN5 is a growth arrest-specific gene that regulates smooth muscle cell proliferation and motility.* Am J Pathol, 2003. **162**(1): p. 219-31.

106. Malaguarnera, G., et al., *Serum markers of hepatocellular carcinoma.* Dig Dis Sci. **55**(10): p. 2744-55.

107. Spangenberg, H.C., R. Thimme, and H.E. Blum, *Serum markers of hepatocellular carcinoma.* Semin Liver Dis, 2006. **26**(4): p. 385-90.

108. Kitamoto, M., et al., *The assessment of proliferating cell nuclear antigen immunohistochemical staining in small hepatocellular carcinoma and its relationship to histologic characteristics and prognosis.* Cancer, 1993. **72**(6): p. 1859-65.

109. Ng, I.O., et al., *Prognostic significance of proliferating cell nuclear antigen expression in hepatocellular carcinoma.* Cancer, 1994. **73**(9): p. 2268-74.

110. Kurki, P., et al., *Expression of proliferating cell nuclear antigen (PCNA)/cyclin during the cell cycle.* Exp Cell Res, 1986. **166**(1): p. 209-19.

111. Celis, J.E. and A. Celis, *Cell cycle-dependent variations in the distribution of the nuclear protein cyclin proliferating cell nuclear antigen in cultured cells: subdivision of S phase.* Proc Natl Acad Sci U S A, 1985. **82**(10): p. 3262-6.

112. Buckley, M.F., et al., *Expression and amplification of cyclin genes in human breast cancer.* Oncogene, 1993. **8**(8): p. 2127-33.

113. Kitahara, K., et al., *Concurrent amplification of cyclin E and CDK2 genes in colorectal carcinomas.* Int J Cancer, 1995. **62**(1): p. 25-8.

114. Marone, M., et al., *Analysis of cyclin E and CDK2 in ovarian cancer: gene amplification and RNA overexpression.* Int J Cancer, 1998. **75**(1): p. 34-9.

115. Zhang, Y.J., et al., *Amplification and overexpression of cyclin D1 in human hepatocellular carcinoma.* Biochem Biophys Res Commun, 1993. **196**(2): p. 1010-6.

116. Ito, Y., et al., *Activation of mitogen-activated protein kinases/extracellular signal-regulated kinases in human hepatocellular carcinoma.* Hepatology, 1998. **27**(4): p. 951-8.

117. Jiang, W., et al., *Altered expression of the cyclin D1 and retinoblastoma genes in human esophageal cancer.* Proc Natl Acad Sci U S A, 1993. **90**(19): p. 9026-30.

118. Hunter, T. and J. Pines, *Cyclins and cancer. II: Cyclin D and CDK inhibitors come of age.* Cell, 1994. **79**(4): p. 573-82.

119. Hartwell, L.H. and T.A. Weinert, *Checkpoints: controls that ensure the order of cell cycle events.* Science, 1989. **246**(4930): p. 629-34.

120. Wimmel, A., et al., *Inducible acceleration of G1 progression through tetracycline-regulated expression of human cyclin E.* Oncogene, 1994. **9**(3): p. 995-7.

121. Birchmeier, W. and J. Behrens, *Cadherin expression in carcinomas: role in the formation of cell junctions and the prevention of invasiveness.* Biochim Biophys Acta, 1994. **1198**(1): p. 11-26.

122. Kandikonda, S., et al., *Cadherin-mediated adhesion is required for normal growth regulation of human gingival epithelial cells.* Cell Adhes Commun, 1996. **4**(1): p. 13-24.

123. Watabe, M., et al., *Induction of polarized cell-cell association and retardation of growth by activation of the E-Cadherin-catenin adhesion system in a dispersed carcinoma line.* J Cell Biol, 1994. **127**(1): p. 247-56.

124. Perez-Moreno, M., C. Jamora, and E. Fuchs, *Sticky business: orchestrating cellular signals at adherens junctions.* Cell, 2003. **112**(4): p. 535-48.

125. Reddy, P., et al., *Formation of E-Cadherin-mediated cell-cell adhesion activates AKT and mitogen activated protein kinase via phosphatidylinositol 3 kinase and ligand-independent activation of epidermal growth factor receptor in ovarian cancer cells.* Mol Endocrinol, 2005. **19**(10): p. 2564-78.

126. Martinez-Rico, C., et al., *Integrins stimulate E-Cadherin-mediated intercellular adhesion by regulating Src-kinase activation and actomyosin contractility.* J Cell Sci. **123**(Pt 5): p. 712-22.

127. Giannelli, G., et al., *Psoriatic lesions in patients with chronic liver disease are distinct from psoriasis vulgaris lesions, as judged on basis of integrin adhesion receptors.* Hepatology, 1994. **20**(1 Pt 1): p. 56-65.

128. Enjoji, M., et al., *Integrins: utility as cell type- and stage-specific markers for hepatocellular carcinoma and cholangiocarcinoma.* In Vitro Cell Dev Biol Anim, 1998. **34**(1): p. 25-7.

129. Mas, V.R., et al., *Differentially expressed genes between early and advanced hepatocellular carcinoma (HCC) as a potential tool for selecting liver transplant recipients.* Mol Med, 2006. **12**(4-6): p. 97-104.

130. Mannello, F. and G. Gazzanelli, *Tissue inhibitors of metalloproteinases and programmed cell death: conundrums, controversies and potential implications.* Apoptosis, 2001. **6**(6): p. 479-82.

131. Murphy, F.R., et al., *Inhibition of apoptosis of activated hepatic stellate cells by tissue inhibitor of metalloproteinase-1 is mediated via effects on matrix metalloproteinase inhibition: implications for reversibility of liver fibrosis.* J Biol Chem, 2002. **277**(13): p. 11069-76.

132. Xia, D., et al., *Overexpression of TIMP-1 mediated by recombinant adenovirus in hepatocellular carcinoma cells inhibits proliferation and invasion in vitro.* Hepatobiliary Pancreat Dis Int, 2006. **5**(3): p. 409-15.

133. Roeb, E., et al., *Enhanced migration of tissue inhibitor of metalloproteinase overexpressing hepatoma cells is attributed to gelatinases: relevance to intracellular signaling pathways.* World J Gastroenterol, 2005. **11**(8): p. 1096-104.

134. Hou, C.H., et al., *WISP-1 increases MMP-2 expression and cell motility in human chondrosarcoma cells.* Biochem Pharmacol. **81**(11): p. 1286-95.

135. Benini, S., et al., *In Ewing's sarcoma CCN3(NOV) inhibits proliferation while promoting migration and invasion of the same cell type.* Oncogene, 2005. **24**(27): p. 4349-61.

136. Shimoyama, T., et al., *CCN3 inhibits neointimal hyperplasia through modulation of smooth muscle cell growth and migration.* Arterioscler Thromb Vasc Biol. **30**(4): p. 675-82.

137. Calvisi, D.F., et al., *Mechanistic and prognostic significance of aberrant methylation in the molecular pathogenesis of human hepatocellular carcinoma.* J Clin Invest, 2007. **117**(9): p. 2713-22.

138. Grzeszkiewicz, T.M., et al., *CYR61 stimulates human skin fibroblast migration through Integrin alpha vbeta 5 and enhances mitogenesis through integrin alpha vbeta 3, independent of its carboxyl-terminal domain.* J Biol Chem, 2001. **276**(24): p. 21943-50.

139. Kireeva, M.L., et al., *Cyr61 and Fisp12 are both ECM-associated signaling molecules: activities, metabolism, and localization during development.* Exp Cell Res, 1997. **233**(1): p. 63-77.

140. Brigstock, D.R., *The CCN family: a new stimulus package.* J Endocrinol, 2003. **178**(2): p. 169-75.

141. Roberts, L.R. and G.J. Gores, *Hepatocellular carcinoma: molecular pathways and new therapeutic targets.* Semin Liver Dis, 2005. **25**(2): p. 212-25.

142. Gollob, J.A., et al., *Role of Raf kinase in cancer: therapeutic potential of targeting the Raf/MEK/ERK signal transduction pathway.* Semin Oncol, 2006. **33**(4): p. 392-406.

143. Leu, S.J., et al., *Identification of a novel integrin alpha 6 beta 1 binding site in the angiogenic inducer CCN1 (CYR61).* J Biol Chem, 2003. **278**(36): p. 33801-8.

144. Schober, J.M., et al., *Identification of integrin alpha(M)beta(2) as an adhesion receptor on peripheral blood monocytes for Cyr61 (CCN1) and connective tissue growth factor (CCN2): immediate-early gene products expressed in atherosclerotic lesions.* Blood, 2002. **99**(12): p. 4457-65.

145. Nakanishi, K., et al., *Akt phosphorylation is a risk factor for early disease recurrence and poor prognosis in hepatocellular carcinoma.* Cancer, 2005. **103**(2): p. 307-12.

146. Howe, A.K., A.E. Aplin, and R.L. Juliano, *Anchorage-dependent ERK signaling--mechanisms and consequences.* Curr Opin Genet Dev, 2002. **12**(1): p. 30-5.

147. Schwartz, M.A. and V. Baron, *Interactions between mitogenic stimuli, or, a thousand and one connections.* Curr Opin Cell Biol, 1999. **11**(2): p. 197-202.

148. Zha, J., et al., *Serine phosphorylation of death agonist BAD in response to survival factor results in binding to 14-3-3 not BCL-X(L).* Cell, 1996. **87**(4): p. 619-28.

149. Datta, S.R., et al., *Akt phosphorylation of BAD couples survival signals to the cell-intrinsic death machinery.* Cell, 1997. **91**(2): p. 231-41.

150. Chen, C.C. and L.F. Lau, *Deadly liaisons: fatal attraction between CCN matricellular proteins and the tumor necrosis factor family of cytokines.* J Cell Commun Signal. **4**(1): p. 63-9.

151. Venkatachalam, K., et al., *WISP1, a pro-mitogenic, pro-survival factor, mediates tumor necrosis factor-alpha (TNF-alpha)-stimulated cardiac fibroblast proliferation but inhibits TNF-alpha-induced cardiomyocyte death.* J Biol Chem, 2009. **284**(21): p. 14414-27.

152. Kaufmann, S.H. and W.C. Earnshaw, *Induction of apoptosis by cancer chemotherapy.* Exp Cell Res, 2000. **256**(1): p. 42-9.

153. Kaufmann, S.H. and G.J. Gores, *Apoptosis in cancer: cause and cure.* Bioessays, 2000. **22**(11): p. 1007-17.

10 Declaration

The work submitted in this dissertation is the result of my own investigation, except where otherwise stated.

_____

11 Curriculum vitae

Name	Sonja Lukowski
Professional Title	Dipl.Chem.
Date of Birth	December, 31st, 1983
Place of Birth	Kiel, Germany
Nationality	German
Marital status	Single

Academic Education

Since 12/2008	Doctoral thesis at the Ruprecht-Karls-Universität Heidelberg in the research group of Prof. Dr. S. Dooley

Studies

10/2007 - 9/2008	Diplom thesis at the Georg-August-Universität Göttingen in the research group of Prof. Dr. C. Steinem
	Topic of diplom thesis: „The HIV-1 Nef protein pertubs artificial membranes: Investigation of the contribution of the myristoyl anchor."
10/2003 -10/2007	Basic and main studies in chemistry at the Georg-August-Universität Göttingen

School education

08/1994 - 06/2003	Grammar school Wellingdorf, Kiel
08/1990 07/1994	Primary school Ellerbek, Kiel

Publications

➢ Dynamin GTPase activity mediates dedifferentiation of cultured hepatocytes via transcriptional changes. *In preparation*
I. Ilkavets, **S. Lukowski**, A. Bachmann, C. Sticht, C. Meyer, N. Gretz, S. Dooley.

- ➢ Role of Wisp1 in liver pathogenesis. *In preparation*.

  S. Lukowski, H. Weng, S. Dooley*,* I. Ilkavets.

- ➢ The HIV-1 Nef protein pertubs artificial membranes: investigation of the contribution of the myristoyl anchor, *Biophys J.* 2009 Apr 22; 96(8):3242-50R. R. Szilluweit, G. Boll, **S. Lukowski**, H. Gerlach, O. T. Fackler, M. Geyer, C. Steinem.

Presentations

- ➢ Wisp1 as a new HCC promoting target gene, AG Prof. Dr. A. Piiper, Medizinische Klinik der Johann Wolfgang Goethe Universität Frankfurt am Main, 19.11.2011

Poster Presentations

<u>2012</u>

SBMC Meeting, Leipzig, Germany

- ➢ Modeling of hepatic stellate cells role in liver function, inflammation and fibrosis - structural changes and functional consequences of the liver lobular/sinusoidal system

  I.Ilkavets, K. Breitkopf-Heinlein, S. Höhme, A. Friebel, **S. Lukowski**, L. Qi, A. Müller, F. Herweck, S. Kh. Hammad, H. Weng, R. Gebhardt, J. Hengstler, D. Drasdo, S. Dooley

- ➢ Hepatic stellate cells as source and target for hepatocellular growth factors and effect of hepatic stellate cells on hepatocyte polarity and transdifferentiation

  I. Ilkavets, K. Breitkopf-Heinlein, F. Herweck, K. Abramovic, **S. Lukowski**, S. Legewie, A. Raue, B. Löffler, A. Voss-Boehme, L. Brusch, M. Thomas, K. Waldow, L. A. D'Alessandro, U. Klingmüller, U. Zanger, A. Deutsch, R. Gebhardt, J. Timmer, S. Dooley

EASD Meeting, Berlin, Germany

- ➢ Effects of the inhibition of insulin degrading enzyme (IDE) activity on the liver cancer cell transcriptome

  O. Pivovarova, I. Ilkavets, C. Sticht, S. Zhuk, A. Malashicheva, C. Bumke-Vogt, **S. Lukowski**, A. Schlag, A. Kostareva, N. Gretz, S. Dooley, A.F.H. Pfeiffer, N.N. Rudovich

CSH Asia Conference, Suzhou, China

➢ TGF-β induced hepatocellular Wisp1 is expressed in hepatocellular carcinoma and drives proliferation of epithelial-type cancer cells

S. Dooley, **S. Lukowski**, H. Weng, X. Gu, C. Gao, Q. Li, I. Ilkavets

GASL, Hamburg, Germany

➢ TGF-β induced hepatocellular Wisp1 is expressed in hepatocellular carcinoma and drives proliferation of epithelial-type cancer cells

S. Lukowski, H. Weng, X. Gu, C. Gao, Q. Li, S. Dooley, I. Ilkavets

<u>2011</u>

GASL, Regensburg, Germany

➢ Wisp1 as a new marker of hepatocellular carcinoma

S. Lukowski, H. Weng, S. Dooley, I. Ilkavets

<u>2010</u>

GASL, Bonn, Germany,

➢ Dynamin GTPase activity mediates dedifferentiation of cultured hepatocytes via transcriptional changes

I. Ilkavets, **S. Lukowski**, A. Bachmann, C. Sticht, C. Meyer, N. Gretz, S. Dooley

➢ Wisp1, a new marker of hepatocellular carcinoma?

S. Lukowski, I. Ilkavets, H. Weng, S. Dooley

SBMC, Freiburg, Germany

➢ Wisp1 is a new player in liver cancer progression

S. Lukowski, I. Ilkavets, H. Weng, S. Dooley

VLN Kick-off meeting, Dresden, Germany

➢ Structural changes and functional consequences of the liver lobular/sinusoidal system during inflammation and fibrosis

S. Dooley, I. Ilkavets, **S. Lukowski,** A. Mueller, F. Herweck, P. Godoy, S. Hammad, J. Hengstler, T. Szekeres, U. Klingmueller, S. Hoehme, D. Drasdo, 5, A. Deutsch, B. Habermann, M. Mann, J. Timmer, M. Zerial, J. Schiller, A. Schevchenko

EASL, Amsterdam, Netherlands

➢ Dynamin GTPase activity mediates dedifferentiation of cultured hepatocytes via transcriptional changes

I. Ilkavets, **S. Lukowski**, A. Bachmann, C. Sticht, C. Meyer, N. Gretz, S. Dooley.

12 Acknowledgements

Finally, it's over!

Many thanks to Dr. Iryna Ilkavets (*Molecular Hepatology - Alcohol Associated Diseases II. Medical Clinic Faculty of Medicine Mannheim* of *Heidelberg University*) for giving me the opportunity to work on such an interesting project!

I would like to thank collegues from the Institute of *Molecular Hepatology.* Thanks to Marlies, Yan, Alex, Anne and Johanna who were always willing to lend an ear or a helpful hand when it was needed!

To my friends and family:

I am grateful to all my friends! You make life real, easy and joyful!

Special thanks to: Tanja, for everything. Angelika, my tower of strength. Moni, always reminding me what is important in life. Sandra, for making me smile. Sarah, giving me hope for a better time. Priyanka, Anayansi and Aline for finally making Mannheim a home for me. Nina, even though you are not anymore with us, you keep me down to earth when I lose my ground.

Dicker, danke! Mein größter Dank gilt meinen Eltern, für ihre bedingungslose Liebe und Unterstützung in allen Lebenslagen! Ich bin so dankbar, dass ich Eltern wie euch habe!

Danke Mutti, dziękuję tato.